1960

The status of gas-lubricated bearings

Bhaskar Dattatraya Shiwalkar

THE STATUS OF GAS - LUBRICATED BEARINGS

BY

BHASKAR DATTATRAYA SHIWALKAR

A

THESIS

submitted to the faculty of the

SCHOOL OF MINES AND METALLURGY OF THE UNIVERSITY OF MISSOURI

in partial fulfillment of the work required for the

Degree of

MASTER OF SCIENCE IN MECHANICAL ENGINEERING

Rolla, Missouri

1960

Approved by

Aaron J. Miles (Advisor) Ralph E. Schowalter

R. F. Davidson John B. Heagler Jr.

S. J. Pagano

ACKNOWLEDGEMENT

The author is indebted to Dr. A.J. Miles, chairman, Department of Mechanical Engineering, for the keen personal interest displayed in the preparation of this thesis and for the encouragement he has received from time to time. He is also grateful to various authors from whose publications the material has been drawn freely in the preparation of this thesis, especially to Dr. J.S. Ausman, whose unpublished work provided some very useful information on the theory of Hydrodynamic Bearings. In the end, the author wishes to thank Mr. B.M. Williams, Assistant Librarian, for the troubles he has taken in procuring some of the articles which were difficult to obtain.

TABLE OF CONTENTS

LIST OF ILLUSTRATIONS

LIST OF TABLES

INTRODUCTION

The idea of gas-lubricated bearings was suggested as far back as 1854 by Hirn (1)*, but it is only very recently that they have aroused a great amount of interest. The interest is centered on the advantages of gas-bearings for the following major applications:

1. High temperature lubrication where ordinary liquid or grease lubrication fails.
2. Bearings operating in radio-active atmospheres where conventional lubrication may break down.
3. Applications sensitive to contamination where fouling from lubricating oil becomes serious.
4. Low-friction devices--an especially important advantage because of the trend to high speed machinery.
5. Applications where positional accuracies down to micro-inches are required.

As a result of the increasing interest, many people are working in this field and gas bearings have been used for a variety of purposes, both in the laboratory and in industry on a small scale. There is a definite lack of published information relating to their systematic design. It is possible to design a gas bearing for a particular purpose and to make it function satisfactorily, but it is often difficult to achieve the optimum design from the standpoint of maximum load, minimum friction, economic gas flow and maximum stability.

---

* The numbers in the parentheses refer to the numbers in the Bibliography-Part I.

It is the purpose of this thesis to collect all possible literature with a view of finding out what has been done up to this time, so that further theoretical and experimental investigations may be carried out with a view of formulating a complete theory for the design and operation of gas bearings in par with the liquid and grease lubricated bearings.

The subject has been divided into two main parts, because the basic principles underlying the two are quite different:

1. Hydrodynamic or Self-acting Bearings.
2. Hydrostatic or Pressurized Bearings.

In each part an attempt has been made to cover the following topics:

1. Basic Theory.
2. Experimental Results and Their Comparison with Theoretical Predictions.
3. Stability.
4. Effects of Various Parameters on the Performance.
5. Some Practical Aspects.

PART I

HYDRODYNAMIC BEARINGS

NOTATION

Symbol	Description	Units
a	Ratio $\frac{\text{Maximum Film Thickness}}{\text{Minimum Film Thickness}}$	
B	Dimension of Pad in the Direction Parallel to Flow	in.
b	Axial Length of Journal Bearing	in.
c	Average Radial Clearance	in. or $\frac{\text{in.}}{\text{in.}}$
c_1, c_2	Dimensions as Shown in Figure 1.5	in.
d	Diameter of Journal Bearing	in.
e	Eccentricity in Journal Bearing	in.
E	Eccentricity Ratio = $\frac{e}{c}$ for Journal Bearings $\frac{h_1 - h_2}{B}$ for Pad Bearings	
f	Friction Coefficient	
g	Acceleration Due to Gravity	$\frac{\text{in.}}{\text{sec.}^2}$
G	Non Dimensional Group $\frac{6\mu\omega r^2}{c^2 P_a}$ for Journal Bearings $\frac{6\mu UB}{h^2 P_a}$ for Pad Bearings $\frac{3\mu UL}{\Delta^2 P_a}$ for Step Bearings	
h	Clearance Between Bearing Surfaces At Any Point	in.

h_1, h_2	Maximum and Minimum Clearance	in.
K, K_o, K_L	Constants	
k	Polytropic Exponent of Density	
L	Axial Length of Journal Bearing	in.
N	Journal Speed	R.P.M.
P_m	Radial Load per Unit Projected Area of Journal Bearing	$\frac{\text{lbs.}}{\text{in.}^2}$
P	Pressure	$\frac{\text{lbs.}}{\text{in.}^2}$
P_a, P_o	Ambient Pressure	$\frac{\text{lbs.}}{\text{in.}^2}$
P_{∞}	Pressure Solution for Journal Bearing of Infinite Length	$\frac{\text{lbs.}}{\text{in.}^2}$
r	Radius of Journal	in.
U	Velocity of Moving Surface of Bearing Pair	$\frac{\text{in.}}{\text{sec.}}$
u, v, w	Fluid Velocity Components in the x,y,z Direction	$\frac{\text{in.}}{\text{sec.}}$
W	Load Carried by the Bearing	lbs.
W_1, W_2	Vector Components of Load Parallel to and Perpendicular to the Plane of Minimum-Maximum Film Thickness in Case of Journal Bearings	lbs.
W_{∞}	Load Carried by a Bearing of Infinite Width	lbs.

x, y, z	Cartesian Coordinate System with Origin in the Plane of the Moving Surface, z axis Perpendicular to Moving Surface and Directed Positive into the Lubricating Film and x Plotted in the Direction of Motion. Origin at the Trailing Edge for Pad Bearings and in the Centre for Journal Bearings.	
β	$\frac{x}{r}$ Angular Coordinate	Radians
ξ	$\frac{y}{r}$ Dimensionless Axial Coordinate	
μ	Absolute Viscosity	$\frac{\text{lbs.sec.}}{\text{in}^2}$
ρ	Density of the Lubricant	$\frac{\text{lbs.sec}^2}{\text{in}^4}$
ϕ	Attitude Angle Between Direction of Radial Load and Plane of Maximum-Minimum Film Thickness	Degrees
ψ	Misalignment Attitude Angle	Degrees
ω	Angular Velocity of Journal	$\frac{\text{Radians}}{\text{Sec.}}$
Δ	$h_1 - h_2$	in.

In addition some other symbols have been used at some specific places. They are defined at the proper place. Also some of the above symbols have been used in a different sense as explained at the proper place.

1. BASIC THEORY

Hydrodynamic or self-acting type of bearing generates its own hydrostatic pressure within the clearance space, by virtue of the fluid in which it is immersed and the relative motion of the bearing elements. These bearings may be divided into two main categories:

1. Thrust Bearings
2. Journal Bearings

First, the basic theory common to both types will be presented. This will be followed by individual treatment of the two types.

The steady-state behaviour of these bearings under constant load can be described completely by the continuity, momentum and energy equations of flow for a Newtonian fluid, a category to which most of the gases belong for all practical purposes. The energy equation is necessary to predict the nature of the expansion and compression process of the gas within the bearings. So far many attempts have been made, but nobody has been able to prove anything conclusively. Some authors assume the process as isothermal, while others assume adiabatic. The actual process lies between the two. Hence it is better to work with a polytropic process in which the value of the exponent k may be adjusted to suit the particular conditions. Thus we obtain the following equations for continuity, momentum and energy equations:

1. Continuity: $\frac{\partial}{\partial x}(\rho u) + \frac{\partial}{\partial y}(\rho v) + \frac{\partial}{\partial z}(\rho w) = 0$

2. Momentum (Navier-Stokes):

$$\rho u \frac{\partial u}{\partial x} + \rho v \frac{\partial u}{\partial y} + \rho w \frac{\partial u}{\partial z} = \mu \left(\frac{\partial^2 u}{\partial x^2} + \frac{\partial^2 u}{\partial y^2} + \frac{\partial^2 u}{\partial z^2} \right) - \frac{\partial P}{\partial x}$$

$$\rho u \frac{\partial v}{\partial x} + \rho v \frac{\partial v}{\partial y} + \rho w \frac{\partial v}{\partial z} = \mu \left(\frac{\partial^2 v}{\partial x^2} + \frac{\partial^2 v}{\partial y^2} + \frac{\partial^2 v}{\partial z^2} \right) - \frac{\partial P}{\partial y}$$

$$\rho u \frac{\partial w}{\partial x} + \rho v \frac{\partial w}{\partial y} + \rho w \frac{\partial w}{\partial z} = \mu \left(\frac{\partial^2 w}{\partial x^2} + \frac{\partial^2 w}{\partial y^2} + \frac{\partial^2 w}{\partial z^2} \right) - \frac{\partial P}{\partial z}$$

3. Energy: $P\rho^{-k} = \text{constant}.$

We can apply the following assumptions to these equations which are justified within the operating range of most bearings:

1. Inertia terms may be neglected with respect to pressure-gradient terms at usual operating speeds.
2. Fluid velocities normal to the surface are neglected with respect to velocities parallel to the surface.
3. The predominant viscous-shear stresses are $\frac{\partial^2 u}{\partial z^2}$ and $\frac{\partial^2 v}{\partial z^2}$, all other viscous-shear stresses being negligible by comparison.
4. The viscosity coefficient μ may be approximated as a constant.
5. Pressure and density are independent of co-ordinate z.
6. There is no slip between the lubricant and bearing surfaces.

After applying these assumptions, the equations reduce to:

1. Continuity: $\frac{\partial}{\partial x}(\rho u) + \frac{\partial}{\partial y}(\rho v) = 0$ ------1

2. Momentum:

$$\frac{\partial P}{\partial x} = \mu \frac{\partial^2 u}{\partial z^2} \qquad \text{------2}$$

$$\frac{\partial P}{\partial y} = \mu \frac{\partial^2 v}{\partial z^2} \qquad \text{------3}$$

$$\frac{\partial P}{\partial z} = 0 \qquad \text{------4}$$

3. Energy: $pe^{-k} = \text{const.}$ ------5

To make the analysis simpler, some authors have introduced further assumptions given below.

1. The bearing is of infinite width, or there is no side leakage.
2. The process is isothermal, or the value of k is unity.

With these assumptions, the equations reduce to:

1. Continuity: $\frac{\partial}{\partial x}(\rho u) = 0$ ------6

2. Momentum: $\frac{\partial p}{\partial x} = \mu \frac{\partial^2 u}{\partial z^2}$. ------7

$\frac{\partial p}{\partial y} = 0$ ------8

$\frac{\partial p}{\partial z} = 0$ ------9

3. Energy: $p\rho^{-1} = \text{const.}$ -----10

These basic equations (1 to 10) have been solved by various authors. The solutions will now be presented in brief.

THRUST BEARINGS

All the normal types of hydrodynamic thrust bearings as commonly used with liquid lubrication may be used with gases. The "thermal wedge" effect, though present in gas-lubricated bearings, is of negligible amount due to low viscosity and compressibility effects. So parallel face slider bearings can not be used with gases. Leaving the parallel face slider bearings, they can be classified in five categories:

1. Pivoted Pad Type.
2. Fixed Inclined Pad Type.
3. Rayleigh Step Type.
4. Hydrodynamic Pocket Type.
5. Grooved Type.

The theory of pad type bearing is the simplest and the most fundamental in hydrodynamic lubrication. The first theoretical work on gas lubrication was done by Harrison (2)*in 1913. Harrison considered an infinitely long bearing along with isothermal pressure-density relationship. In short, he solved equations 6 to 10 with the following boundary conditions:

$u = U$ at $z = 0$ and $u = 0$ at $z = h$

After applying these boundary conditions to equations 6 to 10, we get:

(See appendix 1) $$\frac{dp}{dx} = \frac{12\mu}{h^3}\left[\frac{Uh}{2} - \frac{K}{\rho}\right] \qquad \text{------------(1.2)}$$

This equation can be integrated to obtain the pressure-profile, if we can substitute 'h' as a function of 'x'. In case of pivoted pad bearings, 'h' is a linear function of 'x' and so we can obtain the pressure-profile, from which load, friction and other characteristics may be calculated. Although mathematics of the pad bearing solution is simple, the computation of numerical cases from Harrison's solution is extremely difficult, because the pressure is found to be

*The numbers in the parentheses refer to the numbers in the Bibliography Part I.

contained implicitly in difficult transcendental equations. A few cases have been worked out by Ford et al (3), whose results are shown in figure 1.1. This equation was solved by perturbation methods (to be described later) by Mow and Saibel (4) for pressure distribution and load capacity. Their results are shown in figures 1.2 and 1.3.

Ausman (5) derived the equation relating pressure and film thickness for finite bearings with polytropic expansion and compression which he solved for journal bearings. This is loosely called Reynold's equation for compressible fluids and we will also use this name in the thesis. Reynold's equation can be obtained from equations 1 to 6 by applying the following boundary conditions: (See Appendix 2)

Reynold's Equation: $\frac{\partial}{\partial x}\left[p^{1/k} h^3 \frac{\partial p}{\partial x}\right] + \frac{\partial}{\partial y}\left[p^{1/k} h^3 \frac{\partial p}{\partial y}\right] = 6\mu U \frac{\partial}{\partial x}\left[p^{1/k} h\right]$ ----1.9

Boundary Conditions: $u = U\,;\ v = 0 \quad at \quad z = 0$

$u = 0,\ v = 0 \quad at \quad z = h$

The Reynold's equation has been solved by perturbation method by Mow and Saibel (4). Their results are shown in figure 1.4. However, like all perturbation solutions, the solution is accurate only for small values of E.

In the case of a stepped thrust bearing, the usual difficulties of the pressure solution outlined in the foregoing are largely overcome, that is, the overall qualitative structure of the pressure and

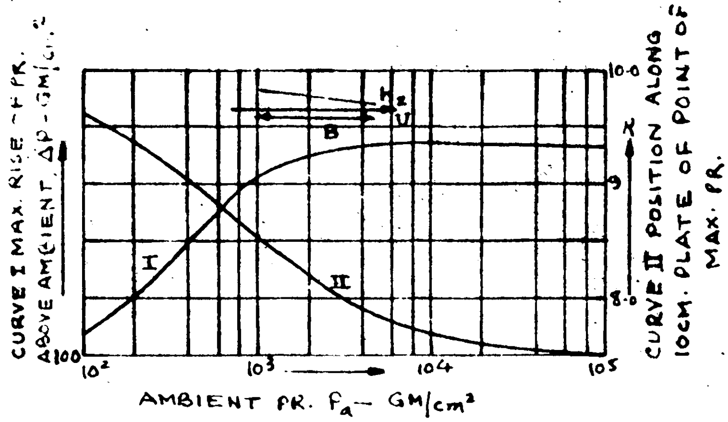

$B = 10$ cm. $h_1 = 3\times10^{-3}$ cm. $h_2 = 10^{-3}$ cm. $U = 2\times10^{3}$ cm/sec.

$\mu = 1.67\times10^{-7}\ \frac{gm.\ sec}{cm^2}$

Results.

r_i = Max. Pr. Ratio for incompressible case
r_c = " " " compressible case.
ΔP_i = Max. Pressure Rise in in-compressible Case.
ΔP_c = " " " " compressible Case.

P_a	G	$a(a-1)G$	r_i	r_c	ΔP_i	ΔP_c	$P_a h_1$
100	200	0.03	9.33	2.69	833	169	0.3
1000	20	0.3	1.83	1.72	833	720	3.0
10,000	2	3.0	1.08	1.08	833	830	30

Pressures in gms/cm².

FIGURE (1.1) - THEORETICAL RESULTS FOR SELF-ACTING. THRUST BEARINGS (FORD, ET AL)

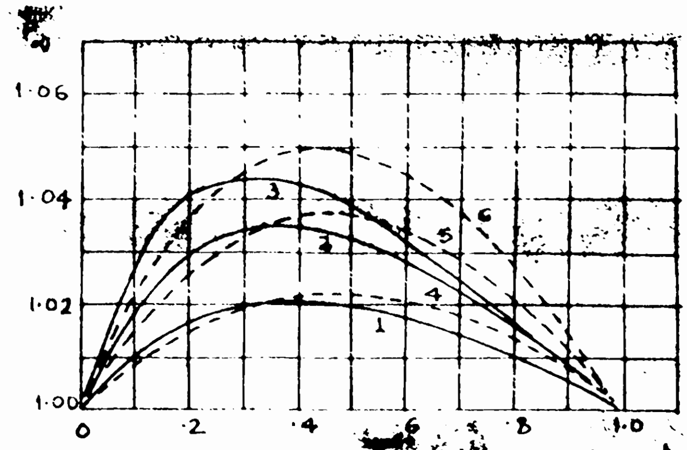

GRAPH OF $\bar{P}_\infty$ VS. $\bar{x}$ at $E = (\cdot 1, \cdot 2, \cdot 3)(\frac{h_2}{B})$ and $G = 2$

1. $E = \cdot 1\,(\frac{h_2}{B})$ } comp.
2. $E = \cdot 2$ (")
3. $E = \cdot 3$ (")

4. $E = \cdot 1\,(\frac{h_2}{B})$ } incomp
5. $E = \cdot 2$ (")
6. $E = \cdot 3$ (")

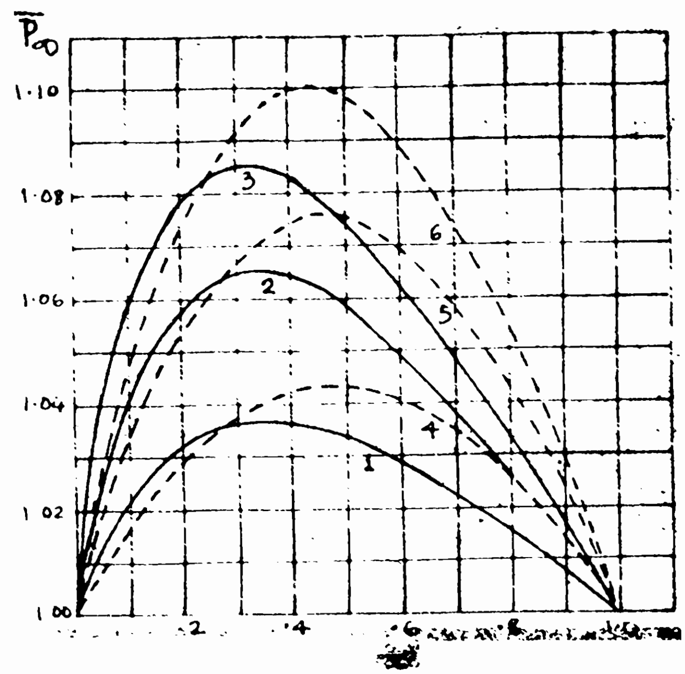

Graph of $\bar{P}_\infty$ vs $\bar{x}$ at $E = (\cdot 1, \cdot 2, \cdot 3)(\frac{h_2}{B})$ and $G = 4$

1. $E = \cdot 1\,(\frac{h_2}{B})$ } comp.
2. $E = \cdot 2$ (")
3. $E = \cdot 3$ (")

4. $E = \cdot 1\,(\frac{h_2}{B})$ } incomp.
5. $E = \cdot 2$ (")
6. $E = \cdot 3$ (")

FIGURE 1.1·2 - MOW'S SOLUTION FOR INFINITE WIDTH SLIDER BEARING

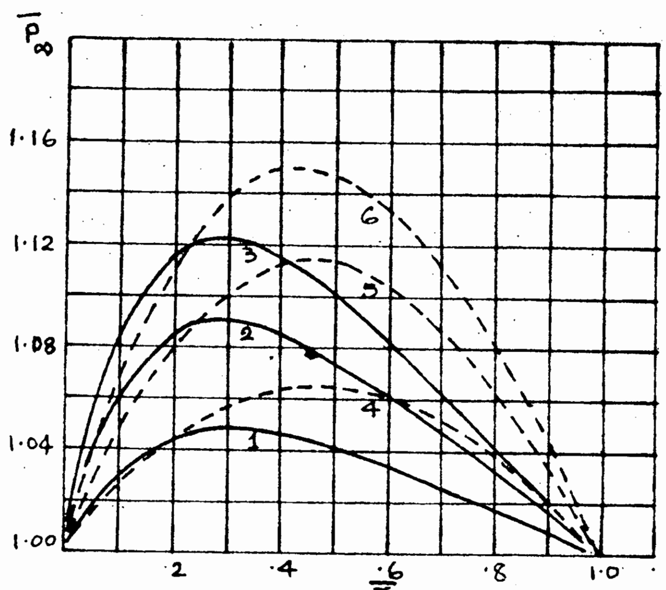

Graph of $\overline{P}_\infty$ vs $\bar{x}$ at E $(\cdot1, \cdot2, \cdot3)(\frac{h_2}{B})$ and G = 6

1. E = ·1 $(\frac{h_2}{B})$, 2. E = ·2 (″), 3. E = ·3 (″) } Comp.

4. E = ·1 $(\frac{h_2}{B})$, 5. E = ·2 (″), 6. E = ·3 (″) } incomp.

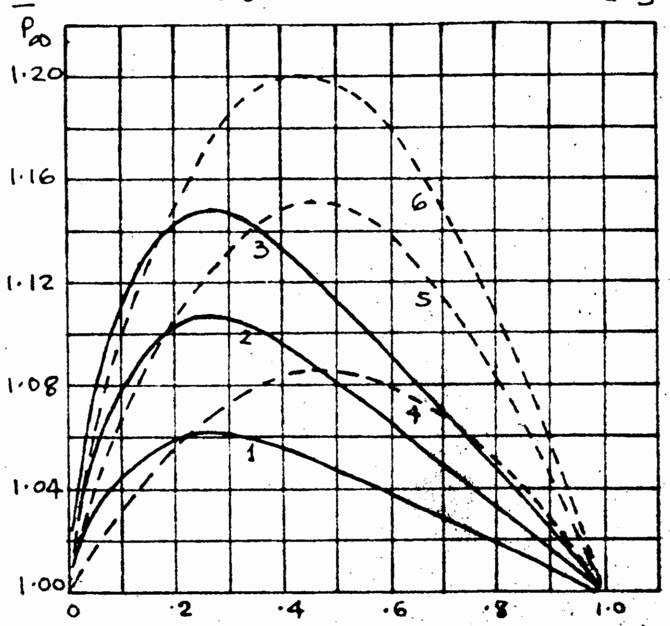

Graph of $\overline{P}_\infty$ vs $\bar{x}$ at E = $(\cdot1, \cdot2, \cdot3)(\frac{h_2}{B})$ and G = 8

1. E = ·1 $(\frac{h_2}{B})$, 2. E = ·2 (″), 3. E = ·3 (″) } Comp.

4. E = ·1 $(\frac{h_2}{B})$, 5. E = ·2 (″), 6. E = ·3 (″) } incomp.

FIGURE (1·3) – MOW'S SOLUTION FOR INFINITE WIDTH SLIDER BEARING.

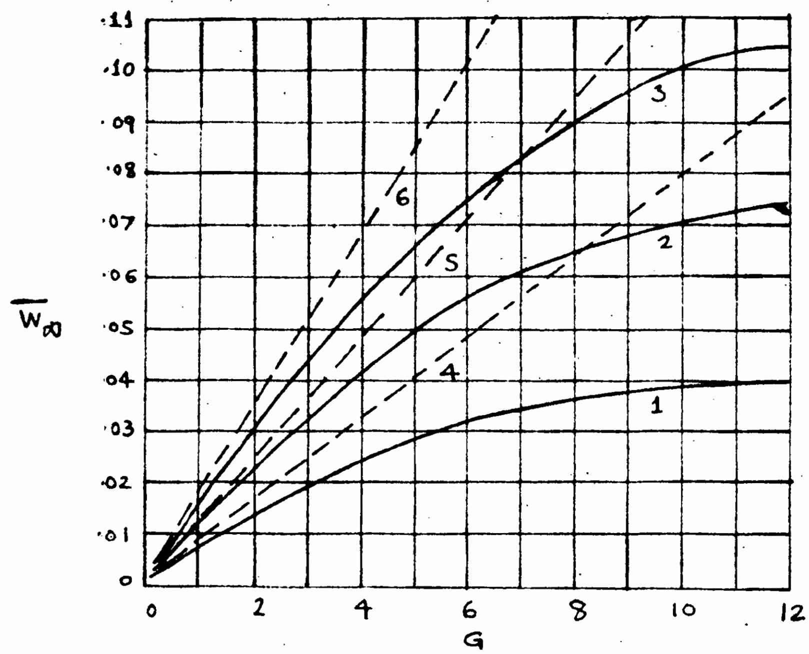

Graph of $\overline{W}_\infty$ vs G at E = (·1, ·2, ·3)$(\frac{h_2}{B})$

1. E = ·1 $(\frac{h_2}{B})$, 2. E = ·2 (″), 3. E = ·3 (″) — Comp.

4. E = ·1 $(\frac{h_2}{B})$, 5. E = ·2 (″), 6. E = ·3 (″) — incomp.

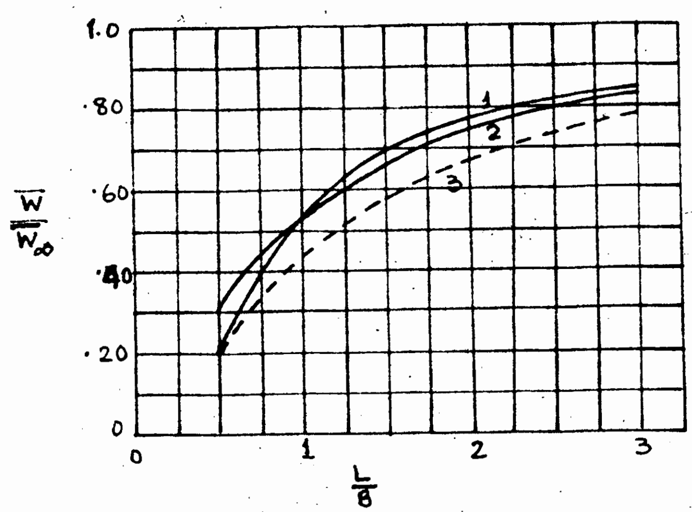

Graph of $\frac{W}{\overline{W}_\infty}$ Vs. $\frac{L}{B}$ at G = 2 and G = 8

1. G = 8, E = ·3 $(\frac{h_2}{B})$ Comp.
2. G = 2 E = ″ ″
3. E = 1.0 incomp.

FIGURE(1.4) MOW'S SOLUTION FOR FINITE SLIDER BEARING.

load, optimum design parameters and design curves can be determined with relative ease. The simplification is obtained due to the fact that the film thickness is constant in different regions as shown in figure 1.5. Kochi (6) has presented a graphical method of solving equation 1.2 for infinite width bearings. He also presented two design curves (figure 1.5) from which an optimum design for load can be obtained. He has introduced the following new variables in plotting these curves:

$$G = \frac{3\mu UL}{P_a \Delta^2}, \quad \eta = \frac{c_1}{L} \quad \text{and} \quad s = \frac{h_2}{\Delta}$$

However, this design does not take into account the effects of end flow in finite bearings. These effects can be accounted for by means of "end flow factors" which can be calculated by solving Reynold's equation by a method which will be shown in the journal bearings section. However, no such curves are available for the present.

The theory and application of Hydrodynamic Pocket Bearings was developed by Drescher (7). His theoretical analysis predicts pressure rise, friction moment, thickness of air film, and permits the selection of optimum dimensions. But his original paper could not be obtained to present the outline of his theory.

The hydrodynamic theory of grooved thrust bearing is extremely complicated. This has been dealt fully by Whipple (8), who has derived the results given in table I for the essential design parameters for maximum pressure rise within the bearing.

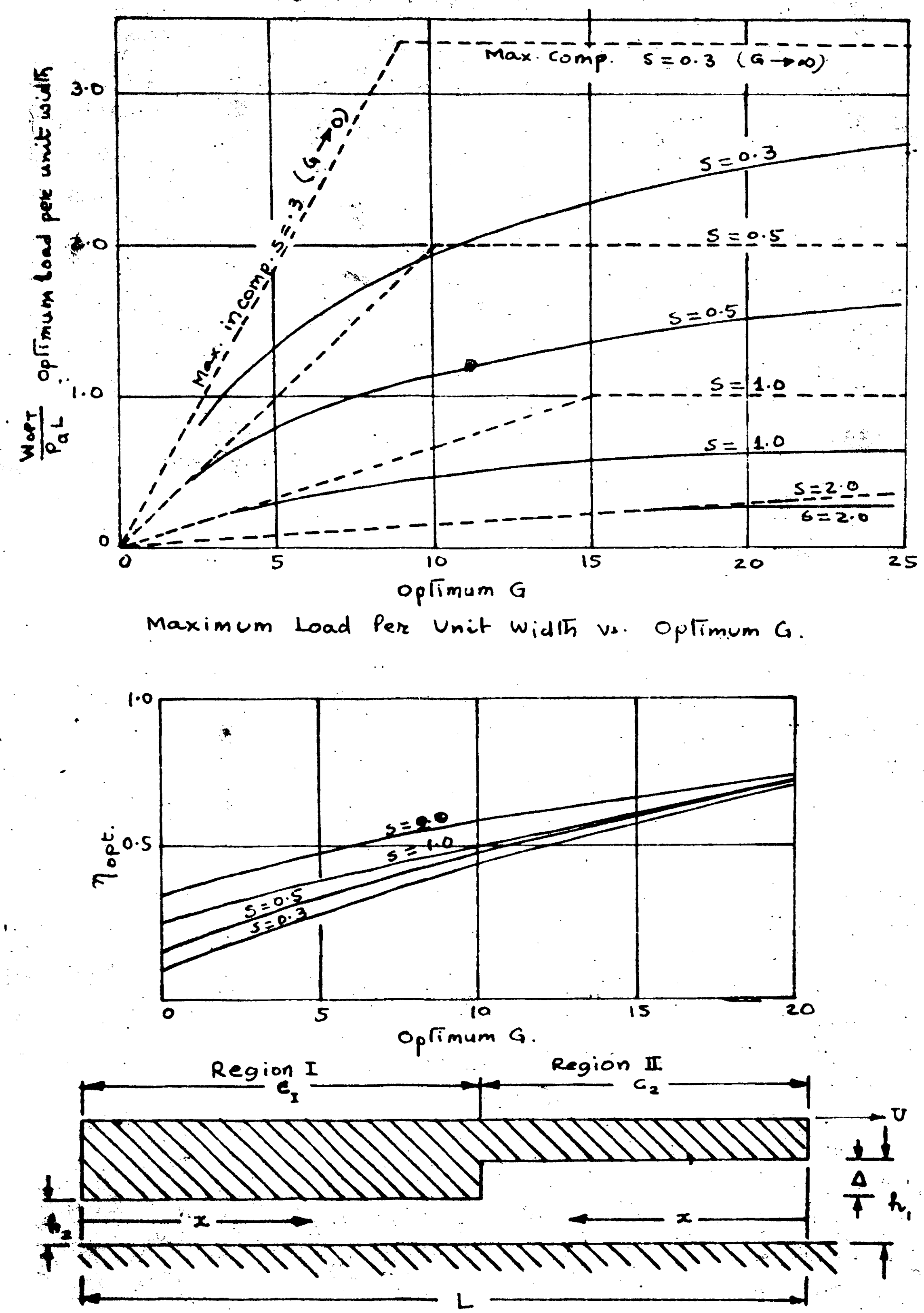

FIGURE (1.5) - KOCHI'S RESULTS FOR RAYLEIGH STEP BEARING.

TABLE I

DESIGN PARAMETERS FOR MAXIMUM PRESSURE RISE

Parameter	Value for Bearing Type	
	Herringbone Type	Spiral Grooved Type
θ	76°	72°
δ/h	2.6	3.05
$b/b+c$	-	0.7
a_1/a_2	1.0	1.8
P	0.547y	0.374y

θ = Angle between the groove centre line and the radius of the plate.

δ = The groove depth.

P = Pressure rise.

h = Clearance between plates.

$y = \frac{Ub}{h^2}$

b = Radial width of groove belt.

c = Radial width of seal belt.

a_1 = Groove width.

a_2 = Land width.

The results for spiral groove bearing have been embodied in a form convenient for design purposes in a paper by Frotescue (9) from which figure 1.6 has been taken.

JOURNAL BEARINGS

There are three main types of journal bearings.

1. Full Bearings.
2. Partial Bearings.
3. Fitted Bearings.

All of the work done so far has been confined to full bearings and so the other types will not be discussed further. Introducing new variables (figure 1.7) β & ξ in equations 1.2 and 1.9 where $\beta = \frac{x}{r}$ and $\xi = \frac{y}{r}$ we get

$$\frac{dP}{d\beta} = \frac{12\mu r}{h^3}\left[\frac{Uh}{2} - \frac{K}{P}\right] \qquad \text{-----------------11}$$

$$\frac{\partial}{\partial\beta}\left[P^{1/k}h^3\frac{\partial P}{\partial\beta}\right] + \frac{\partial}{\partial\xi}\left[P^{1/k}h^3\frac{\partial P}{\partial\xi}\right] = 6\mu\omega r^2\frac{\partial}{\partial\beta}\left[P^{1/k}h\right] \qquad \text{-----------------12}$$

These equations give the pressure in terms of film thickness 'h'. If we substitute 'h' as a function of β we can solve the equations for pressure profile and other characteristics. In case of journal bearings 'h' can be approximated by the following equation:

$$h = c\,(1 + E\cos\beta) \qquad \text{-----------------13}$$

By substituting for 'h' in equation 11, we get Harrison's equation for journal bearing:

$$\frac{dP}{d\beta} = \frac{6\mu\omega r^2}{c^2(1+E\cos\beta)^2}\left[1 - \frac{2K}{UPc(1+E\cos\beta)}\right] \qquad \text{-----------------14}$$

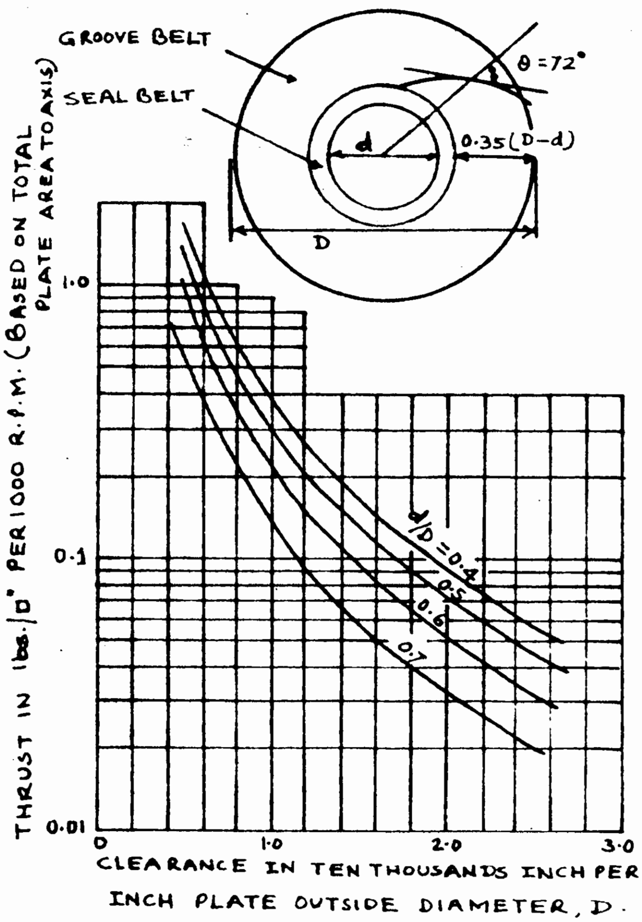

FIGURE: 1.6. GENERALIZED WHIPPLE SOLUTION FOR SPIRAL-GROOVED THRUST PLATES

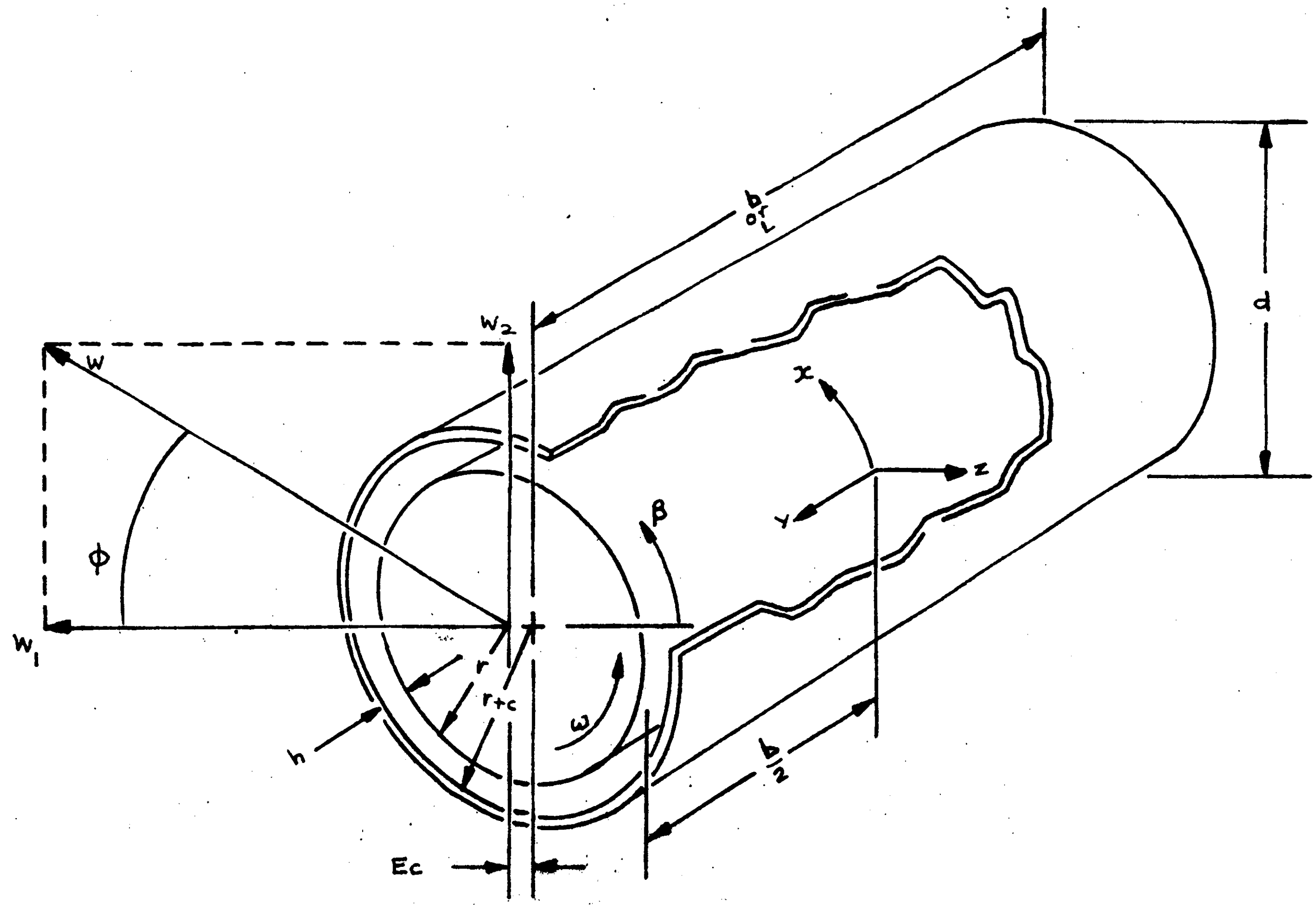

FIGURE (1·7) - FINITE JOURNAL BEARING.

Harrison could not integrate this equation analytically, but he solved some specific cases by numerical integration to compare his results with Kingsbury's (10) experimental results. To evaluate the constant of integration K, he assumed that the gas within the bearing remains constant, whether or not the bearing is rotating. Mathematically, this condition is expressed by:

$$\int_0^{2\pi} Ph \, d\beta = \text{const.}$$

His results are shown in figure 1.8 along with Kingsbury's experimental results. Harrison suggested an approximation to journal bearings which may be called "Double Wedge". This gives an approximate analytical solution for journal bearings, but the evaluation of specific cases is extremely tedious.

In 1950, Katto and Soda (11) obtained a series solution to Harrison's equation and proved convergence (see Appendix 3). In this way they were able to generate a large family of curves (figure 1.9) for infinitely long bearings. However, the large effects of side leakage on finite bearings, plus the "constant mass of gas" condition embodied in Harrison's method, limit the practical value of their results.

Scheinberg (12) avoided Harrison's (2) "constant mass of gas" condition and at the same time succeeded in evaluating the effects of end-flow on finite journal bearings. The basic steps in his method are:

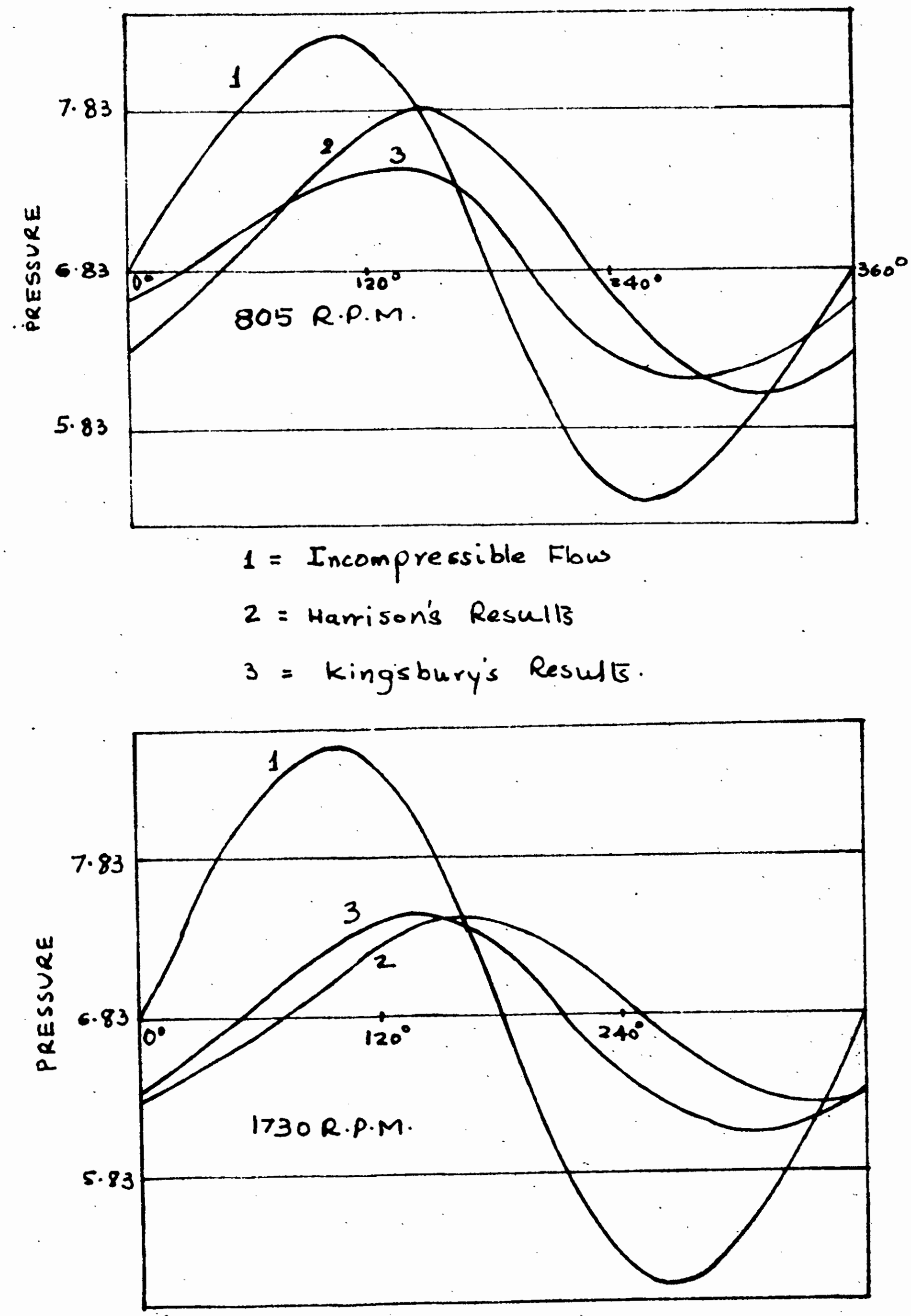

FIGURE (1·8) – HARRISON'S RESULTS FOR A JOURNAL BEARING

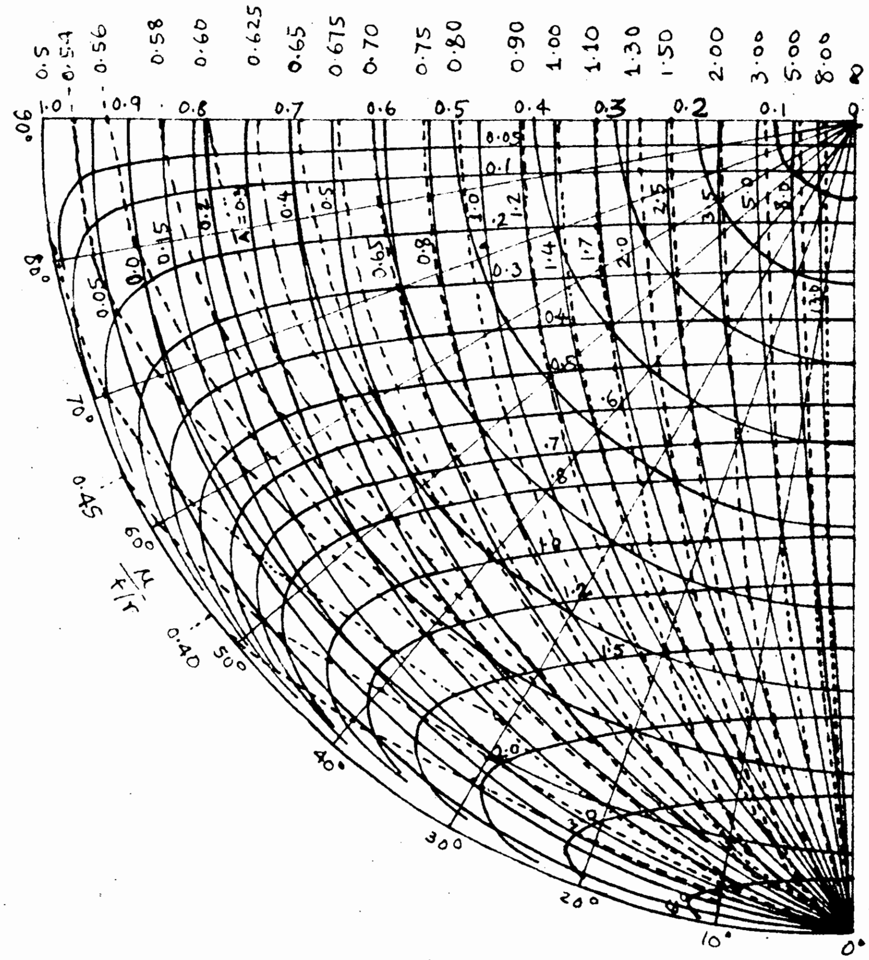

$\bar{A}' = \dfrac{\bar{A}}{\bar{P}_m}$

FIGURE (1.9) - KATTO AND SODA'S RESULTS FOR JOURNAL BEARINGS

1. An infinite length solution is obtained by numerically integrating Harrison's equation, leaving the constant of integration (initial pressure) undetermined.

2. The axial pressure is assumed to be geometrically similar, that is, independent of β , which assumption yields a condition for the determination of the constant of integration in the infinite width solution. The resulting condition is:

$$\int_0^{2\pi} P_\infty h^3 d\beta = P_a \int_0^{2\pi} h^3 d\beta = \text{const.} \qquad \text{----------------15}$$

3. The pressure distribution is assumed to be of the form

$$P - P_a = (P_\infty - P_a)\left[1 - \frac{\cosh \frac{\xi}{K_L}}{\cosh \frac{b}{K_L d}}\right] \qquad \text{----------------16}$$

in which the coefficient of leakage, K_L is determined by a mass balance (equating inflow and outflow of gas) over that portion of the lubricating film bounded by the planes $\beta = 0$, $\beta = \pi$ and the ends of the bearing. In choosing the limits of 0 to π the method is somewhat empirical. This was necessary because equation 16 is not a solution of Reynold's equation and hence does not satisfy the continuity relationships macroscopically. So to force the assumed pressure distribution to satisfy the continuity relationships, the limits had to be chosen arbitrarily on the basis of experimental results.

Assumptions 15 and 16, though not exact duplications of the true pressure distribution, are reasonably accurate, because at small values of G ($G \to 0$) they match the solution for liquid-lubricated bearings, and because the pressure distribution approaches the infinite length solution (as it should) at very high values of G ($G \to \infty$). Scheinberg was probably the first to show that at small bearing numbers ($G \to 0$) the Reynold's equation becomes the same as that for liquid lubricated bearings, while at high bearing numbers ($G \to \infty$) the finite and infinite length equations become identical.

Scheinberg's condition 15 which determines the constant of integration, is still not quite the correct one as derived by Elrod and Burgdorfer (13), but it is much closer than Harrison's "constant mass of gas" condition. Scheinberg's results are shown in figures 1.20 to 1.24.

In 1957, Ausman (5) proposed another method of solving the Reynold's equation. It is based on the assumption that the ratio of fluid pressure changes to ambient pressure is of the same order of magnitude as the eccentricity ratio. This method can be considered accurate for small values of $E < \frac{1}{2}$ but the approximation does not hold for higher values of $E > \frac{1}{2}$. For small values of E Ausman developed a perturbation solution from which he calculated load and attitude angles. (See Appendix 2) To circumvent the limitation of small E, Ausman suggested the following approach, which extends the range of usefulness:

1. To compute end-flow factors $\frac{W}{W_\infty}$ where both W and W_∞ are first

order solutions. (See Appendix 2)

2. To use these factors to modify the best available infinite width solution for end-flow effects.

In this attempt, Ausman (14) combined his finite width solution with Katto and Soda's infinite width solution to get design curves. In doing this, he assumed that the effects of end-leakage on heavily loaded bearings would be the same as on lightly loaded bearings. This assumption has no rigorous proof and the only alternative is to compare with experimental results. This was done by Ausman (15) and the comparison was quite satisfactory. The comparison will be shown in a later section.

In 1959, Elrod and Burgdorfer showed that the proper condition for the evaluation of the integration constant K in Harrison's (2) equation is:

$$\int_0^{2\pi} P_\infty^2 h^3 \, d\beta = P_a^2 \int_0^{2\pi} h^3 \, d\beta = \text{const.}$$

With this condition they have obtained a solution for infinite width bearing which seems to be the best available solution. The condition used by these authors seems to be logical, because if a comparison is made with the equation for viscous flow in thin passages, the quantity ($P_\infty^2 h^3$) seems to be the accurate representation of mass flow rather than ($P_\infty h$) as assumed by Harrison.

After getting the solution of Elrod and Burgdorfer, Ausman has plotted another set of curves, combining his finite width with their infinite width solution. In plotting these curves, he also makes an arbitrary choice for values of k to fit his results to the experimental data. He uses k = 1.4 for load calculations and k = 1 for attitude-angle calculations. These curves seem to be the best available design curves and are shown in figures 1.10 to 1.13.

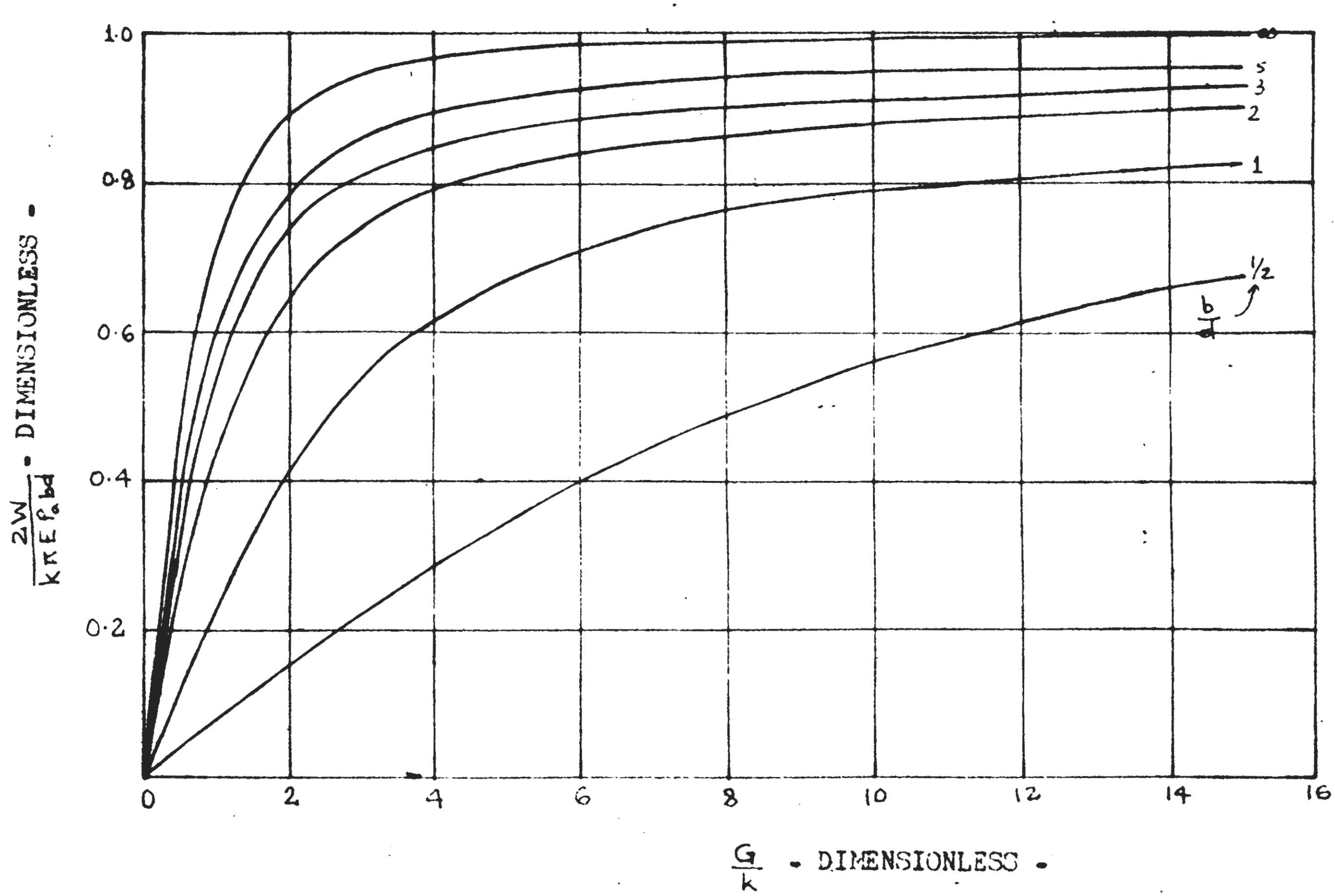

FIGURE (1.10) - AUSMAN'S DESIGN CURVE FOR JOURNAL BEARING.

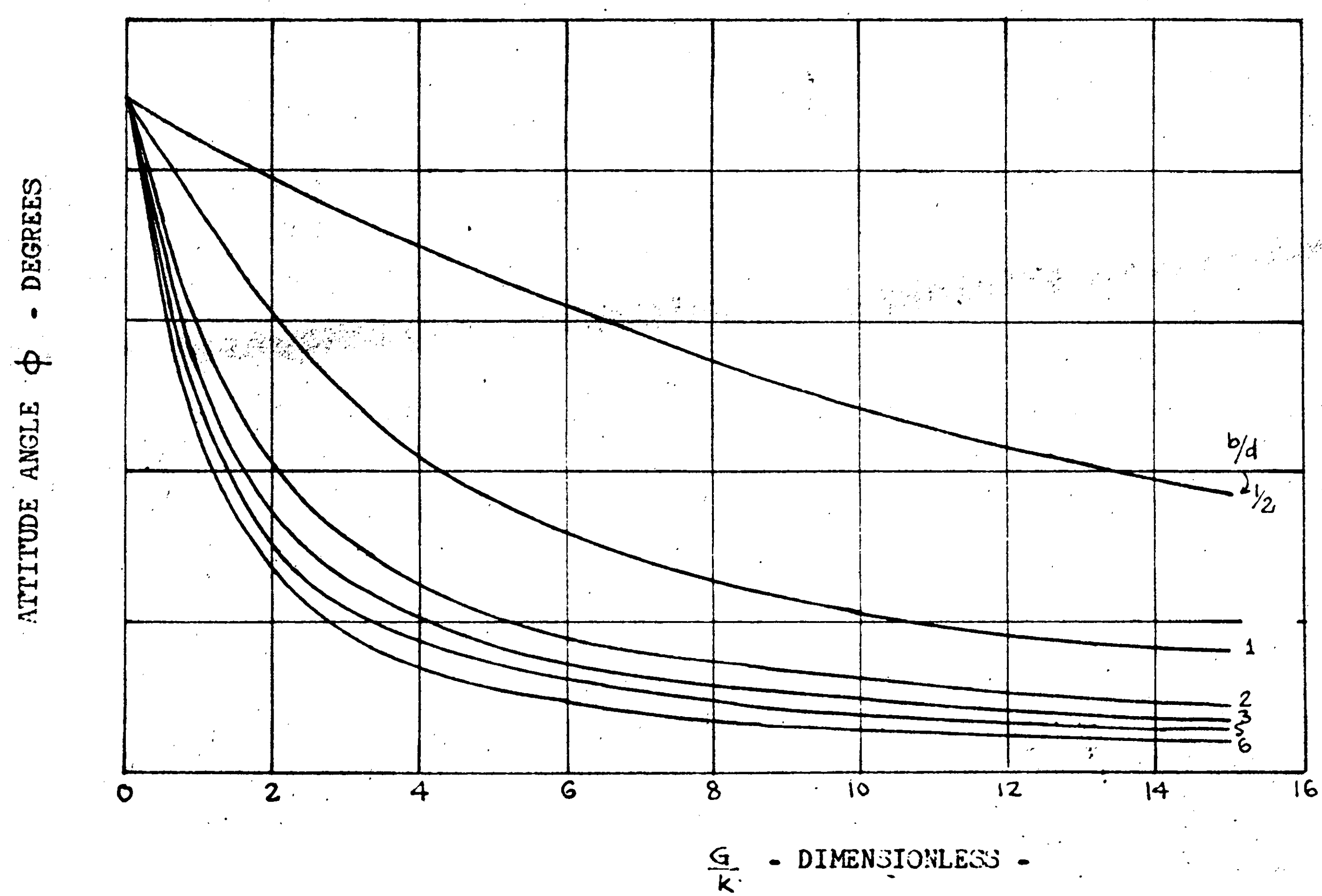

FIGURE (1·11) – AUSMAN'S DESIGN CURVE FOR JOURNAL BEARING.

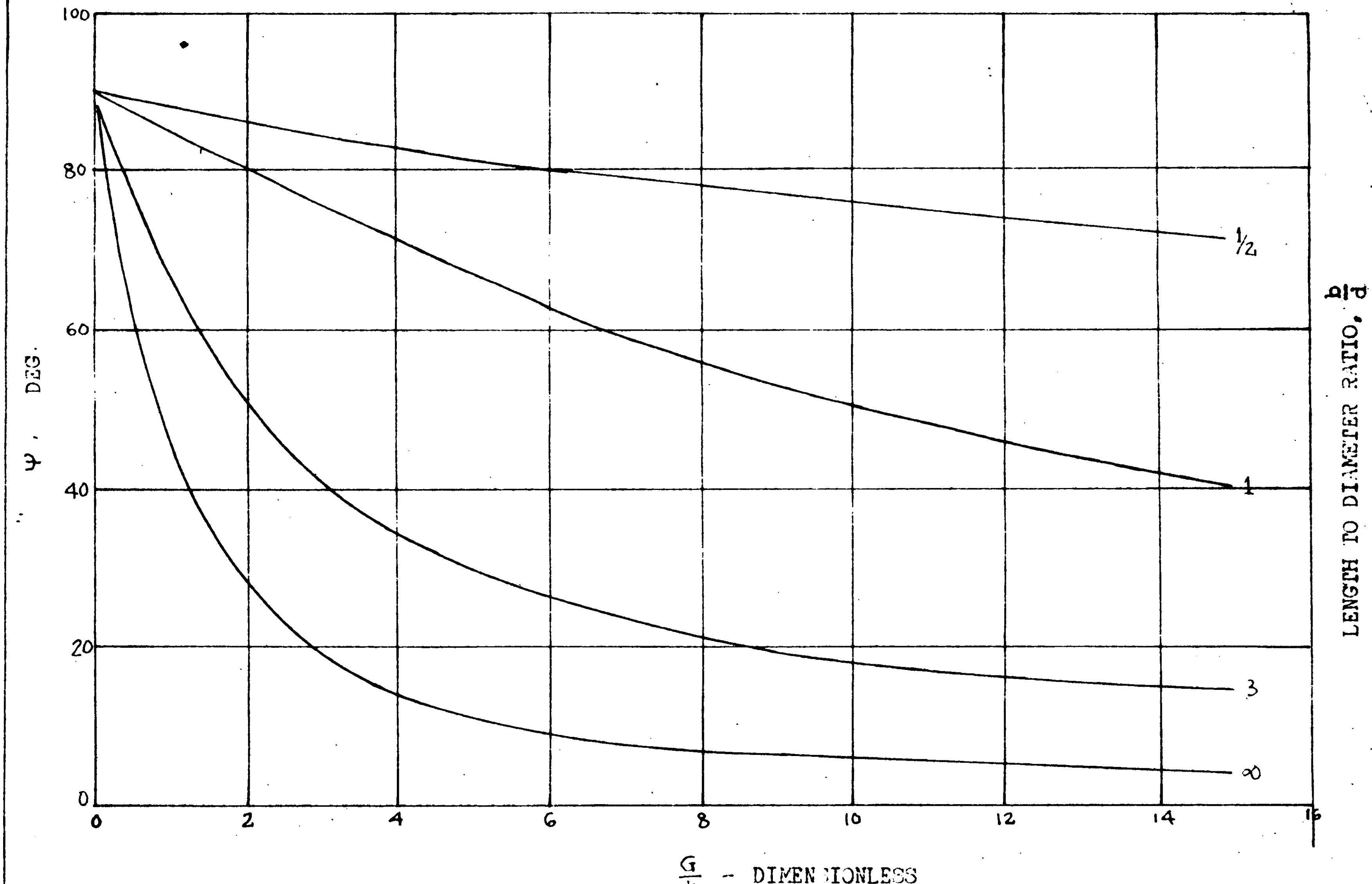

FIGURE (1·12) – AUSMAN'S DESIGN CURVE FOR JOURNAL BEARING.

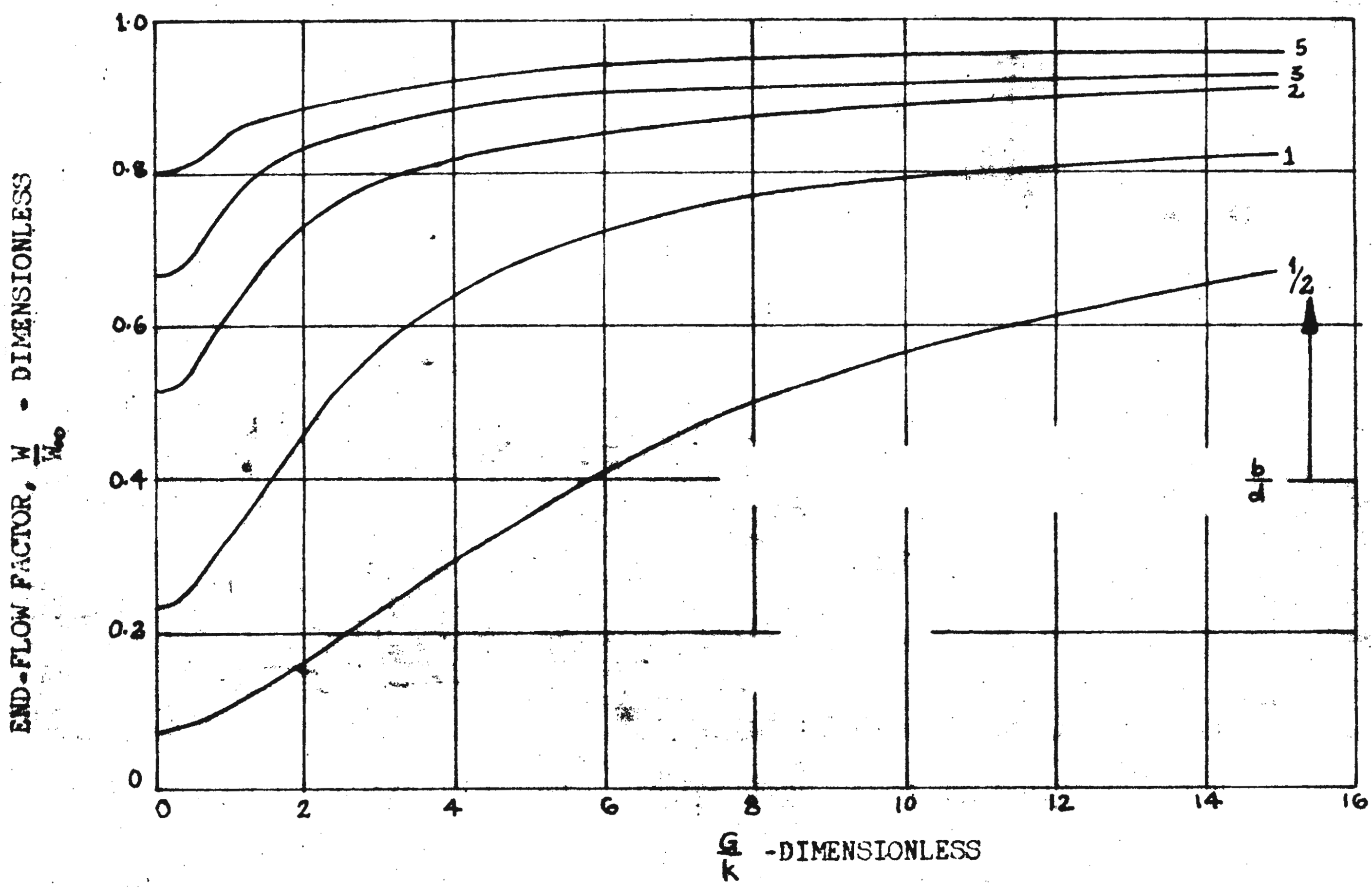

FIGURE (1.13) - AUSMAN'S DESIGN CURVE FOR JOURNAL BEARING.

2. EXPERIMENTAL RESULTS AND THEIR COMPARISON WITH THEORETICAL PREDICTIONS

Experimental work on thrust bearings is that of McNeilly (16) and Brunner et al (17). McNeilly has investigated Kingsbury's (10) thrust bearing using air as a lubricant. But his paper could not be obtained. Brunner et al have investigated the pivoted pad bearings. They have found that pivoted flat surface bearings proved unstable. The wedge-effect with air as the lubricant apparently is too weak to support much of a load. The wedge was thus magnified by investigating a cylindrical convex surface slider. This improved significantly the stability and increased load carrying ability considerably. Maximum load capacity for a given film thickness was obtained at a crown height (chord to curve) of around 350 micro-inches. For a given minimum film thickness the angle of inclination was also found to increase with crown height. Speed tests indicated the film-thickness variation with speed for a given load is nearly linear. They also found that the isothermal flow conditions are a little closer than adiabatic.

Excellent experimental work has been done on journal bearings by Kingsbury, Ford et al (3), Wildmann (18), Scheinberg (12), and Sternlicht et al (19). Out of these the experimental results of Ford et al and Wildmann are most extensive. They used a number of different gases for lubrication. However, the original paper of

Wildman could not be obtained. His experimental results have been plotted in the comparison section along with the results of other workers.

Ford et al tested bearings from 1 inch in diameter to 7 inches in diameter, but the work on bearings larger than 2 inches is limited. The summary of their results is shown in table II. Their results are plotted in figures 1.14 to 1.16.

Sternlicht et al tested bearings of 2 inches and 2.5 inches diameter with a length diameter ratio of 1.5 at constant speed. They obtained pressure distribution curves for various axial positions. Their results are shown in figures 1.17 to 1.19. From their experiments they concluded that the turbulent incompressible case is closer than the laminar incompressible case to the compressible solution.

Dr. Ausman (15) has compared the theoretical predictions of various authors with the experimental results available so far. From earlier discussion we know that the finite bearings have been dealt with by only two authors:

a) Scheinberg's (12) solution.

b) Combined solution of Ausman and Elrod-Burgdorfer.

Ausman has plotted curves to compare the above two solutions and his first order perturbation solution with the experimental results of Kingsbury (10), Ford et al (3), Wildman (18), Scheinberg (12) and Sternlicht (19). Figure 1.20 shows some typical pressure distribution

TABLE II

SUMMARY OF EXPERIMENTAL RESULTS OF FORD ET. AL

Variable	Range of Variation	Effects and Remarks
1. Speed N	0-15000 R.P.M.	W increases with N
2. Mean radial clearance, c	$0.2\text{-}4.0 \times 10^{-3}$ inch	W increases as c decreases
3. Ambient pressure P_a	2-225 lbs. per sq. in. abs.	W increases with P_a in compressible flow
4. Viscosity	2:1 (using hydrogen and air, k = 1.41 for both)	W increases with μ
5. Ratio of specific heat k	1.11 to 1.67 (ether to helium)	Little effect, slight tendency for W to increase with k
6. Length-radius ratio L/r	1 to 8 (for r = 1 in)	P_m increases with (1/r)
7. Radius r	0.5 to 1.25 in	P_m independent of r for constant G

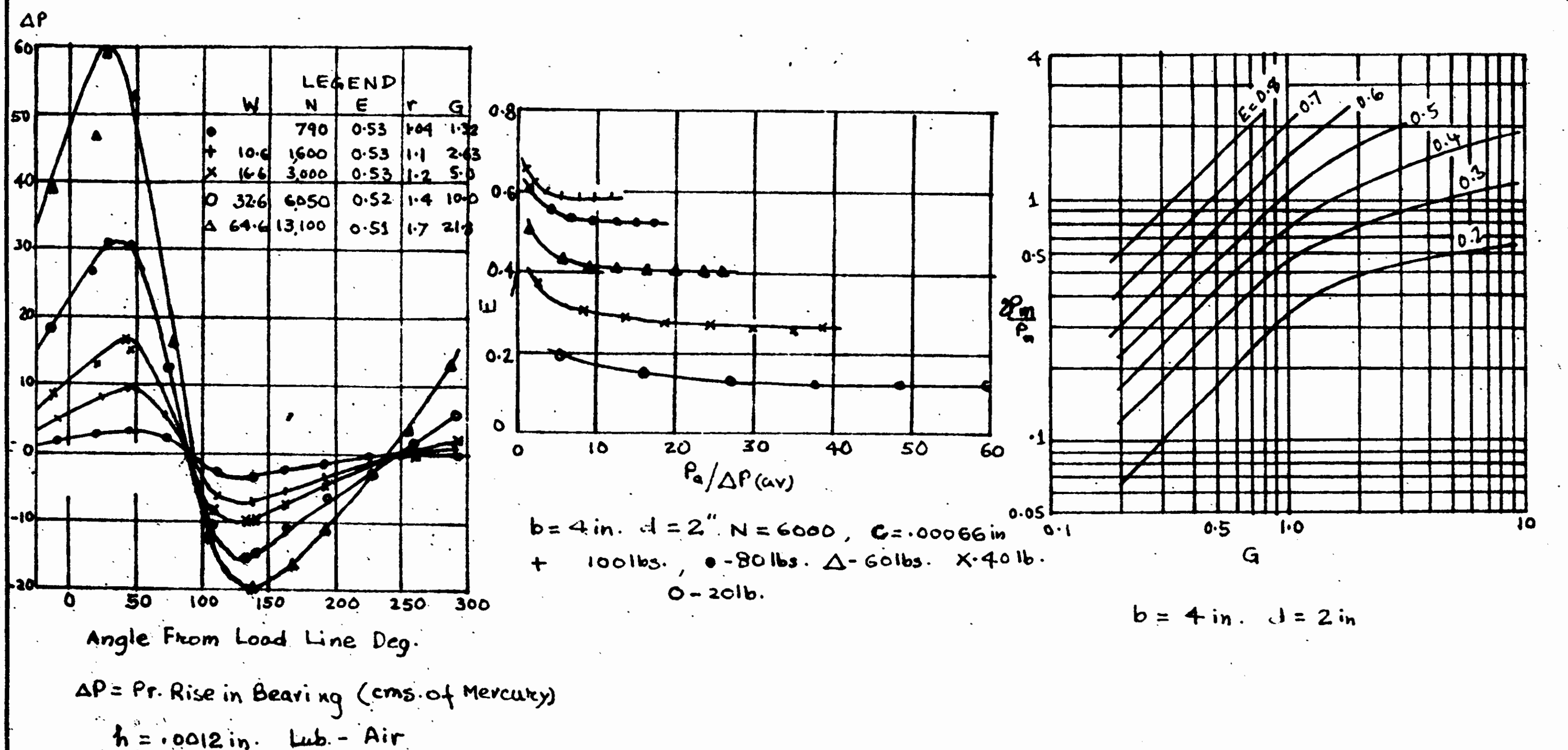

FIGURE (1·14) – EXPERIMENTAL RESULTS OF FORD, ET AL.

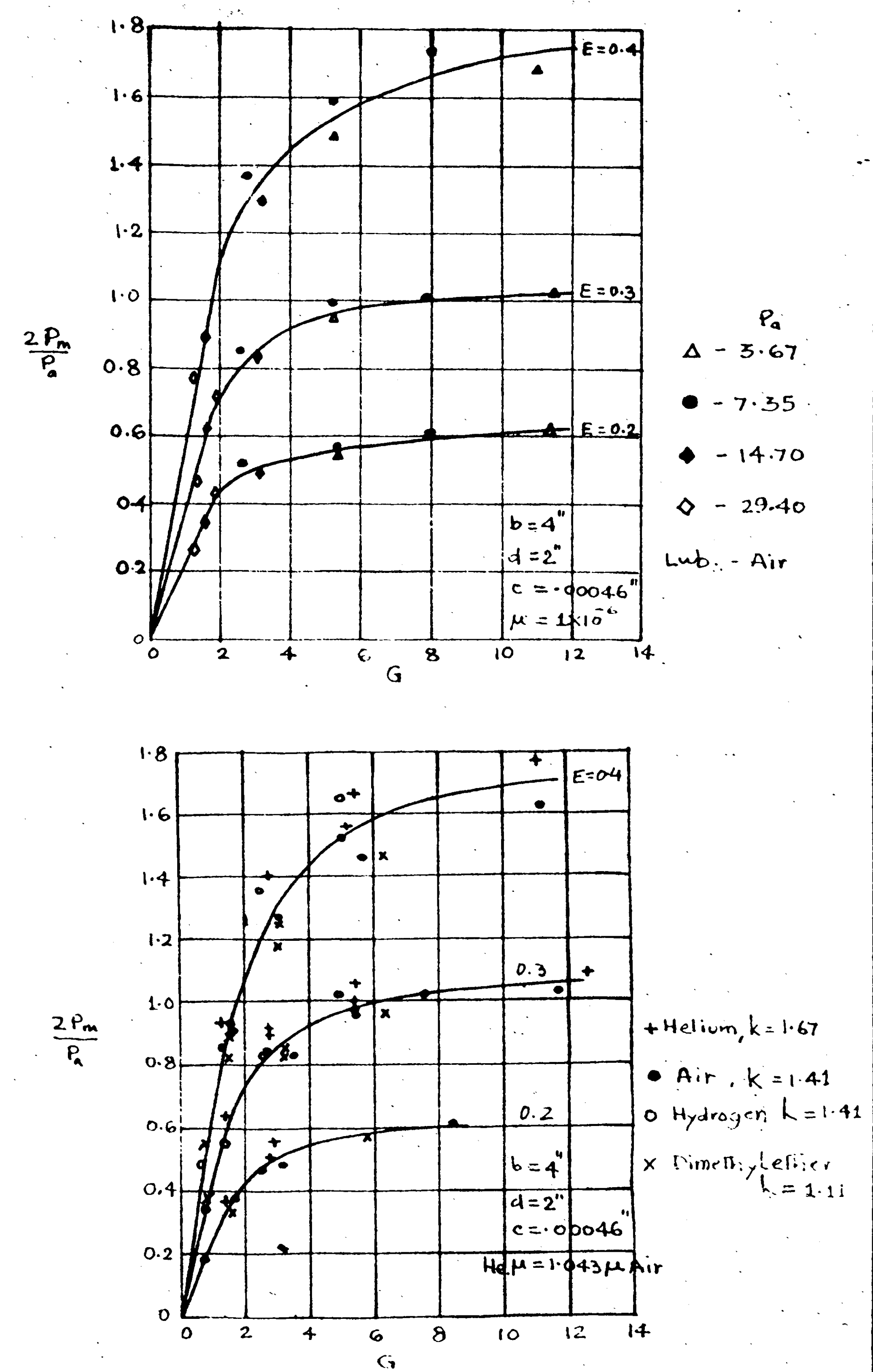

FIGURE (1·15) - EXPERIMENTAL RESULTS OF FORD, ET AL

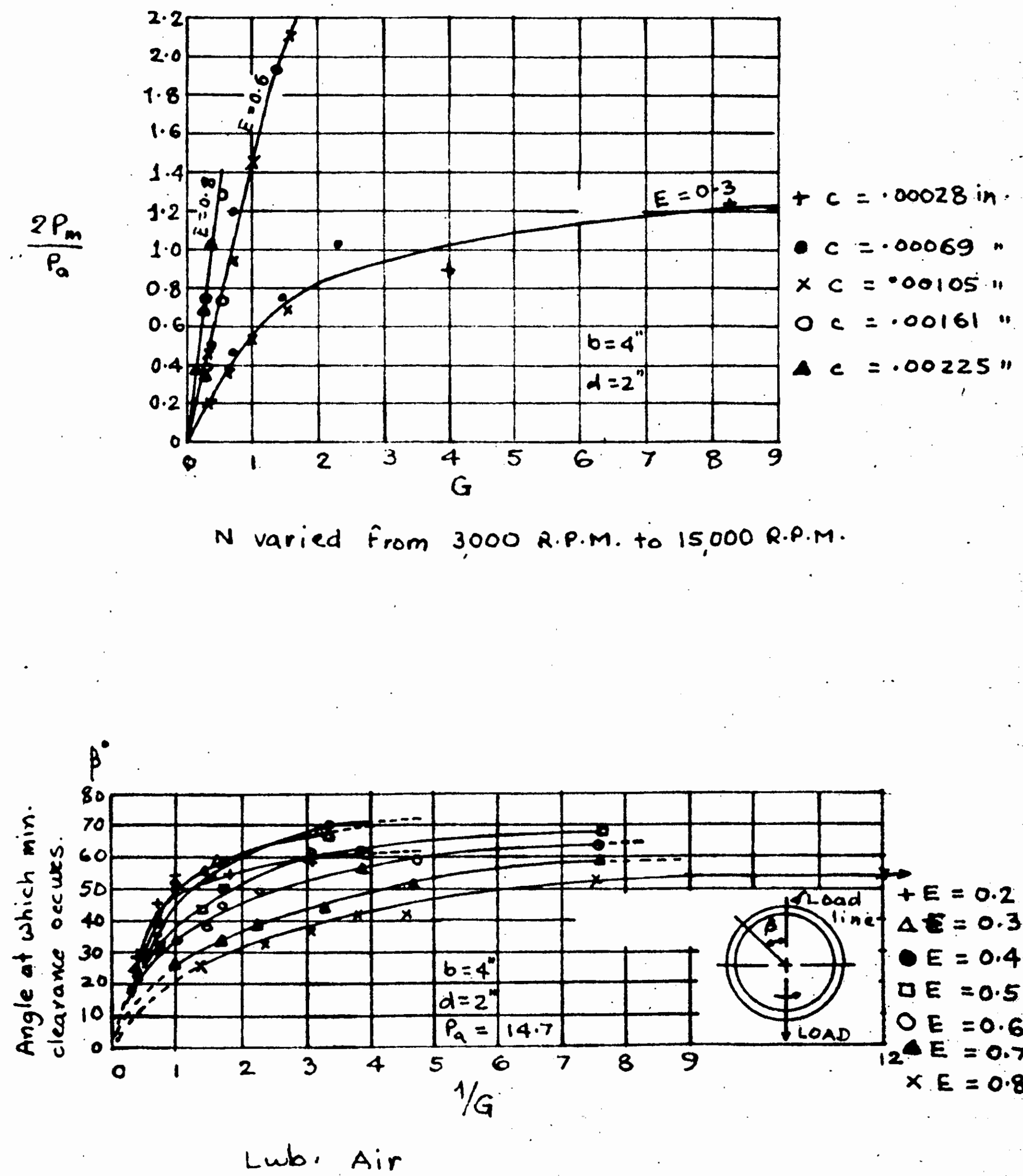

FIGURE (1.16) - EXPERIMENTAL RESULTS OF FORD, ET AL.

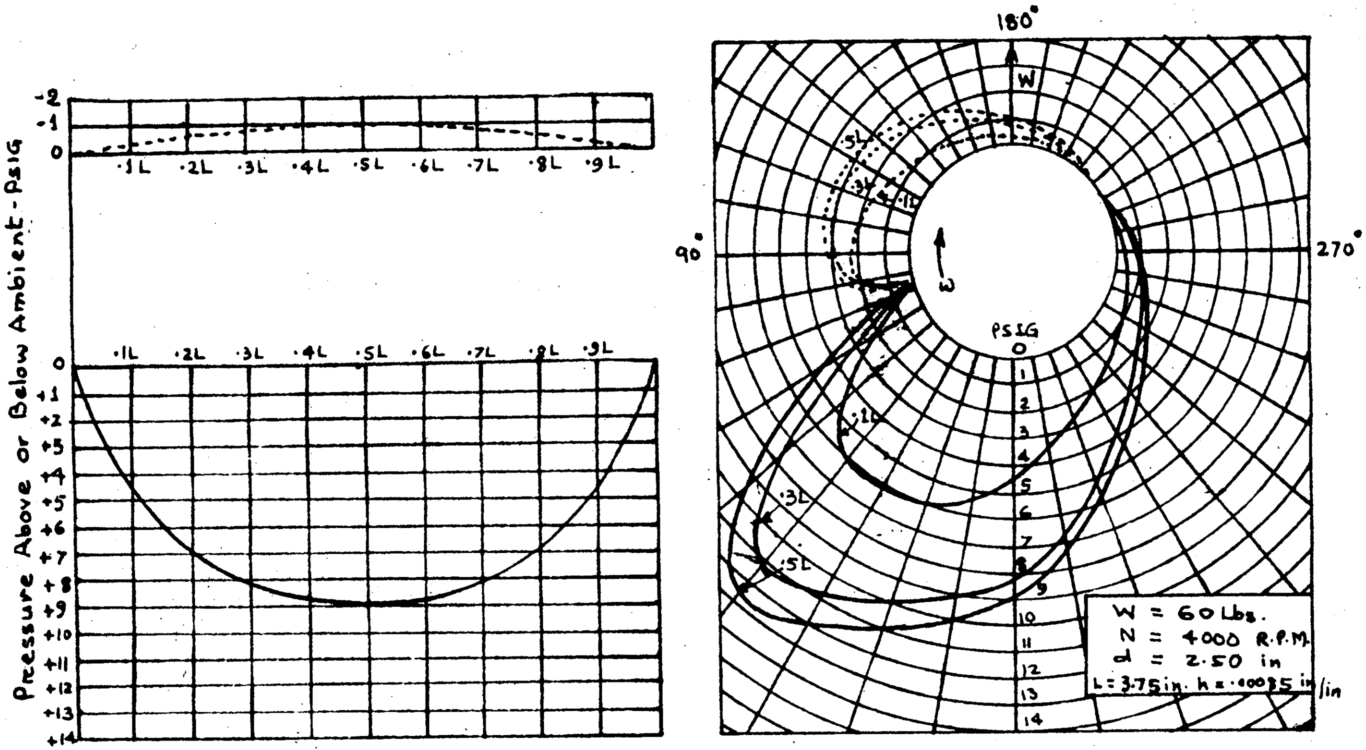

FIGURE (1·17) — STERNLICHT'S EXPERIMENTAL PRESSURE DISTRIBUTION IN A JOURNAL BEARING.

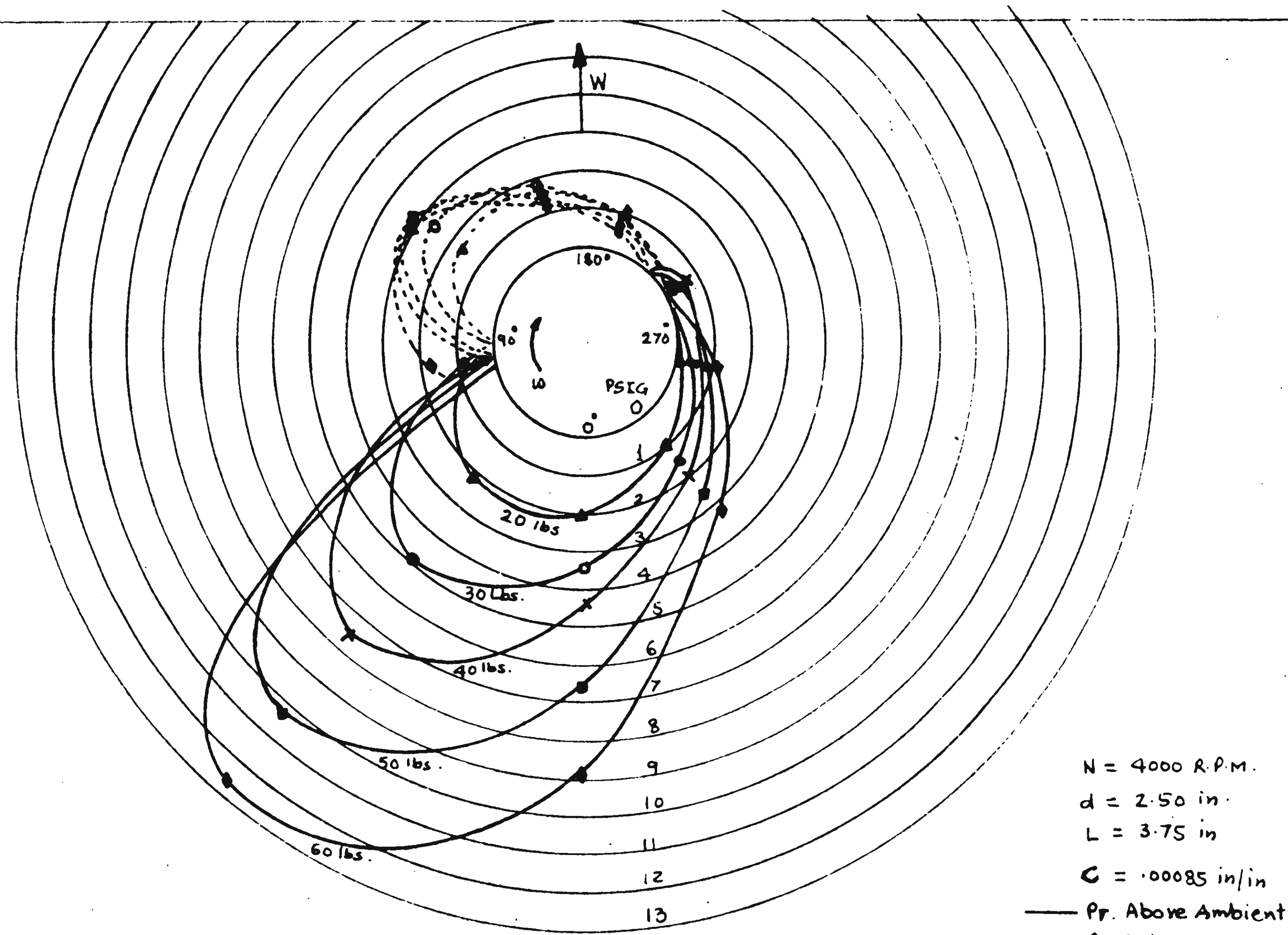

FIGURE (1.18) - STERNLICHT'S EXPERIMENTAL PRESSURE DISTRIBUTION IN JOURNAL BEARING.

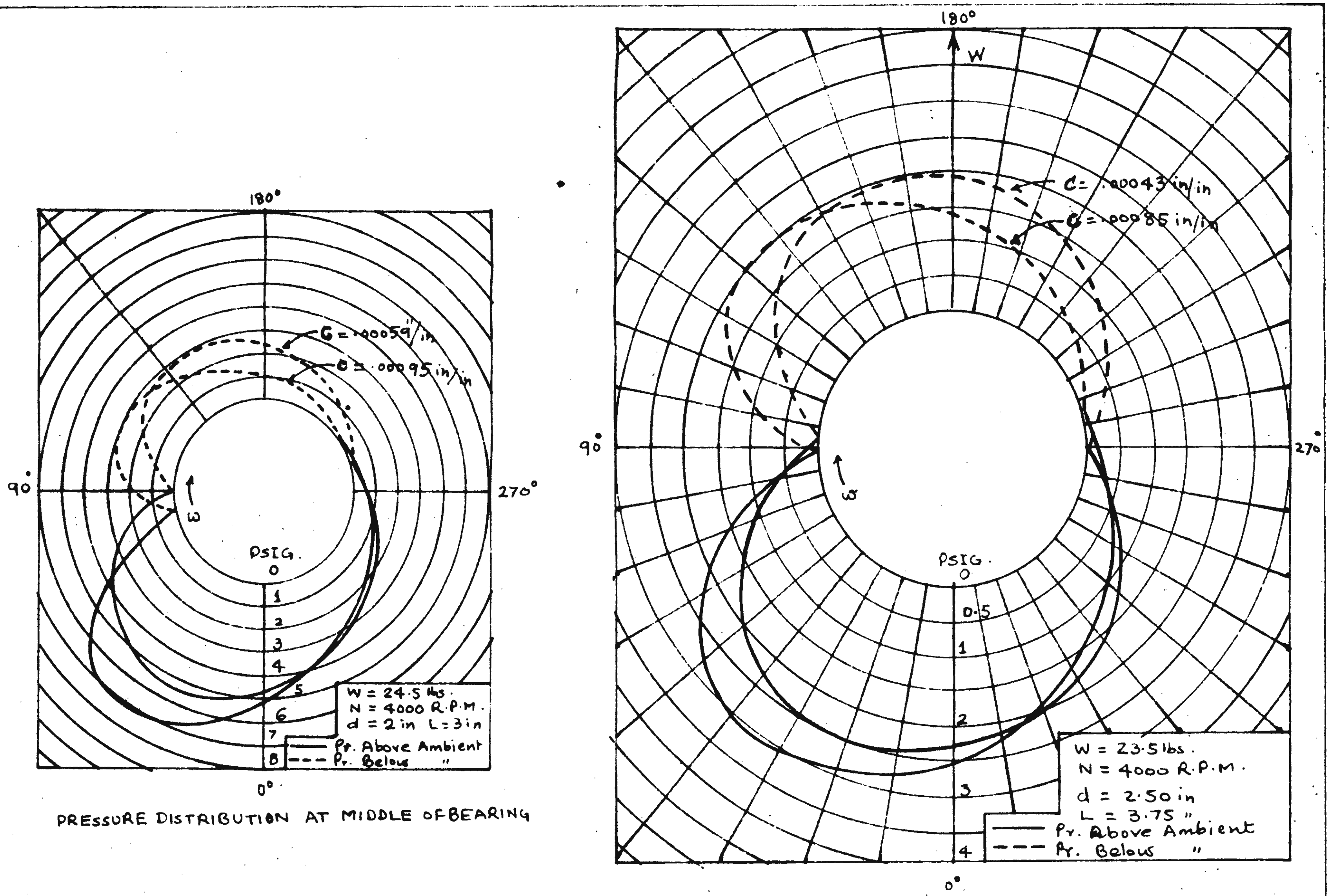

FIGURE (1.19) - STERNLICHT'S EXPERIMENTAL PRESSURE DISTRIBUTION IN JOURNAL BEARING.

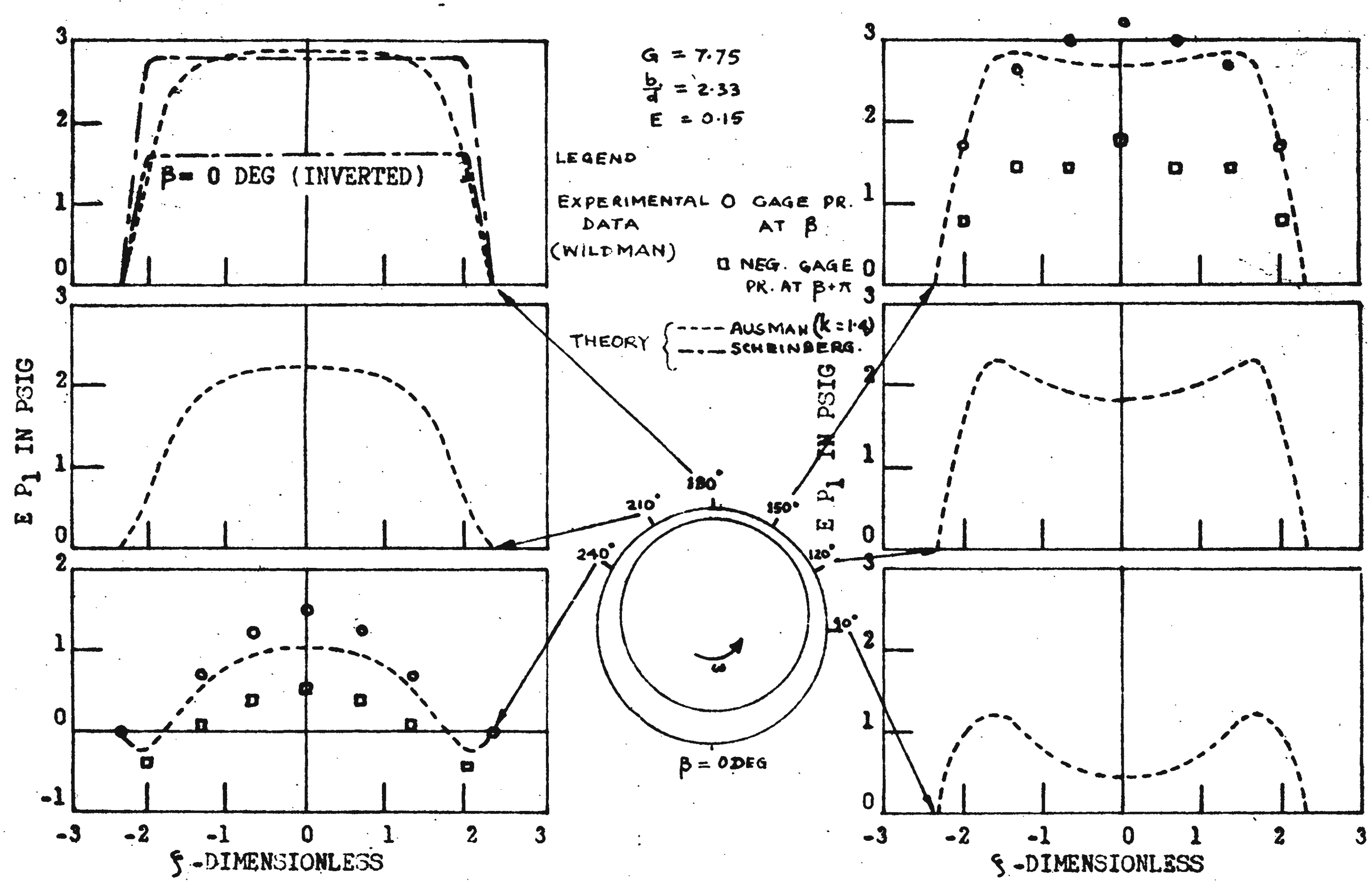

FIGURE (1.20) - COMPARISON OF PRESSURE DISTRIBUTION IN JOURNAL BEARING curves from the two theoretical solutions and Wildman's experiments. The experimental results show that the positive peak pressure is more positive than the negative pressure is negative. But Ausman's (15) first order perturbation solution gives equal peaks because the second order terms are neglected. However, the load or integrated pressure is not affected by second order terms. For this reason, the load characteristics predicted by his solution are better approximations than the pressure comparison of figure 1.20 would lead one to expect.

Scheinberg's (12) similarity assumption, though not a true representation of the actual physical behaviour, gives a reasonable approximation in the regions of peak pressures, which regions have the greatest effect on determining the magnitude of load. The asymmetry effect about the ambient pressure is included in his pressure distribution as shown in figure 1.20. The double peaking phenomenon indicated by Ausman's first order perturbation solution and substantiated by Wildman's data is not accounted for in Scheinberg's solution which is qualitatively the same as shown for $\beta = 180^\circ$ and 0° for other values of β. But this phenomenon occurs at relatively low pressures and at β values of roughly 90° away from the load line. For these reasons it may be expected that Scheinberg's solution yields good results for the magnitude of the load, but not for the attitude angle which is strongly influenced by pressure profiles in the regions 90° away from the load. This conclusion is substantiated by figure 1.24

Figures 1.22 to 1.24 demonstrate the manner in which the actual load carrying ability of the bearing increases more and more above the straight line load eccentricity characteristic predicted by first order solution. The more accurate curves of Scheinberg (12) and Ausman's (15) combined solution show better approximation. In the attitude angle versus bearing parameter curve of figure 1.24, the first order theory of Ausman is seen to be in better agreement with the experimental results of Scheinberg and Kingsbury (10). In contrast, Scheinberg's theoretical predictions yield substantially poorer results as anticipated.

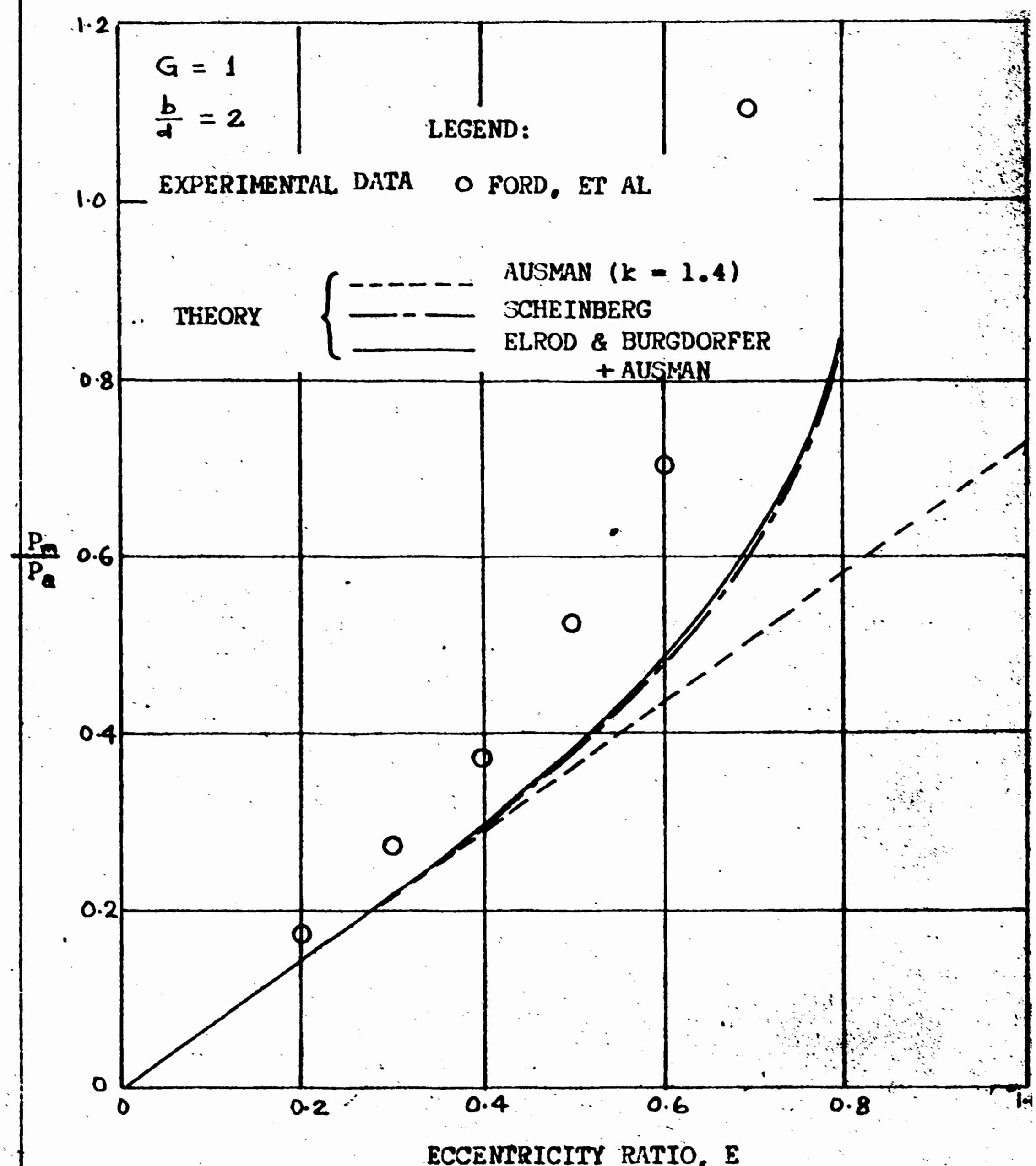

FIGURE (1·21) – MEAN BEARING PRESSURE VS. ECCENTRICITY RATIO.

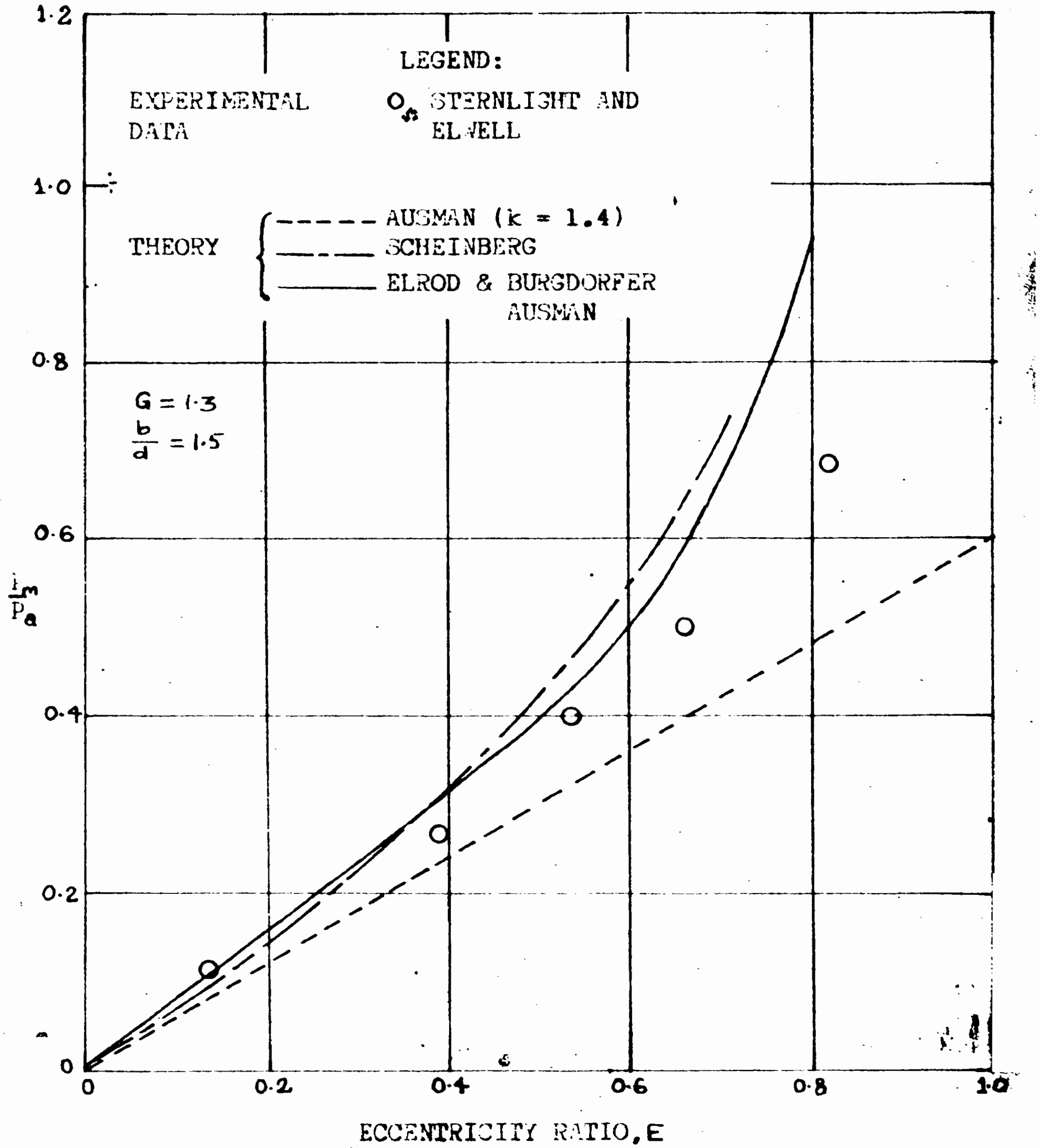

FIGURE (1·22) – MEAN BEARING PRESSURE VS. ECCENTRICITY RATIO

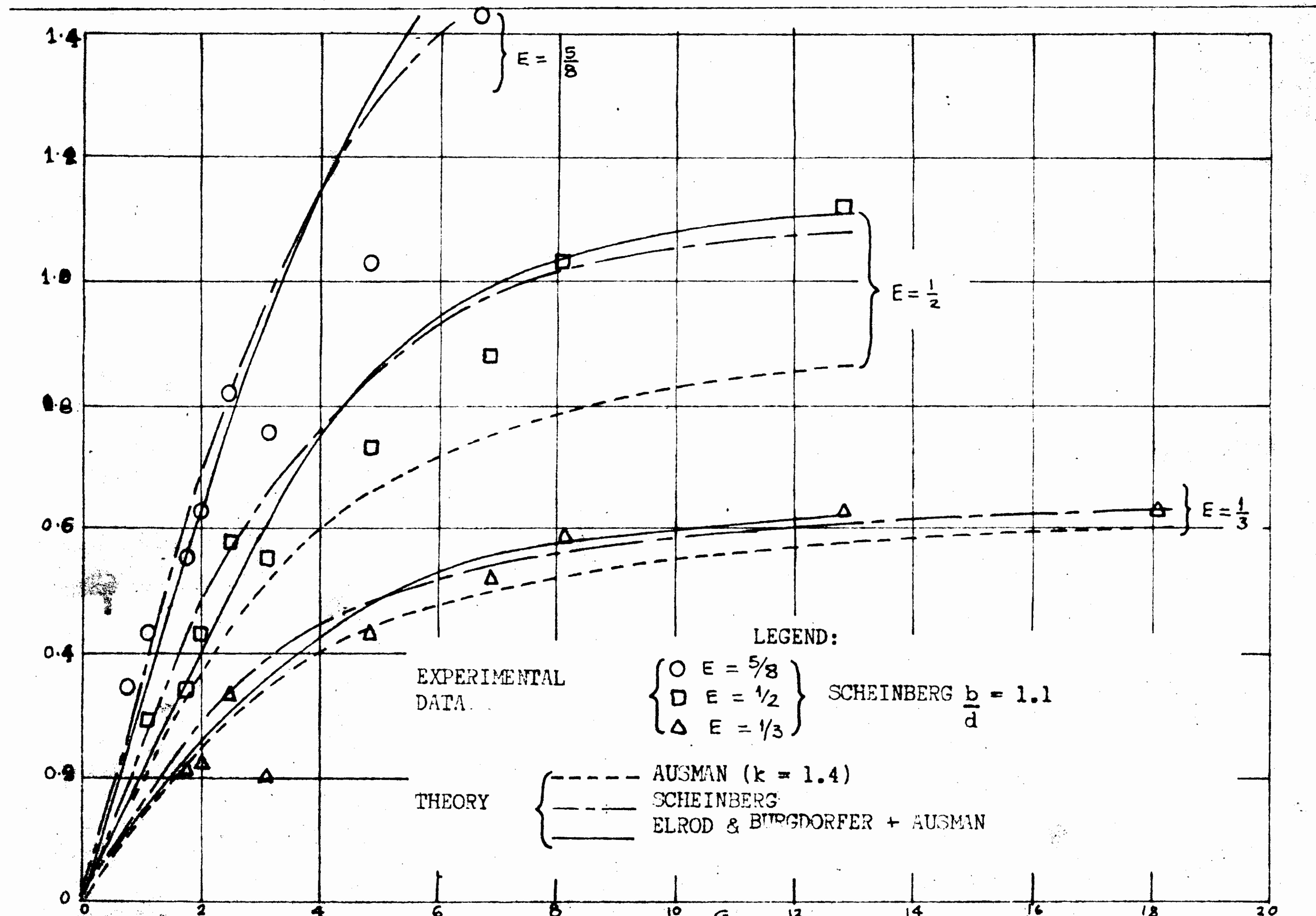

FIGURE (1.23) – MEAN BEARING PRESSURE VS BEARING PARAMETER

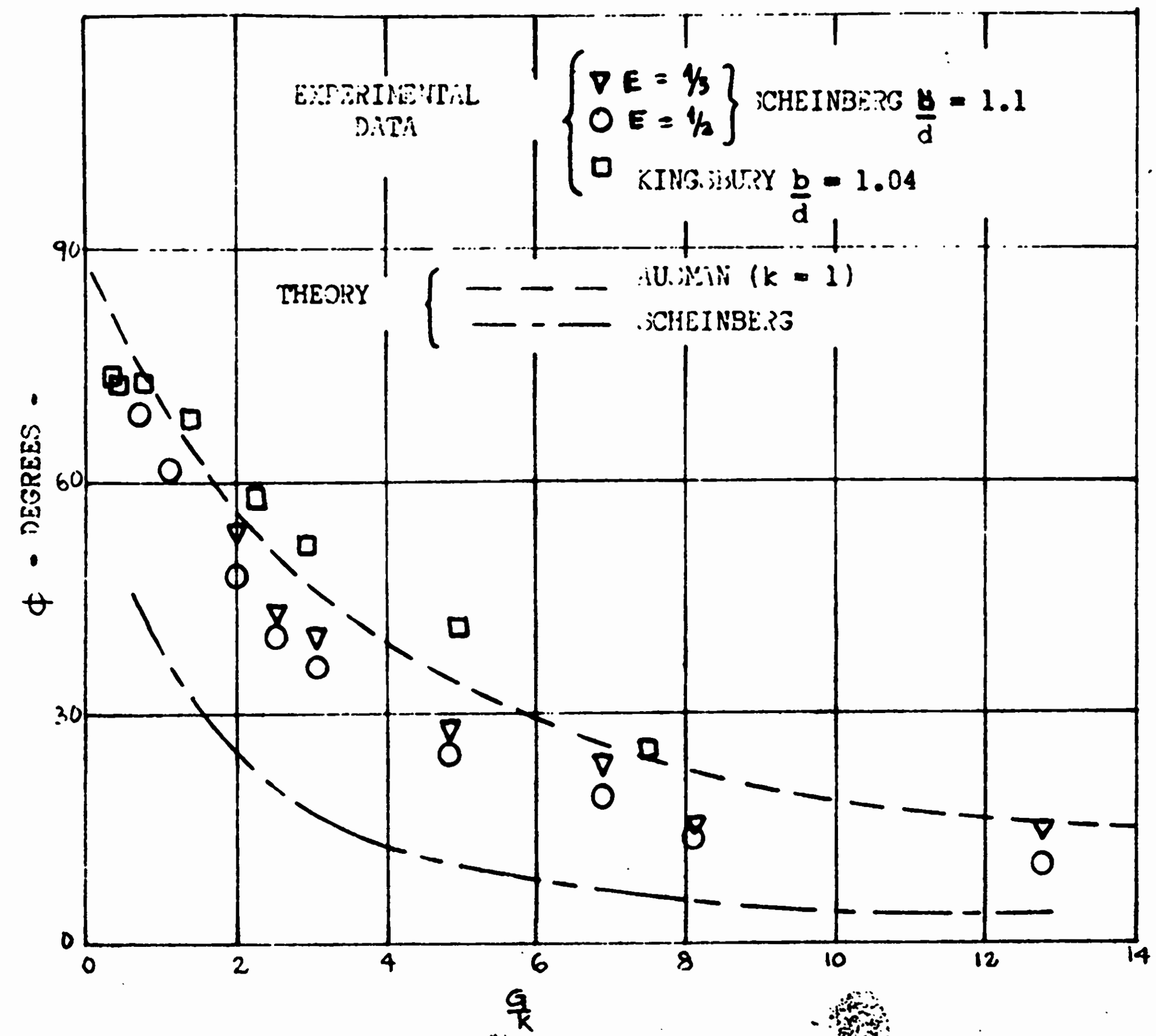

FIGURE (1.24) – ATTITUDE ANGLE VS BEARING PARAMETER

3. STABILITY

Due to the low damping characteristics of gas films, certain dynamic instabilities need to be anticipated and controlled which might have been suppressed or passed unnoticed with liquid lubricants where the damping action is greater. Pivoted pad shoes used in self acting thrust bearings have a number of instabilities of their own. Decrease in film thickness as load increases may cause a flat shoe to become parallel to the runner and the bearing becomes unable to support a load and collapses. A crowned shoe will not exhibit this tendency. Pitching, rolling and vertical bounce are other forms of shoe instability, and all of these modes of action require investigation if the application is to be completely successful. The problem of instability in thrust bearings has been analysed by Brunner et al (17) who found that crowned pads are more stable than flat pads.

In journal bearings there are two types of instabilities which may occur singly or simultaneously. They are:

1) Synchronous whirl.
2) Half speed whirl, commonly known as "oil whip" in liquid bearings.

In both types of whirl, if the motion of the whole shaft is considered it is found that whirling motion of the ends of the shaft may be in phase (cylindrical whirl) or antiphased (conical whirl). When rotational speeds are increased indefinitely or clearance decreased, attitude angle tends to zero and gas film stiffness becomes constant.

The vibrations produced under such conditions which are excited by the disturbing force due to residual unbalance in the shaft are called "synchronous whirl" because they have the same frequency as the rotating shaft. On the other hand, in lightly loaded bearings rotating under high speeds, attitude angle ϕ tends to 90° and the shaft tends to run into the "half-speed whirl."

"Synchronous whirl" has been dealt with by Brix (20) by semi-empirical methods. He has given equations for spring constant of gas films for low eccentricities ($\epsilon < 1/2$). He has recommended the following methods to avoid synchronous whirl:

1) Bearings should be spaced as far as possible in cases where the conical mode gives the lower of the two critical speeds.
2) Overhung masses should be avoided.
3) The best way to raise the lowest critical speed is to increase the film stiffness by reducing clearance, a very powerful variable.

"Half speed whirl" is usually the main source of trouble for high speed operation. It manifests itself as a vibration of the journal in the bearing clearance space with a frequency equal to half the running speed, and may be complicated by shaft elasticity if the machine is running at or above twice its critical speed. There is a much simplified qualitative explanation of this effect. In a self-acting bearing the lift is produced by the differential shearing of the fluid as it is squeezed between the converging surfaces of the bearing. The average speed of the fluid is of the order of one half the speed of the moving surface. If now the position of the wedge journal between the moving and fixed surfaces also moves in the direction of the fluid at the average speed of the fluid, no lift producing action can occur. Thus, motion of the shaft centre about the bearing centre of about half shaft speed, which produces the same effect, destroys the action of the bearing. When this phenomenon takes place in oil bearings the motion is observed to occur at between one third and one half shaft speed. In gas bearings, however, the effect has only been observed to take place at very close to half the shaft speed. By extension of existing theories Fischer et al (21) have developed a procedure for predicting and controlling half speed whirl under hydrodynamic as well as hydro-dynamic-hydrostatic operation. But their publication could not be obtained to present the details here.

The methods of suppression are similar to those used in liquid bearings and include:

1) Misalignment of bearings.
2) Reduction of bearing length and clearance.
3) Application of extra bearing load.
4) Application of asymmetric hydrostatic pressure to the bearings by means of a feed hole or groove in the bearing.
5) Use of stabilizing pockets.

However, the grooving of the bearing reduces the load capacity. Doescher (7) has described the effects of stabilizing pockets which are shown in figure 1.25 along with typical pressure distribution in the grooves. The idea of asymmetric hydrostatic loading has been used by Brewster (22) and seems to be the most powerful method of raising the threshold of whirl instability. Experiments show that modest pressures and a very small flow of gas is enough to stabilize the bearing. In the case of horizontal machines the same effect is obtained if a hole is drilled through the bearing wall in the regions where subatmospheric pressures exist. This simple device is surprisingly effective and Ford et al (3) have been able to raise the threshold of whirl instability from 5000 R.P.M. to 14000 R.P.M.

Preloaded multiple pad gas bearings do not suffer from half speed whirl instability, a fact already observed in connection with liquid lubricated pad bearings. Besides this advantage, pad journal bearings offer no better load carrying performance than plain journals and present considerable complexity in manufacture, gauging and installation.

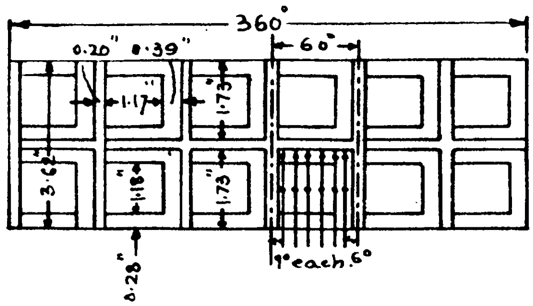

Developed contact Face of a Full Bearing shell with stabilising Recesses ·0008 inch deep.

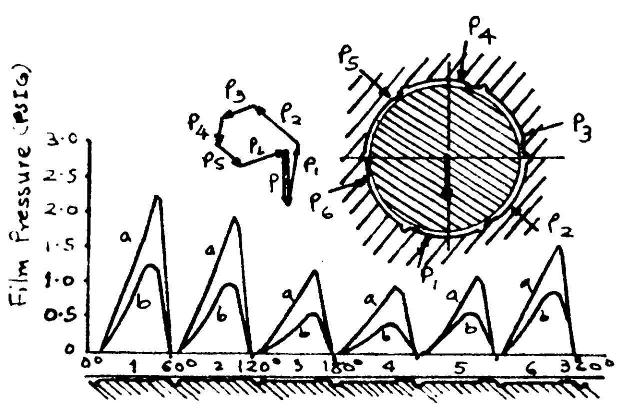

Pressure Distribution in The Developed Bearing Shell

a) Pressure distribution along centre line of recess.

b) Pressure distribution along edge of recess.

FIGURE (1·25) — EFFECTS OF STABILISING POCKETS ON THE PRESSURE DISTRIBUTION.

4. EFFECTS OF VARIOUS PARAMETERS ON THE PERFORMANCE.

SPEED:

The load carrying capacity increases with the speed in the beginning, but ultimately settles down to a constant value which depends on the ambient pressure and is independent of speed, viscosity and bearing clearance. The attitude angle also increases as the speed is increased. It is also shown by Hughes and Osterle (23) that the inertia terms can not be neglected at very high speeds. Their results show inertia effects can be significant in laminar regime. Error in load capacity depends more on speed than eccentricity ratio, amounting to 11% at 200,000 R.P.M. At low speeds inertia effects are negligible.

RATIO OF SPECIFIC HEATS:

Ford et al (3) have used various gases in their experiments. The value of k varied from 1.11 to 1.67 but they have found very little effect except for a slight tendency of increase in load capacity with k.

MEAN MOLECULAR FREE PATH:

Burgdorfer (24) has shown that the lubricating gas does not form a continuous medium in case of hydrodynamically lubricated bearings which operate mostly with narrow gap widths. The assumption of continuous medium is limited to flows where the molecular mean free path of the gas is negligible compared with the dimensions of flow passages. By selecting some values from Wildman's (18) experimental data he has shown that the ratio of molecular mean free path to radial clearance is not negligible and hence, the fluid flow phenomenon in gas lubricated bearings should be treated on a microscopic rather than macroscopic basis, at least in some cases. When the molecular free path becomes comparable to the film thickness, the following effects must be taken into account:

a) Slipping between the gas and walls.

b) Discontinuity in temperature between the solid boundary and gas.

As long as the ratio of molecular mean free path and the film thickness is between 0 and 1 (which is usually the case), then, as a first approximation the flow may be still treated by Reynold's equation but with modified boundary conditions to take into account the above mentioned effects. He has solved Reynold's equation for a Step bearing and inclined pad slider bearing using the perturbation method. The analysis of the influence of the ratio m (molecular mean free path to a representative film thickness at a reference location) on the performance of gas lubricated bearings shows that:

a) Values of m greater than .01 will have a noticeable effect on the bearing performance such as load carrying capacity and the friction coefficient.

b) The load carrying capacity decreases with increasing value of m. This decrease is most pronounced at low speeds. On the other hand, the influence of m at very high speeds is negligible

c) The friction coefficient decreases with increasing value of m.

MISALIGNMENT OF BEARINGS:

In some applications of gas lubricated journal bearings, the misalignment torque or angular stiffness of the bearing is of interest. For example, a very high angular stiffness is required for gyroscope rotor bearings in order to accurately define the spin reference axis. Dr. Ausman (25) has developed a perturbation solution for the torque produced by the misalignment of journal bearings. A numerical example gives a misalignment torque of 0.16 pound inch per second of arc misalignment.

5. SOME PRACTICAL ASPECTS

In the case of thrust bearings, a disadvantage of the pivoted pad type of bearing is that the pivots need extremely accurate setting because of the smaller running clearances (usually between .0001 inch to .001 inch) necessary with the gases. Alternatively a system of load equalizing levers and pivots may be employed or if the axial setting of the thrust bearing may be allowed to move, spring loaded pads may be used. The other types of bearing avoid this difficulty. Drescher (7) describes the application of hydrodynamic pocket bearings to an asynchronous motor. Application of spiral grooved thrust bearings to a carbon dioxide circulator is described by Ford et al (3). They are easy to make and reliable in service. Thrust plates are usually ground and machine lapped. The flatness obtained is within one or two fringes of sodium light as measured using an optical flat. Pumping grooves are ground into the surface on a special machine after lapping. The fixed plate is mounted on a ball pivot gymbal mounting to provide self alignment. The material used for the fixed plate was carbon.

Satisfactory bearings can be made using simple and familiar machining and finishing processes but care must be taken at appropriate stages in manufacture to ensure that adequate stress relieving heat treatment is carried out. Normally the surface finish required for gas bearings is of the order of 1 to 5 microinches rms. This can be obtained by honing.

Radial clearances in gas bearings range from 0.0001 inch to 0.001 inch rather than 0.001 inch and up, as in oil bearings. This calls for careful design of supports. The self aligning mountings are arranged to cause the least possible distortion. In practical machines, journal bearings are mounted in thin metal diaphragms whose thickness is chosen by trial and error as a compromise between being so thin as to cause bearing flutter and being so thick as to allow adequate self alignment. These diaphragms are usually made from sheet metal by grinding their internal and external diameters when assembled as a firmly clamped stack in a jig.

Bearing materials present a problem because of starting and stopping conditions when the hydrodynamic film is inoperative and contact occurs. Suggestions have been made that the difficulty of starting should be overcome by using either a hydrostatic lubrication or a liquid lubricant which boils off as the bearing accelerates to full speed. Current practice is to use conservative bearing load (1 to 2 PSI of projected area) and hard bearing materials such as chrome, nitrided steel or tungsten carbide. Corrosivity of the lubricating gas also influences choice of bearing material, hence the employment of inert gas atmospheres. Recently some applications have been described where ceramics have been used with helium due to the excellent anti-galling properties of ceramics. At very high temperatures, in the region of 500° centigrade, it may be possible to make use of the good boundary lubrication properties of the reactive gases such as sulphur hexafluoride in conjunction with certain alloys, but no information is available. The areas of application of air bearings comprise of precision grinders, turbo expanders, gas circulators, air cycle refrigerating machines, instruments, gyros etc. Applications are being contemplated from -200° farenheit to 3000° farenheit and from very low speeds to 500,000 R.P.M.

APPENDIX 1

From equation 7, 8, and 9 we note that pressure is a function of $\underline{x}$ only , so we can integrate equation 7 twice to get:

$$u = \frac{1}{\mu}\frac{dP}{dx}\frac{z^2}{2} + C_1 z + C_2$$ where C_1 and C_2 are constants.

Applying boundary conditions:

$$u = 0 \quad at \quad z = h$$

$$\& \quad u = U \quad at \quad z = 0$$

we get $$u = U\left[1 - \frac{z}{h}\right] - \frac{z}{2\mu}\frac{dP}{dx}\left[h - z\right] \qquad \text{------1.1}$$

The mass flow through any section can be represented by:

$$\int_0^h \rho u dz \quad or \quad \int_0^h P u dz \quad because \quad P\rho^{-1} = const.$$

$$\therefore \int_0^h P u dz = P\int_0^h u dz = K$$

Substituting for u from equation 1.1 and integrating we get:

$$\frac{K}{P} = \frac{Uh}{2} - \frac{h^3}{12\mu}\frac{dP}{dx}$$

$$or \quad \frac{dP}{dx} = \frac{12\mu}{h^3}\left[\frac{Uh}{2} - \frac{K}{P}\right] \qquad \text{------1.2}$$

For a pad bearing referring to the figure:

$$h = h_1 - (h_1 - h_2)x \qquad \begin{bmatrix} Let\ Ph = w \\ h_1 - h_2 = \Delta \end{bmatrix}$$

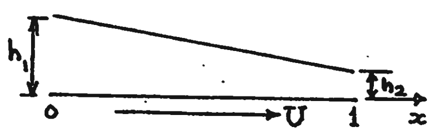

Then from equation 1.2 we have:

$$\frac{\Delta h^3}{\mu}\frac{dP}{dh} + 6Uh = \frac{K}{P}$$

$$\frac{\frac{\Delta}{\mu} w\, dw}{\frac{\Delta}{\mu} w^2 - 6Uw + K} - \frac{dh}{h} = 0 \qquad \text{------1.3}$$

The form of the integral depends on the sign of $(\mu K\Delta - 9\mu^2 U^2)$ and for our present purpose this will be found positive within the required range of U. Hence integrating equation 1.3 we get

$$\frac{1}{2}\ln\left(\frac{\Delta\omega^2}{\mu} - 6U\omega + K\right) + \frac{3\mu U}{(\mu K\Delta - 9\mu^2U^2)}\tan^{-1}\frac{\omega\Delta - 3\mu U}{(\mu K\Delta - 9\mu^2U^2)^{1/2}} - \ln h = c_1$$

Boundary conditions are:

$$P = P_a \quad at \quad x = 0$$

$$h = h_1 \quad at \quad x = 0 \quad and \quad h = h_2 \quad at \quad x = 1$$

Substituting these boundary conditions and subtracting the two equations so obtained, we have an equation from which to determine K.

$$\ln\frac{h_1}{h_2} = \frac{1}{2}\ln\frac{\left(\frac{\Delta P_a h_1^2}{\mu} - 6UP_a h_1 + K\right)}{\left(\frac{\Delta P_a h_2^2}{\mu} - 6UP_a h_2 + K\right)} + \frac{3\mu U}{(\mu K\Delta - 9\mu^2U^2)^{1/2}}\left[\tan^{-1}\frac{\Delta P_a h_1 - 3\mu U}{(\mu K\Delta - 9\mu^2U^2)^{1/2}} - \tan^{-1}\frac{\Delta P_a h_2 - 3\mu U}{(\mu K\Delta - 9\mu^2U^2)^{1/2}}\right] \quad \text{-----1.4}$$

To find the value and position of the maximum pressure we get:

$$\frac{dP}{dx} = 0 \qquad \therefore \quad 6UPh = K \quad \text{from equation 1.2.}$$

Therefore the position x, of maximum pressure is given by the equation:

$$\ln\frac{h_1 - \Delta x_1}{h_1} = \frac{1}{2}\ln\frac{2\left(\frac{K}{6U}\right)^2}{\frac{\Delta P_a^2 h_1^2}{\mu} - 6UP_a h_1 + K} + \frac{3\mu U}{(\mu K\Delta - 9\mu^2U^2)^{1/2}}\left[\tan^{-1}\frac{\frac{\Delta K}{6U} - 3\mu U}{(\mu K\Delta - 9\mu^2U^2)^{1/2}} - \tan^{-1}\frac{\Delta P_a h_1 - 3\mu U}{(\mu K\Delta - 9\mu^2U^2)^{1/2}}\right] \quad \text{-----1.5}$$

Having found x_1 from this equation the value of maximum pressure can be found. As will be seen, it is extremely difficult to calculate results for any specific case from these equations.

APPENDIX 2

From equation 4 we note that pressure is not a function of z and so equations 2 and 3 can be integrated to give:

$$u = \frac{1}{\mu}\frac{\partial p}{\partial x}\frac{z^2}{2} + c_1 z + c_2$$
$$v = \frac{1}{\mu}\frac{\partial p}{\partial y}\frac{z^2}{2} + c_3 z + c_4$$

Applying boundary conditions:

$u = U$ at $z = 0$ and $u = 0$ at $z = h$

$v = 0$ at $z = 0$ and $z = h$

we get

$$u = U\left(1 - \frac{z}{h}\right) - \frac{z}{2\mu}\frac{\partial p}{\partial x}(h - z) \qquad \text{-----1.6}$$

$$v = \frac{z}{2\mu}\frac{\partial p}{\partial y}(h - z) \qquad \text{-----1.7}$$

Now considering equation 1 for continuity and integrating it with respect to z we get

$$\int_0^h \frac{\partial}{\partial x}(\rho u)dz + \int_0^h \frac{\partial}{\partial y}(\rho v)\,dz = 0 \qquad \text{-----1.8}$$

From calculus we get

$$\frac{\partial}{\partial x}\int_0^h \rho u\,dz = \frac{\partial h}{\partial x}(\rho u)_{z=h} + \int_0^h \frac{\partial(\rho u)}{\partial x}dz$$

$$\frac{\partial}{\partial y}\int_0^h \rho v\,dz = \frac{\partial h}{\partial y}(\rho v)_{z=h} + \int_0^h \frac{\partial(\rho v)}{\partial y}dz$$

Substituting for $\int_0^h \frac{\partial(\rho u)}{\partial x}dz$ and $\int_0^h \frac{\partial(\rho v)}{\partial y}dz$ from these equations in 1.8 we get

$$\frac{\partial}{\partial x}\int_0^h \rho u\,dz + \frac{\partial}{\partial y}\int_0^h \rho v\,dz = \frac{\partial h}{\partial x}(\rho u)_{z=h} + \frac{\partial h}{\partial y}(\rho v)_{z=h}$$
$$= 0 \quad [\text{Because } u = v = 0 \text{ at } z = h]$$

Substituting for ρ from equation 5 and noting that P is not a function of z we get:

$$\frac{\partial}{\partial x}\left[P^{1/k}\int_0^h u\,dz\right] + \frac{\partial}{\partial y}\left[P^{1/k}\int_0^h v\,dz\right] = 0 \qquad \text{-----1.9}$$

Substituting for u and v from equation 1.6 and 1.7 and integrating:

$$\frac{\partial}{\partial x}\left[P^{1/k} h^3 \frac{\partial P}{\partial x}\right] + \frac{\partial}{\partial y}\left[P^{1/k} h^3 \frac{\partial P}{\partial y}\right] = 6\mu U \frac{\partial}{\partial x}(P^{1/k} h)$$

This is called Reynold's equation for compressible fluids. For journal bearing, introducing new variables β and ξ where $\beta = \frac{x}{r}$ and $\xi = \frac{y}{r}$ we get(Refer figure 1.7)

$$\frac{\partial}{\partial \beta}\left[P^{1/k} h^3 \frac{\partial P}{\partial \beta}\right] + \frac{\partial}{\partial \xi}\left[P^{1/k} h^3 \frac{\partial P}{\partial \xi}\right] = 6\mu\omega r^2 \frac{\partial}{\partial \beta}\left[P^{1/k} h\right]$$

$$\frac{\partial}{\partial \beta}\left[\left(\frac{P}{P_0}\right)^{1/k}\left(\frac{h}{c}\right)^3 \frac{\partial P}{\partial \beta}\right] + \frac{\partial}{\partial \xi}\left[\left(\frac{P}{P_0}\right)^{1/k}\left(\frac{h}{c}\right)^3 \frac{\partial P}{\partial \xi}\right] = GkP_0 \frac{\partial}{\partial \beta}\left[\left(\frac{P}{P_0}\right)^{1/k}\left(\frac{h}{c}\right)\right] \qquad \text{----1.10}$$

from equation 13: $h = c(1 + E\cos\beta)$

The partial differential equation 1.10 is still non-linear in the pressure P but a perturbation solution can be developed if the pressure is expressed as a power series of increasing order in the eccentricity ratio E.

$$P = P_0 + EP_1 + E^2P_2 + \text{-----} \qquad \text{----1.11}$$

If we substitute for h and P from equations 13 and 1.11 into equation 1.10 and group the terms according to powers of E, the following set of linear, partial differential equations is obtained:

$$\frac{\partial^2 P_1}{\partial \beta^2} - G\frac{\partial P_1}{\partial \beta} + \frac{\partial^2 P_1}{\partial \xi^2} = -\,GkP_0 \sin\beta \qquad \text{----1.12}$$

$$\frac{\partial^2 P_2}{\partial \beta^2} - G\frac{\partial P_2}{\partial \beta} + \frac{\partial^2 P_2}{\partial \xi^2} = \frac{3}{2}GkP_0\sin 2\beta - \frac{1}{kP_0}\left[\left(\frac{\partial P_1}{\partial \beta}\right)^2 + \left(\frac{\partial P_1}{\partial \xi}\right)^2\right]$$
$$+\left(3\sin\beta - 2G\cos\beta - G\frac{P_1}{P_0}\right)\frac{\partial P_1}{\partial \beta} \qquad \text{----1.13}$$

$$\frac{\partial^2 P_3}{\partial \beta^2} - G\frac{\partial P_3}{\partial \beta} + \frac{\partial^2 P_3}{\partial \xi^2} = \text{------}$$

In principle, the first equation can be solved for P_1, which can then be substituted into the right hand side of the second equation as a known function. This enables the second equation to be solved for P_2 which in turn can be used to obtain the solution for P_3. As the "driving functions" on the right hand side soon become lengthy, the process is, in practice, restricted by algebraic complexity to obtaining only one or two terms beyond P_o in the pressure series. Fortuneately the second order solution P_2 does not contribute to the bearing load support, so that load characteristics can be determined fairly accurately with first order solution P_1 alone. Ausman (5) has obtained the first order solution which is quite lengthy. Now from this solution we can obtain the load capacity and "end flow factors". Referring to figure 1.4 we have

$$W_1 = -r^2 \int_{-b/d}^{b/d} d\xi \int_0^{2\pi} P \cos\beta \, d\beta$$

$$W_2 = r^2 \int_{-\frac{b}{d}}^{b/d} d\xi \int_0^{2\pi} P \sin\beta \, d\beta$$

If we substitute for P from equation 1.11 and neglect third and higher order terms, the only term which will contribute to load capacity will be EP_1, and so:

$$W_1 = -r^2 \int_{-b/d}^{b/d} d\xi \int_0^{2\pi} EP_1 \cos\beta \, d\beta$$

$$W_2 = r^2 \int_{-b/d}^{b/d} d\xi \int_0^{2\pi} EP_1 \sin\beta \, d\beta$$

After evaluation of these integrals from the first order solution

$$W = \sqrt{W_1^2 + W_2^2} \qquad \text{-----1.14}$$

$$\tan\phi = \frac{W_2}{W_1} \qquad \text{-----1.15}$$

End flow factors will be equal to:

$$\frac{W}{W_{\infty}} = \frac{\sqrt{W_1^2 + W_2^2}}{\sqrt{W_{1\infty}^2 + W_{2\infty}^2}} \qquad \text{-----1.16}$$

APPENDIX 3

The equation to be used for journal bearing solution is equation 14:

$$\frac{dP}{d\beta} = \frac{6\mu\omega r^2}{c^2(1+E\cos\beta)^2}\left[1 - \frac{2K}{UPC(1+E\cos\beta)}\right] \qquad \text{-----14}$$

Conditions which equation 14 must satisfy:

1) The pressure P must be a continuous and periodic function of β, its period being 2π.
2) The total mass of air contained in the bearing clearance must be constant or

$$\int_0^{2\pi} Ph\, d\beta = 2\pi c P_o \qquad \text{----1.17}$$

Where P_o is the pressure which determines the mass of air in the bearing clearance. Introducing new variables (A, S, τ, ψ, θ & ν) equation 14 can be transformed in terms of ψ and θ instead of P and β as shown below:

$$\frac{d\psi}{d\beta} = \frac{\tau}{\nu}\left(1 - \frac{\tau}{\psi}\right) \qquad \text{----1.18}$$

where,

$$A = 6\mu U \qquad \nu = S\frac{cK}{Ar}$$

$$S^2 = 1 - E^2 \qquad \tau = 1 - E\cos\theta$$

$$\cos\theta = \frac{E + \cos\beta}{1 + E\cos\beta} \qquad P = \frac{1}{S^2}\left(\frac{K}{c}\right)\psi$$

Katto and Soda (11) have shown that the solution of equation 1.18 is:

$$\psi = \tau\left[1 + \frac{\nu}{\tau}\frac{d\psi}{d\theta} + \left(\frac{\nu}{\tau}\frac{d\psi}{d\theta}\right)^2 + \text{-----}\right] \qquad \text{----1.19}$$

By disregarding all terms proportional to the second or higher powers of $\frac{\nu}{T}\frac{d\psi}{d\theta}$ we can obtain an approximate solution for ψ. Thus:

$$\psi = 1 - \frac{E}{1+\nu^2}\cos\theta + \frac{E\nu}{1+\nu^2}\sin\theta + - - - - - \qquad ----1.20$$

The validity of the approximation decreases with the increase of the value of ν and E and vice-versa. But it is verified that the magnitude of ν appearing in bearing problems is not so large in general and therefore the error caused by the above approximation is not practically very large. Now converting the ψ and θ in the equation 1.20 into the original notations P and β, we can obtain the air film pressure distribution as a function of β involving E and ν as parameters. The relation between the velocity of the bearing ($A = 6\mu U$) and the parameters (E and ν) is obtained by substituting the above film pressure function into equation 1.17. Hence, given the mean load P_m and the velocity of the bearing, the eccentricity ratio E and the eccentric angle ϕ are determined as functions of running conditions. The moment of the frictional force or the friction coefficient f can be easily calculated in the same way as for usual bearing problems. In order to represent them in dimensionless forms we write:

$$\bar{A} = \frac{Ar}{c^2 P_a}$$

$$\bar{P}_m = \frac{P_m}{P_a}$$

$$\bar{P} = \frac{P}{P_a}$$

where bar represents dimensionless quantities. Using above we have

$$\bar{A} = \frac{1+\nu^2}{\nu} \cdot \frac{s^3}{s^2+\nu^2} \qquad \text{----1.21}$$

$$\bar{P}_m = \pi\left(\frac{s-s^2}{E}\right)\frac{\sqrt{1+\nu^2}}{s^2+\nu^2} \qquad \text{----1.22}$$

$$\tan\phi = \nu \qquad \text{----1.23}$$

$$\bar{p} = \frac{1+\nu^2}{s^2+\nu^2}\left[1 - \frac{E}{1+\nu^2}\,\frac{E+\cos\beta}{1+E\cos\beta} + \frac{Es\nu}{1+\nu^2}\,\frac{\sin\beta}{1+E\cos\beta}\right] \qquad \text{----1.24}$$

$$\frac{f}{c/r} = \frac{1}{2}\,\frac{E}{1-s}\,\frac{\sqrt{1+\nu^2}}{\nu}\left[\frac{s}{3} \pm \frac{\nu^2}{1+\nu^2}(1-s)\right] \qquad \text{----1.25}$$

Figure 1.9 shows the results calculated from the equations 1.21 to 1.25. Given the mean load P_m and the velocity of the journal A, we can find the position of the journal centre in the diagram and in addition know the friction coefficient at the position. When it is necessary to know the pressure distribution we may calculate it by equation 1.24 substituting corresponding values of E and ν .

BIBLIOGRAPHY - PART I

(Hydrodynamic Bearings)

1. HIRN, G. (1854) "Sur les Principaux Phenomenes qui Presentent les Frottements Mediats". Bull. soc. ind. Mulhouse, Vol. 26. p. 188.

2. HARRISON, W.J. (1913) "The Hydrodynamical Theory of Lubrication with Special Reference to Air as a Lubricant". Trans-Cambridge Philosophical Society, Vol. 22. pp. 39-54.

3. FORD, G.W.K., D.M. HARRIS and D. PANTALL (1956) "Principles and Applications of Hydrodynamic Type Gas Bearings". Proc. Inst. of Mech Eng. (London). Vol. 171, No. 2. pp. 93-128

4. MOW, C.C. and E. SAIBEL (1959) "The Gas Lubricated Finite Slider Bearing". Proc. 6th Midwest Conf. Fluid Mech. Austin, Texas. pp. 383-401.

5. AUSMAN, J.S. (1957) "Finite Gas Lubricated Journal Bearing" Paper 22, Conference on Lubrication and Wear, Inst. of Mech Eng. (London)

6. KOCHI, K.C. (1959) "Characteristics of a Self Lubricated Stepped Thrust Pad of Infinite Width with Compressible Lubricant". Trans. ASME, Series D, Vol. 81, No. 2. pp. 135-146.

7. DRESCHER, H. (1953) "Plain Bearings With Air Lubrication" Ministry of Supply Translation T.I.B./T4309 August 1954 or "Gleitlager mit Luftschmierung" Z.V.D.I., Bd. 95, Nr.35 11th Dec. 1953, pp. 1182-1190.

8. WHIPPLE, R.T.P. (1951) "Theory of Spiral Grooved Thrust Bearing with Liquid or Gas Lubricant". A.E.R.E.T./R 622.

9. FORTESCUE, P. (1955) "The Derivation of a Generalized Chart for Viscosity Plate Performance". A.E.R.E. ED/M21.

10. KINGSBURY, A. (1897) "Experiments with an Air Lubricated Journal Bearing". Journ. Am. Soc. Naval. Eng. Vol. 9. p. 267.

11. KATTO, Y. and SODA, N. (1953) "Theory of Lubrication by Compressible Fluid with Special Reference to Air Bearings". Proc. IInd Japanese National Congress on Appl. Mech. National Committee for Theoretical and Appl. Mech. p. 267.

12. SCHEINBERG, S.A. (1953) "Gas Lubrication of Sliding Bearings (Theory and Calculations)" Friction and Wear in Machines, Institute of Machine Sciences, Academy of Sciences of the USSR, Vol. 8. pp. 107-204.

13. ELROD, H. and A. BURGDORFER (1960) "Refinements of the Theory of the Infinitely Long, Self-Acting, Gas Lubricated Journal Bearings". Report No. I-A2049-10, The Frankline Institute Laboratories for Research and Development.

14. AUSMAN, J.S. and M. WILDMANN (1957) "How to Design Hydrodynamic Gas Bearings". Product Eng. pp. 103-106.

15. AUSMAN, J.S. "Theory and Design of Self-Acting Gas-Lubricated Journal Bearings Including Misaligning Effects" (Not Yet Published).

16. MCNEILLY, D.K. (1953) "Investigation of Kingsbury Thrust Bearing Using Air as the Lubricant". Soc. of Automotive Engineers, Paper for Meeting 19th Jan. 1953.

17. BRUNNER, R.K., J.M. HARKER, K.E. HAUGHTON and A.G. OSTERLUND. (1959) "A Gas Film Lubrication Study Part 3: Experimental Investigation of Pivoted Slider Bearings" IBM J. Res. Devel. 3. pp. 260-274.

18. WILDMANN, M. (1956) "Experiments on Gas Lubricated Journal Bearing". ASME Paper No. 56-Lub-8.

19, STERNLICHT, B and R.C. ELWELL. (1958) "Theoretical and Experimental Analysis of Hydrodynamic Gas Lubricated Journal Bearings". Trans. ASME, Vol. 80, No. 4. pp. 865-879.

20. BRIX, V.H. (1959) "Shaft Stability in Gas-Film Bearings" Engineering, Vol. 187. pp. 178-182.

21. FISCHER, G.K., J. CHERUBIM, and O. DECKER. (1959) "Some Static and Dynamic Characteristics of High Speed Shaft Systems Operating with Gas Lubricated Bearings". Paper presented at 1st International Symposium on Gas Lubricated Bearings. Oct. 26-28, 1959, Washington, D.C.

22. BREWSTER, O.C. (1953) Trans. ASME, Vol. 75. pp. 518-519.

23. HUGHES, W.F. and J.F. OSTERLE. (1958) "High Speed Effects in Pneumodynamic Journal Bearing Lubrication". Applied Scientific Research, Section A, Vol. 7, No. 2-3.

24. BURGDORFER, A. (1959) "The Influence of the Mean Molecular Free Path on the Performance of Hydrodynamic Gas Lubricated Bearings". Trans. ASME, Series D, Vol. 81, No. 1. pp. 94-100.

25. AUSMAN, J.S. "Torque Produced by Misalignment of Hydrodynamic Gas Lubricated Journal Bearings." ASME Paper No.59-Lub-3.

26. GROSS, W.A. (1959) "A Gas Film Lubrication Study, Part 1: Some Theoretical Analyses of Slider Bearings".IBM J. Res. Devel. 3, 3. pp. 237-255.

27. MICHAEL, W.A. (1959) "A Gas Film Lubrication Study, Part 2: "Numerical Solution of the Reynold's Equation for Finite Slider Bearings". IBM. J. Res. Devel. 3,3. pp. 256-259.

28. CONSTANTINESCU, V.N. (1957) "About a Class of Boundary Layer Flow of Viscous Compressible Fluid". (in French) 9th Congres intern. Mecan. Appl., Univ. Bruxelles, 3, pp. 294-305.

29. CONSTANTINESCU, V.N. (1956) "On the Theory of Gas Bearings" (in French) Acad. Repub. Pop Romane Rev. Mecan. Appl. 1, 1. pp. 141-155.

30. CONSTANTINESCU, V.N. (1957) "On Unsteady Lubrication" (in French) Acad. Repub. Pop. Romane Rev. Mecan Appl. 2,2.

31. TIPEI, N. (1956) "Contributions to the Study of Hydrodynamic Lubrication". (in French) Rev. Mecan. Appl 1,1. pp. 107-139.

32. ELROD, H.G. (1960) "A Derivation of the Basic Equation for Hydrodynamic Lubrication with a Fluid Having Constant Properties". Quart. of Appl. Math. Vol. 17, No. 4. pp. 349-359.

33. CASTELLI, V. and H.G. ELROD (1960) "Perturbation Analysis of the Stability of Self-Acting, Gas-Lubricated Journal Bearing". Franklin Institute Laboratories Interim Report No. I-A2049-11.

34. WEBER, R.R. (1949) "The Analysis and Design of Hydrodynamic Gas Bearings". North American Aviation Inc. Report AL-699, Los Angeles, California.

35. FULLER, D.D. (1958) "Annual Report ONR Project A2049" Franklin Institute Laboratories Interim Report No. I-A2049-3. July 15, 1958.

36. SNELL, L.N. (1959) "Gas Bearings with Gas Lubrication". Engineering, 188, Oct. 2, 1959. pp. 285-286.

37. SCIULLI, E.B. (1959) "A Bibliography on Gas Lubricated Bearings". Report PB 161017, U.S. Dept. of Commerce.

38. STERNLICHT, B. and H. PORITSKY. (1959) "Dynamic Stability Aspects of Gas Lubricated Journal Bearing". Paper presented at the 1st International Symposium on Gas Lubricated Bearings. Washington, D.C.

39. TIPEI, N. and V.N. CONSTANTINESCU. (1959) "On High Speed Self-Acting Gas Bearings". Paper presented at the 1st International Symposium on Gas Lubricated Bearings October, 1959, Washington, D.C.

40. SLIBAR, A. (1959) "Theory of Self-Acting Gas Lubricated Journal Bearing of Finite Width". Paper presented at the 1st International Symposium on Gas Lubricated Bearings. October, 1959, Washington, D.C.

PART II

HYDROSTATIC BEARINGS

NOTATION

Symbol	Description	Units
A	Area	inches^2
A_o	Effective Orifice Area	inches^2
b	Breadth of the Pad for a Thrust Bearing or Circumferential Distance between two Inlet Holes in a Journal Bearing	inches
c	Eccentricity in a Journal Bearing	
C_d	Orifice Discharge Coefficient	
d	Diameter of Inlet Orifice or Capillary Tubes	inches
D	Depth of Recess in the Pad	inches
f	Pressure Ratios with Respect to Supply Pressure	
F	Total Force Exerted by the Gas on the Bearing Pad	pounds
g	Acceleration due to Gravitational Force	$\frac{\text{inches}}{\text{sec}^2}$
h	Film Thickness Between the Bearing Elements	inches
k	Ratio of Specific Heats	
l	Length of the Capillary Tubes	inches
L	Length of the Bearing in the Direction of flow	inches
m	Mass of the Gas in the Bearing	pounds
M	Mass of the Vibrating Parts of the Bearing	pounds
n	Number of Inlet holes or Number of Pads	
p	Change in Pressure	$\frac{\text{pounds}}{\text{inches}^2}$
P	Absolute Pressure	$\frac{\text{pounds}}{\text{inches}^2}$
q	$\left(\frac{\partial m}{\partial P}\right)_{\tau}$	
Q	Volumetric Flow Rate	$\frac{\text{inches}^3}{\text{sec}}$

r	Radius to any General Point	inches
R_o	Radius of the Recess	inches
R	Outer Radius of the Bearing Pad, Radius of Sphere	inches
R'	Gas Constant	$\frac{in^2}{sec^2 1\,^{\circ}R}$
s	$\left(\frac{\partial m}{\partial h}\right)_q$	
T	Absolute Temperature	$^{\circ}R$
u	Component of Gas Velocity in the x Direction	$\frac{in}{sec}$
v_s	Effective Pad Volume	$inches^3$
V	Velocity	$\frac{in}{sec}$
w	Weight Flow Rate of Gas	$\frac{lbs}{sec}$
W	Load on the Bearing	pounds
x, y	Cartesian co-ordinates	inches
τ	Viscous Shear Stress	$\frac{lbs}{in^2}$
μ	Absolute Viscosity	$\frac{lbs.sec}{in^2}$
ρ	Density of the Gas	$\frac{lbs.sec^2}{in^4}$
ϵ	Eccentricity Ratio	
η	Efficiency of the Bearing	
δ	Small Change in Film Thickness	inches
α	$-\left(\frac{\partial w_{in}}{\partial P}\right)_q$	
β	$\left(\frac{\partial w_{out}}{\partial P}\right)_q$	
θ	$\left(\frac{\partial w_{out}}{\partial h}\right)_q$	

SUBSCRIPTS

Symbol	Description
e	Exhaust from the Bearing
f	Effective
i	Initial
o	Downstream of orifice, i.e. in the Recess
q	Equilibrium
s	Supply

In addition some other symbols have been used at some specific places. They are defined at the proper place. Also some of the above symbols have been used in a different sense as explained at the proper place.

1. BASIC THEORY

In hydrostatic or externally pressurized bearings, the load is supported by the static gas pressure in the clearance space between the two elements of the bearing. There is always a definite outward leakage of gas which must be replaced by gas pumped from an external source through feed holes in the bearing wall. The pumping power thus consumed will increase roughly as the cube of the bearing clearance because flow through a slot of very small height is proportional to the cube of the height. In any application of the hydrostatic bearings not only must this pressure source be provided, but in addition suitable provision must be made to dispose of the gas. Hydrostatic bearings are preferred to hydrodynamic bearings in a case of high unit loads, low coefficient of friction and high positional accuracies.

To promote stability and to economize in pump capacity, it is desirable to use flow restrictors in series with the gas admission holes or recesses. They may take the form of capillaries or orifices. The hydrostatic bearings are classified on the basis of these restrictors. On this basis, they may be divided in two categories:

1. Orifice Compensated Bearings
2. Capillary Compensated Bearings

Similar to hydrodynamic bearings, the hydrostatic bearings may be either Journal or Thrust bearing. In the case of thrust bearings, almost any configuration can be used with hydrostatic lubrication.

Generally, the following configurations are used:

1. Flat
2. Spherical
3. Conical

However, the mechanics of a loaded sphere or cone floated on a seat by a jet of high pressure air are drastically different from those of conventional bearing geometries. Very little theoretical work has been done on bearings of these configurations except for some semi-empirical equations which will be given later.

The items so far studied on hydrostatic bearings are:

1. Load Capacity
2. Gas Consumption
3. Stability

All these items are studied for steady load without any rotation. No study has been undertaken on the effects of rotation on the performance, in a quantitative manner. We will, first of all, develop equations for the flow through orifices, narrow slots and capillaries.

a. Flow through orifices: The weight flow rate for adiabatic compressible flow through an orifice is given by:(see Appendix 4)

$$w_{in} = C_d A_o P_s g\left[\frac{2K}{(K-1)R'T_s}\left(f_o\right)^{2/K}\left\{1 - f_o^{\frac{K-1}{K}}\right\}\right] \qquad \text{--------2.1}$$

b. Flow through narrow slots: This represents the flow out of bearing clearance. It is given by: (see Appendix 4)

1) Rectangular Slots:

$$w_{out} = \frac{g b h^3 P_s^2}{24\mu R' T_s L}\left[f_o^2 - f_e^2\right] \qquad \text{--------2.2}$$

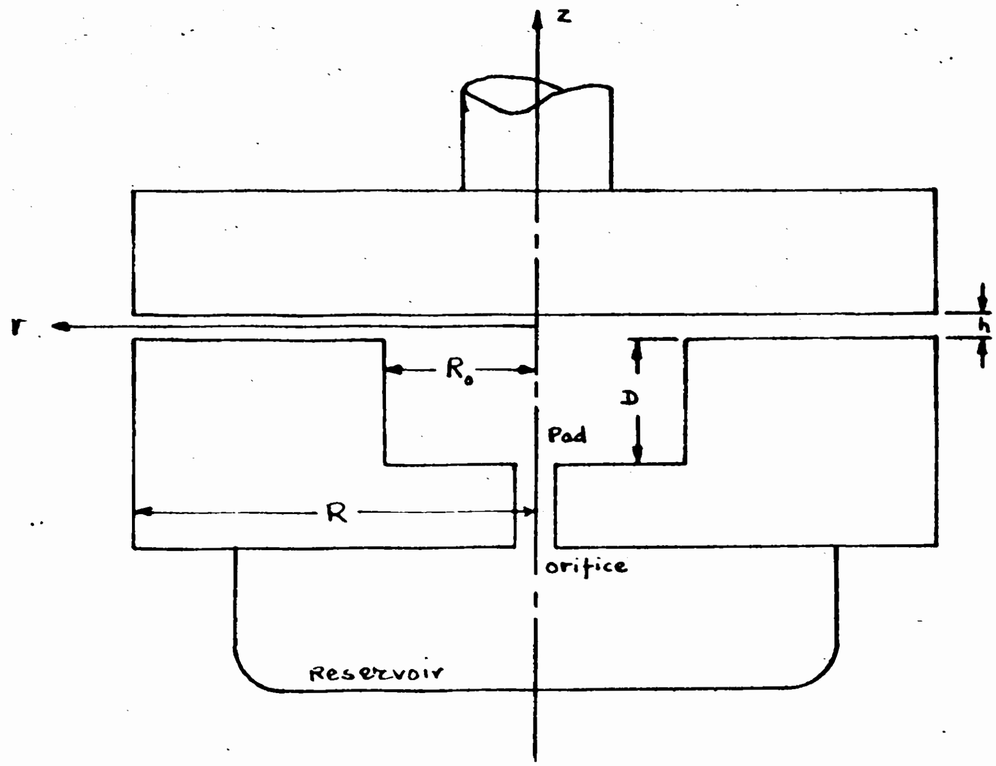

(a) Circular Step Bearing

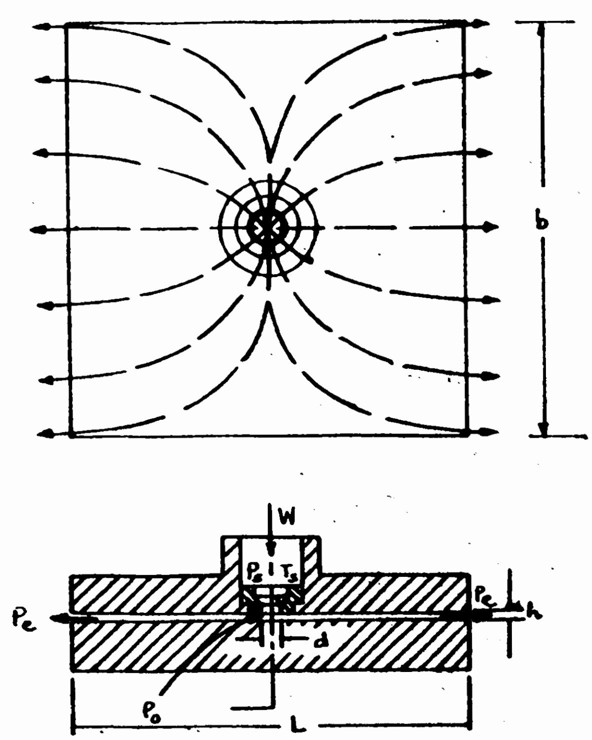

(b) Rectangular Pad Thrust Bearing

FIGURE (2.1) - STEP THRUST BEARINGS

2) Circular Slots:

$$\omega_{out} = \frac{g \pi h^3 P_s^2}{12 \mu R' T_s \ln \frac{R}{R_o}} \left[f_o^2 - f_e^2 \right] \qquad \text{------2.4}$$

c. Flow through capillaries: The flow through a capillary under isothermal conditions is given by: (see Appendix 4)

1) Laminar Flow:

$$\omega_{in} = \frac{g \pi d^4 P_s^2}{256 \mu R' T_s l} \left(1 - f_o^2 \right) \qquad \text{------2.5}$$

2) Turbulent Flow:

$$\omega_{in} = \left[\frac{20.8 \times 10^8 d^5 \left(P_s^2 - P_o^2 \right)}{T_s f' l} \right]^{1/2} \qquad \text{------Ref.4}$$

In steady state conditions, the weight flow coming in through orifices or capillaries must be equal to the weight flow out of the bearings. Mathematically,

$$W \text{ in} = W \text{ out}$$

It is possible to obtain the pressure profile, load capacity, gas flow and other characteristics of the bearings from this relation. This has been done by Laub (1)* for flat thrust bearings and by McNeilly (2) and Richardson et al (3) for journal bearings. Laub has developed an expression for load capacity in terms of Error Functions which can be found in most sets of mathematical tables. (see Appendix 5) He has also plotted the load carrying capacities of bearings of one square inch area against R/R_o which is shown in figure 2.2.

---

*The numbers in the parentheses refer to the numbers in the Bibliography, Part II.

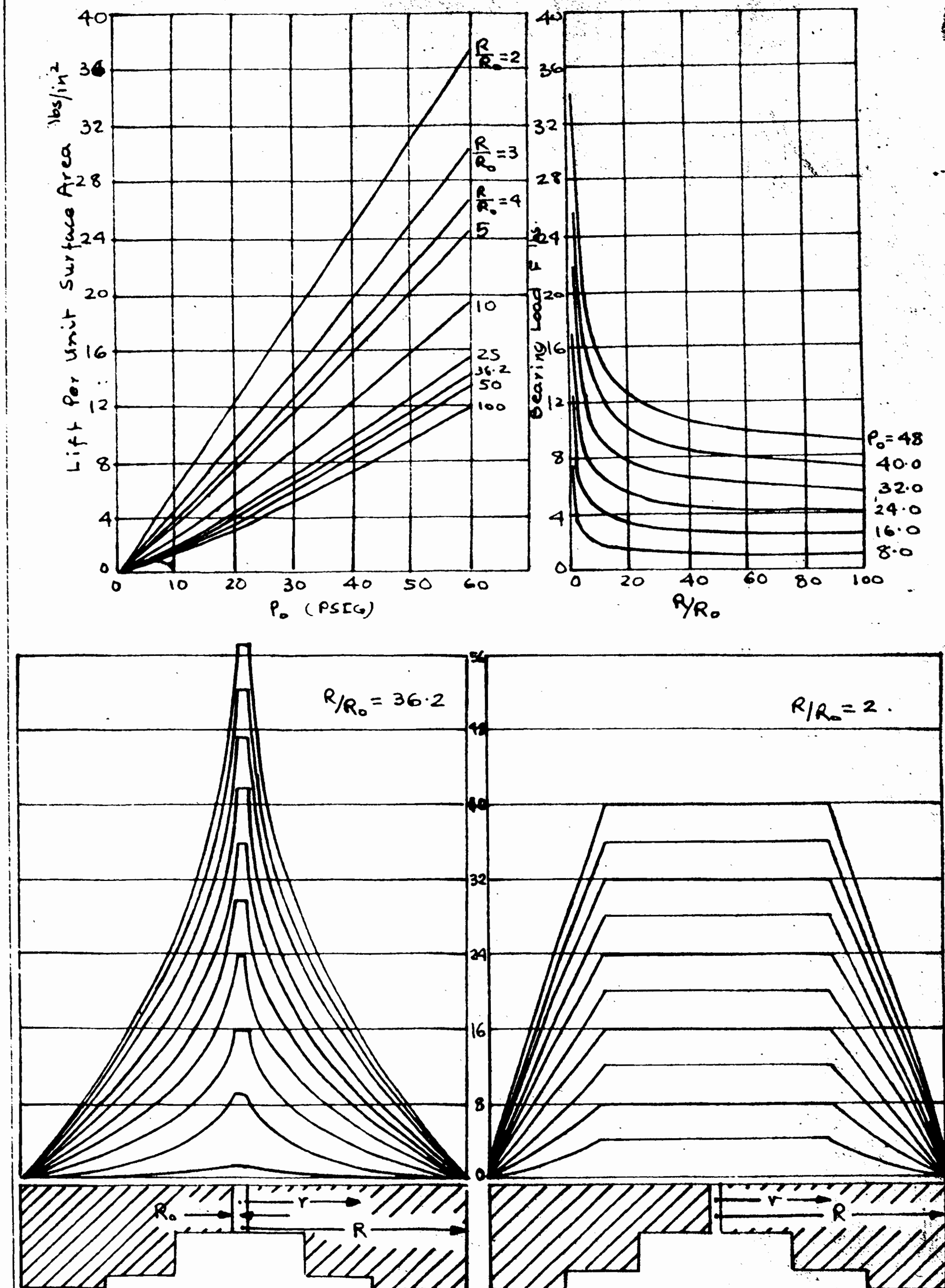

FIGURE (2.2) – PRESSURE PROFILES IN A STEP BEARING.

McNeilly (2) has treated thrust and journal bearings. He has approximated the journal bearing by considering a set of opposed thrust discs. He has developed a design procedure for these bearings and has put forth some recommendations for the number of holes in different sizes of journal bearings. (see Appendix 6)

Richardson et al (3) have also developed a design procedure for journal bearings on the same lines as McNeilly. (see Appendix 7) The only difference is in the shape of the discs, which is rectangular in Richardson's case and circular in McNeilly's case. McNeilly has assumed a radial flow and Richardson has assumed only axial flow, the circumferential flow being neglected. So the designs obtained by these methods should be used with caution. These assumptions will be discussed in greater detail while comparing the theoretical predictions with experimental results.

Very little work has been done on capillary compensated bearings when compared to orifice compensated bearings. In the equation of turbulent flow through capillaries, f' is the friction factor which must be determined experimentally. Pigott and Macks (4) have dealt with this type of bearings in brief.

SPHERICAL BEARINGS

There is no exact analytical treatment of these bearings. However, Corey et al (5) have developed some semi-empirical equations to determine the basic parameters of these bearings.

They are given below: (figure 2.3a)

a. Minimum pressure required to raise a given load (psig):

$$P_{min} = \frac{W}{2R^2} \qquad \text{for } \theta = 60°$$

$$P_{min} = \frac{W}{1.80R^2} \qquad \text{for } \theta = 30°$$

$$P_{min} = \frac{W}{2.21R^2} \qquad \text{for } \theta = 90°$$

b. Air flow versus air pressure:

$$P = (18 + 1.5P_{min}) - (18 + 0.5P_{min})\sqrt{1 - \left(\frac{Q}{Q_{max}}\right)^2}$$

$$Q_{max} \approx 57.4$$

c. Air pressure versus lift:

$$\text{Lift} = \frac{P + 25R - 5}{5000\left[(0.37 + .025R^3)\sqrt{P_{min}}\right]} \qquad P \geq P_o + 25$$

$$\text{Lift} = \frac{P_{min} + 20 + 25R}{5000\left[(0.37 + .025R^3)\sqrt{P_{min}}\right]}\sqrt[3]{\frac{P - P_o}{25}} \qquad P \leq P_o + 25$$

Agreements of these equations with experimental data is within 5%. They have also suggested a design which will provide maximum load carrying capacity for minimum flow. They have suggested that the seat should be machined to two different radii as shown in figure 2.3b.

CONICAL BEARINGS

Semi-empirical equations have been developed for these bearings by Gottawald (6). He has developed equations for load capacity, volume flow and frictional moment for the air bearing shown in figure 2.4.

$$W = C_1 P$$

$$W = \frac{C_2 Q \mu}{h^3}$$

$$X = .0032\,\omega$$

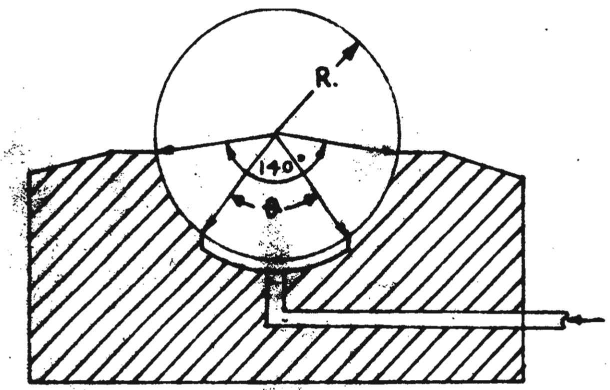

ⓐ Spherical Thrust Bearing.

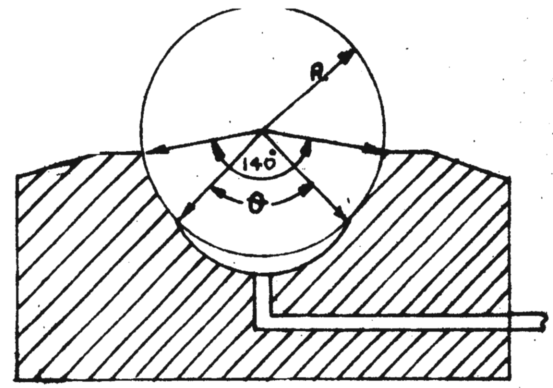

ⓑ Spherical Thrust Bearing.

FIGURE (2·3) - SPHERICAL THRUST BEARINGS

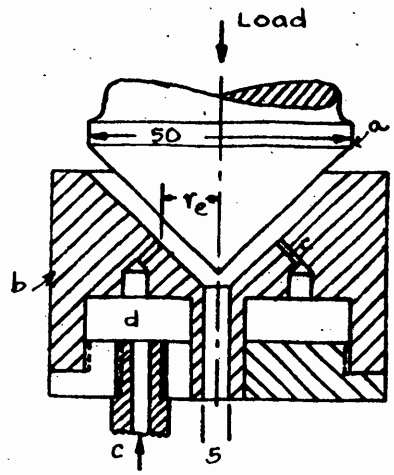

Section through a Model Bearing for Water or Air Lubrication.

a) Shaft Pivot
b) Bearing
c) Lubricant Entrance
d) Ring Shaped Supply Chamber
e) Eight Distribution Perforations
f) Distance of Intake Gap from Axis of Bearing

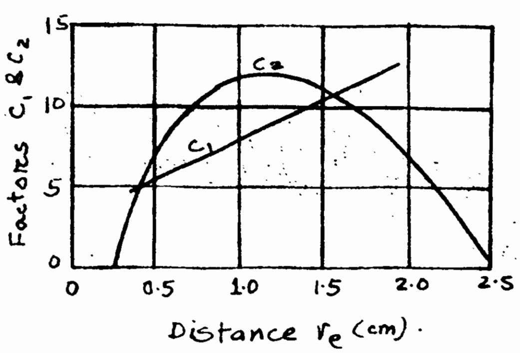

Relationship of Factors c_1 and c_2 from the Location of the Entrance Gap.

r_e - Distance of Entrance Gap from Middle of Bearing

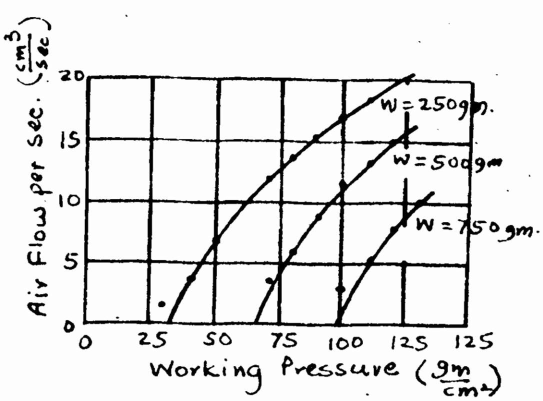

Relationship between Air Supplied per Second, Q, and Working Pressure p_o, for different Loads W of the Air Bearing

FIGURE (2.4) - DESIGN CURVES FOR CONICAL BEARINGS.

where c_1 and c_2 are constants to be determined from figure 2.4. These constants depend on the radius r_e as shown in figure 2.4. The pressure P, volume flow Q film thickness h and frictional moment X must be substituted in C.G.S. units. The value of these equations is very limited, because they apply to the particular bearing tested. However, it indicates a procedure for determining the pertinent characteristics of a bearing from a model.

A recent development in hydrostatic bearings is a step bearing as shown in figure 2.5. A description of this type of bearing is given by Adams (7) along with certain empirical design equations.

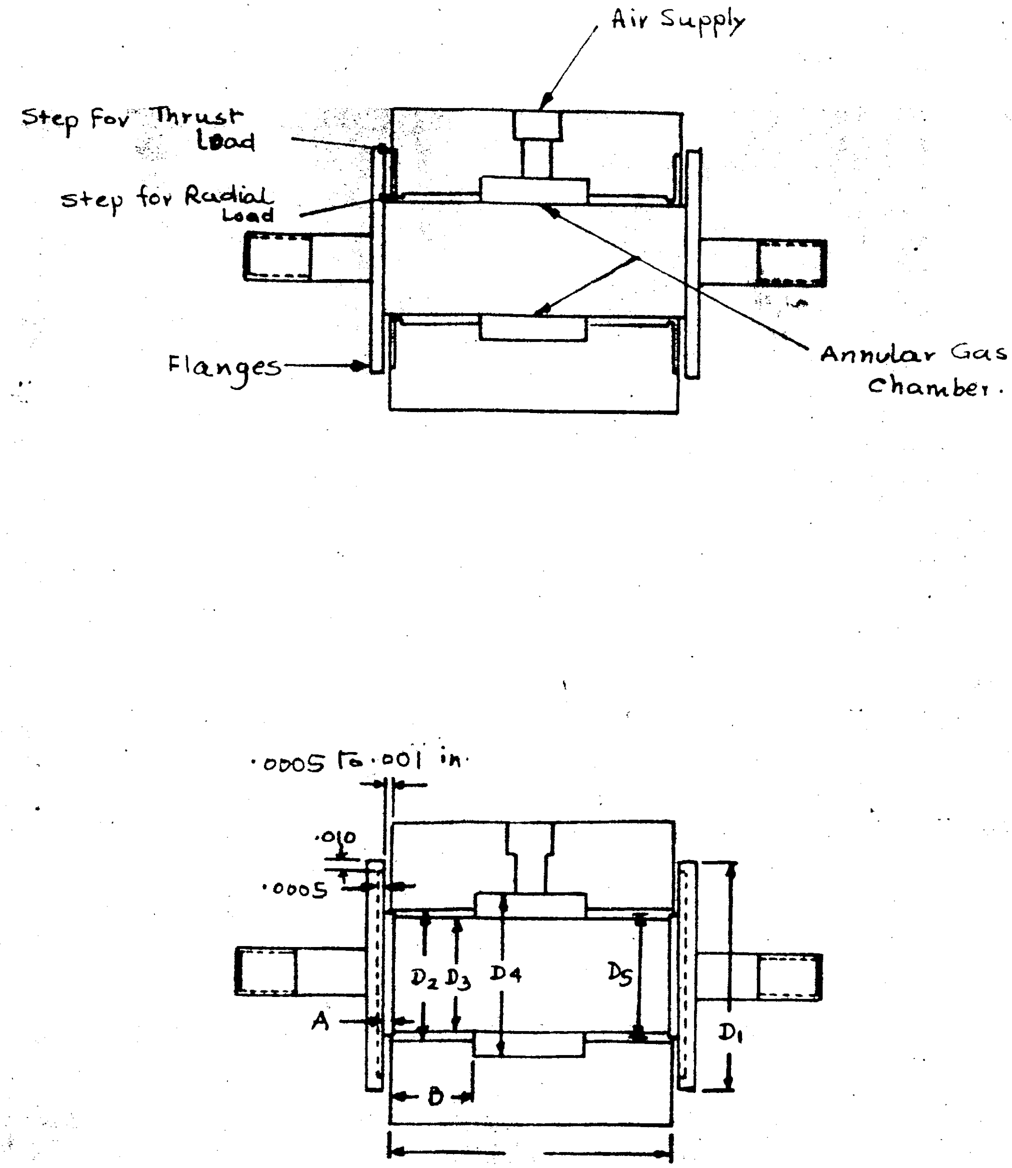

$A > .040$ in, $\quad \frac{A}{B} \approx \frac{1}{6}$, $\quad D_2 = D_3 + 2c$, $\quad c \approx .0005$ in.

$D_4 = D_2 + 0.2$, $\quad D_5 = D_3 + c$

$$P_a = \frac{5W}{LD}$$

FIGURE (2.5) - HYDROSTATIC STEP BEARING.

2. EXPERIMENTAL RESULTS AND THEIR COMPARISON WITH THEORETICAL PREDICTIONS

The major part of the experimental work on these bearings has been carried out by Laub (1), Richardson et al (3), Wunsch (8) and Pigott and Macks (4). Laub has conducted experiments on thrust bearings of the following parameters: (Refer figure 2.1a)

$$R = .565''$$

$$R/R_o = 2,\ 3,\ 36.2$$

The range of pressure variation was from 8 to 48 psig. His results are shown in figure 2.6 and 2.7, along with his theoretical predictions. It is very encouraging to note the excellent agreements between the theoretical and experimental results within the range of pressures and step radii investigated. The author has also made a reference to his work on journal bearings, but it is not yet published.

Richardson has tested thrust bearings with rectangular pads to approximate the conditions in journal bearings. He determined the pressure distribution and flow rate data for a range of pressure ratios f_e from 2 to 12. To minimize leakage problem, he ran the tests with supply pressures P_s near atmospheric and the exit pressures P_e in the vacuum range. The dimensions b and L (figure 2.1b) were fixed at 6.25" and 4" respectively for all tests.

The values of d and h were varied as follows:

$d = 0.013''$, $0.020''$, $0.040''$, $0.078''$ and $0.156''$

$h = .001''$ to $.006''$

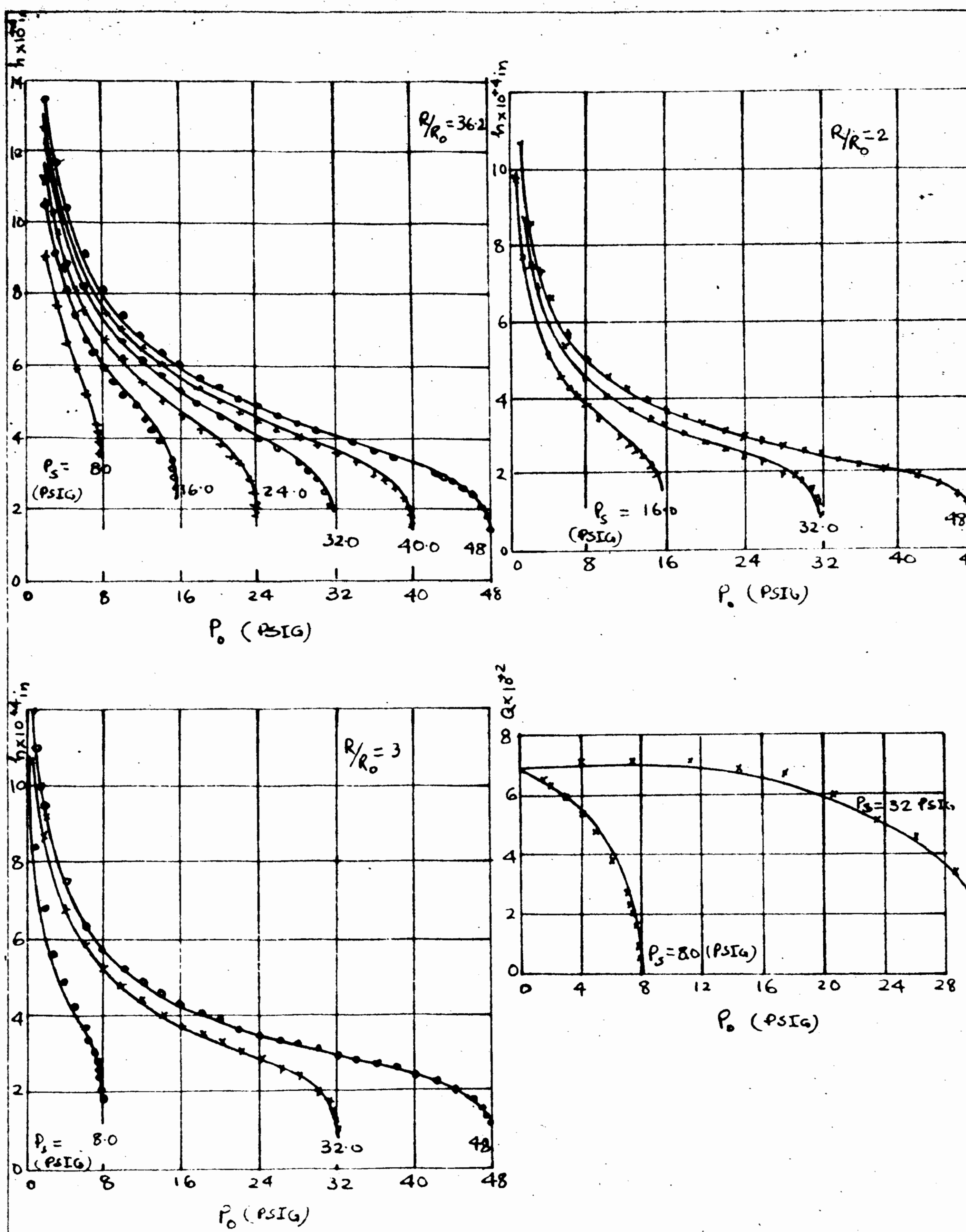

FIGURE (2.6) - EXPERIMENTAL RESULTS OF LAUB.

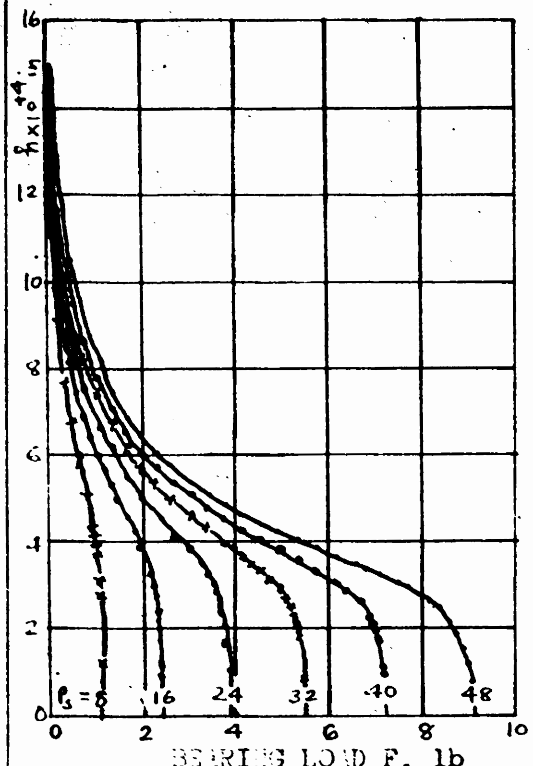

Bearing stiffness, pad bearing
R/R_o = 36.2

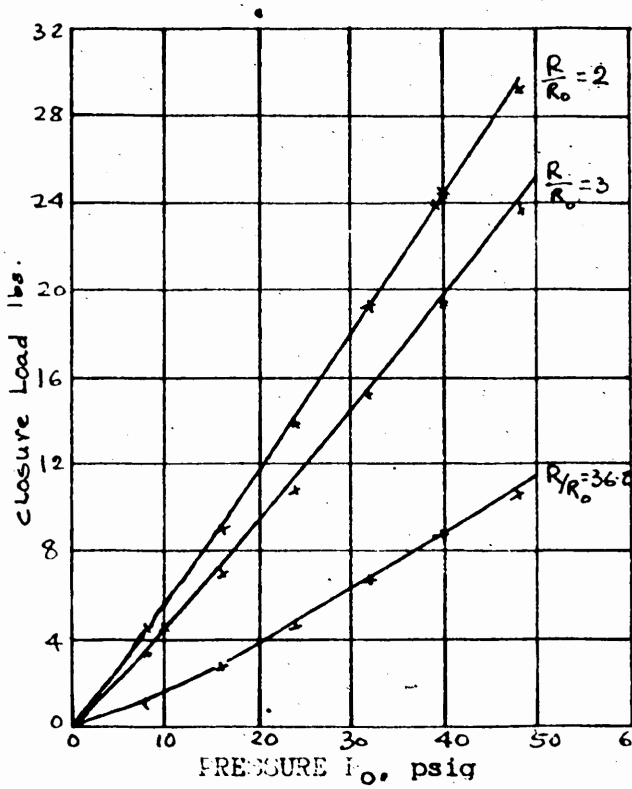

Closure load of pad bearings

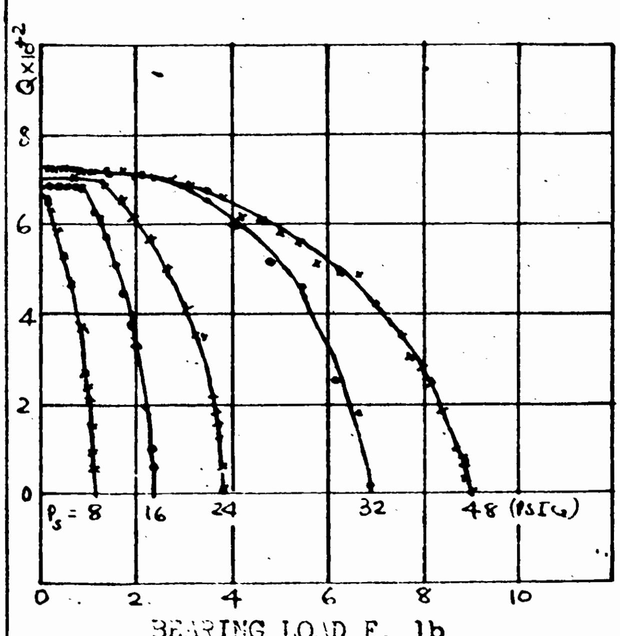

Rate of gas flow for pad bearing

FIGURE (2.7) – EXPERIMENTAL RESULTS OF LAUB.

His results are given in figure 2.8. From these figures it can be seen that

1. The pressure distribution is sensibly linear for a wide range of pressure ratios.
2. The change in pressure ratios with respect to h is most rapid for higher pressure ratios.
3. The pressure distribution in the secondary direction is linear but not constant as assumed in the earlier analysis of journal bearings.

Richardson also tested journal bearings. He subjected the test bearing to a wide range of loads with supply pressures up to 200 psi. His experimental results agree with his theoretical predictions within 20%. The discrepancies may be due to the assumptions of one dimensional flow.

Wunsch (8) has done experiments on thrust bearings with various amounts of set-back of the orifice plug as shown in figure 2.9. His experiments indicate that there is an optimum value of set-back for maximum load capacity. He also changed the orifice diameter, but found no effect on load capacity. His results are shown in figure 2.10.

Experiments on capillary compensated bearings were performed by Pigott and Macks (4). The parameters of their test bearings were as follows: (figure 2.1a)

1) $R_o = .905''$ $R = 1.079''$ $D = .062''$ and $.005''$ $d = .040''$ $L = 10'$, $n = 1$

2) $R_o = 2.5''$ $R = 3''$ $D = .005''$ $d = .040''$ $L = 10'$, $n = 4$

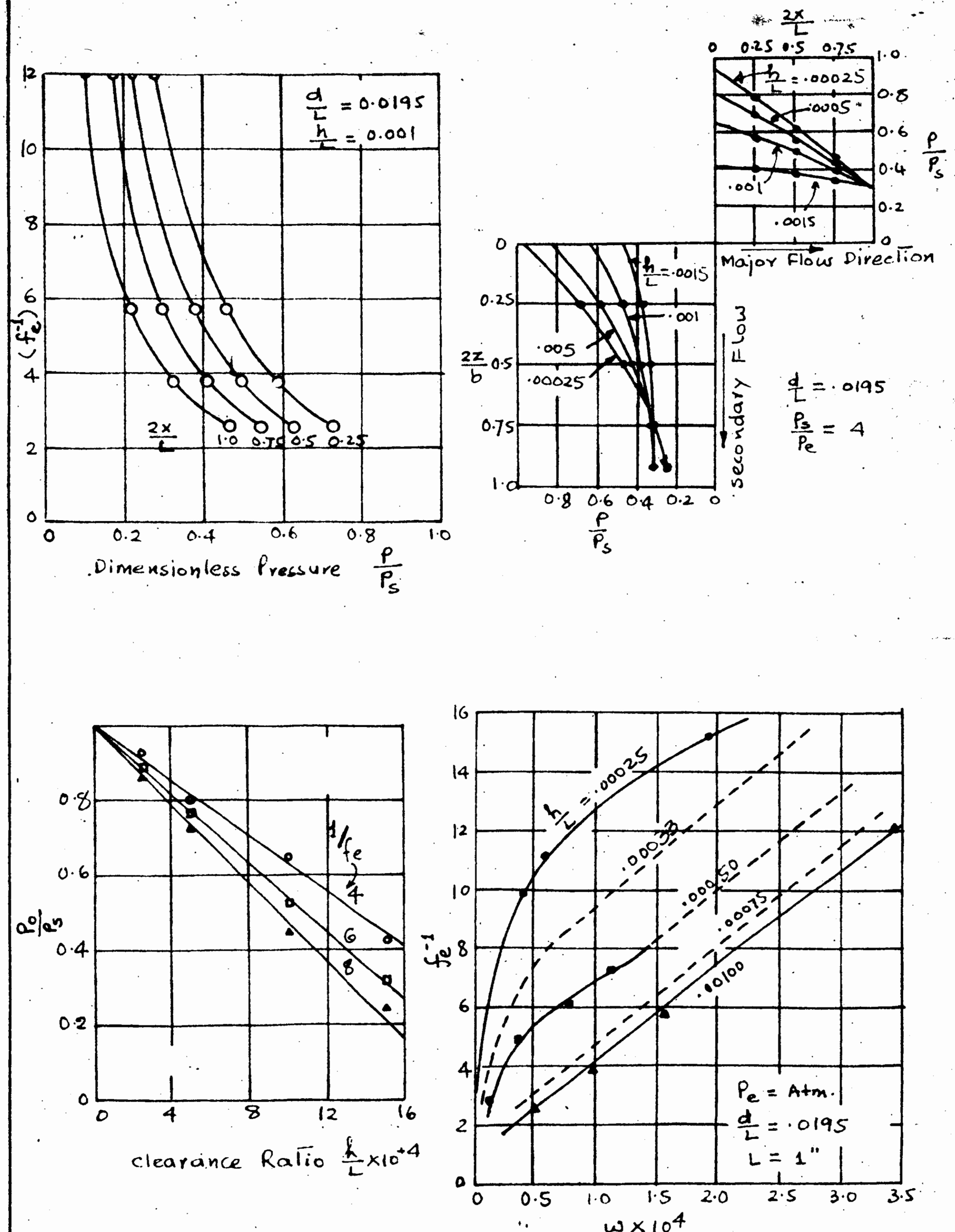

FIGURE (2.8) – EXPERIMENTAL RESULTS OF RICHARDSON.

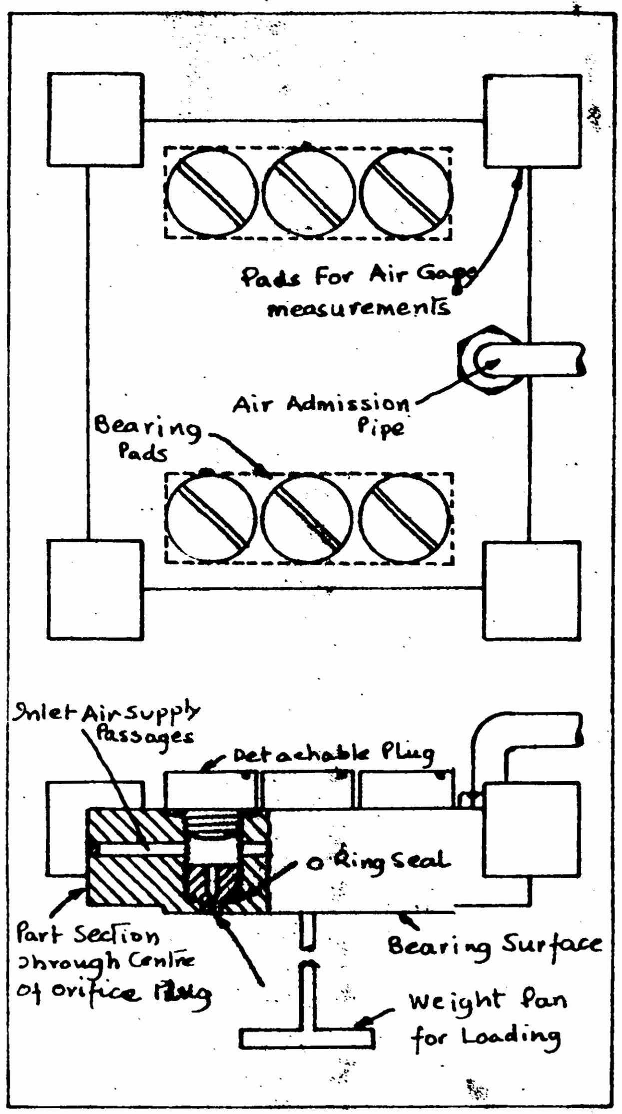

FIGURE (2·9) - GENERAL ARRANGEMENT OF WUNSCH's EXPERIMENTAL EQUIPMENT

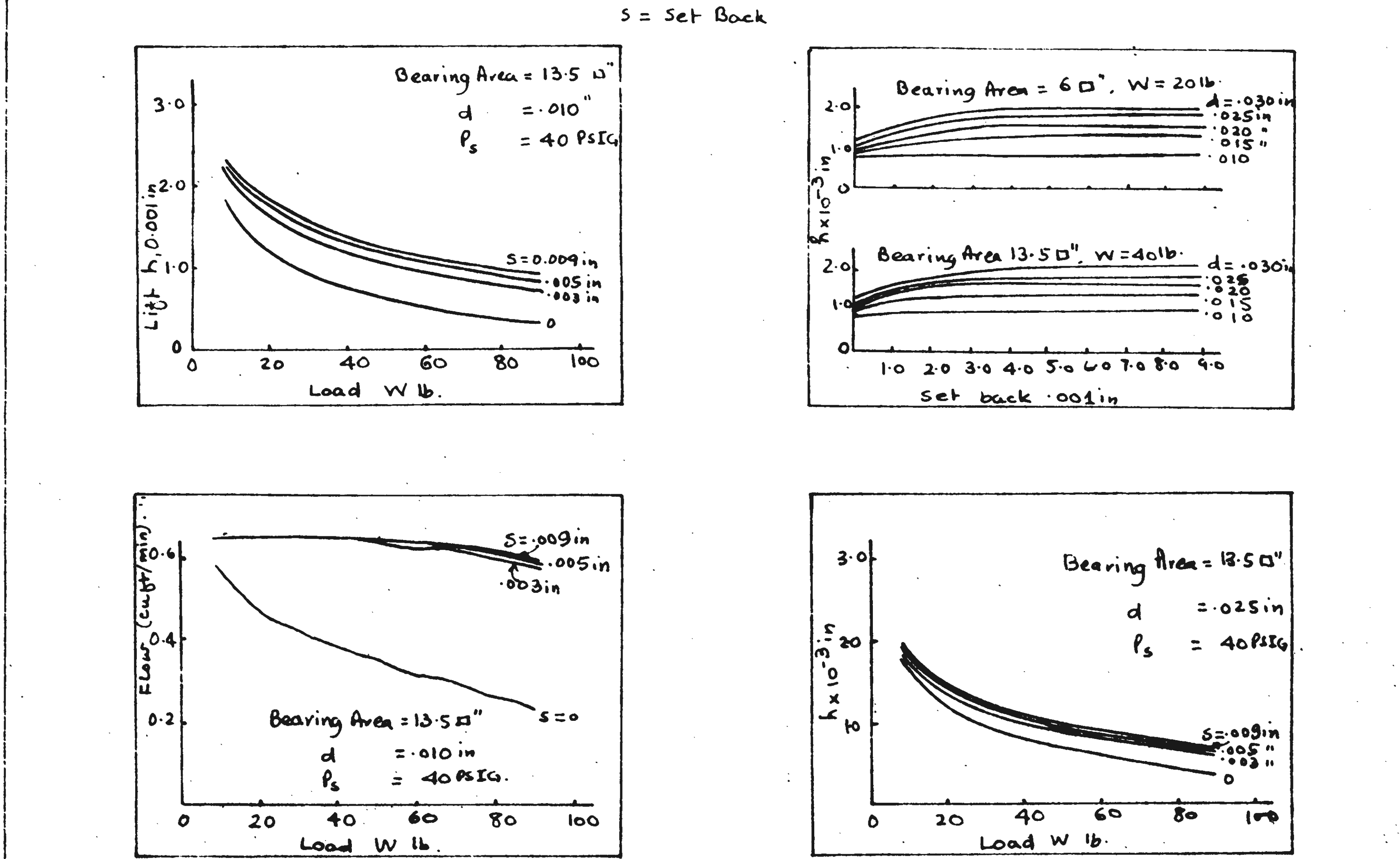

FIGURE (2.10) - EXPERIMENTAL RESULTS OF WUNSCH

They kept the temperature of the capillary tubes constant at 80° F and varied the bearing temperature from 80° F to 1000° F. Their results are shown in figure 2.11. From the experiments they concluded that:

1. The load carrying capacity increases with the increase in operating temperature.
2. The multiple pad design is more stable than the single pad design.

Experiments on spherical bearings were conducted by Corey et al (5), from which they derived the equations given earlier. They used spheres of 2", 4", and 6" diameters. Their results can be found in the reference (5).

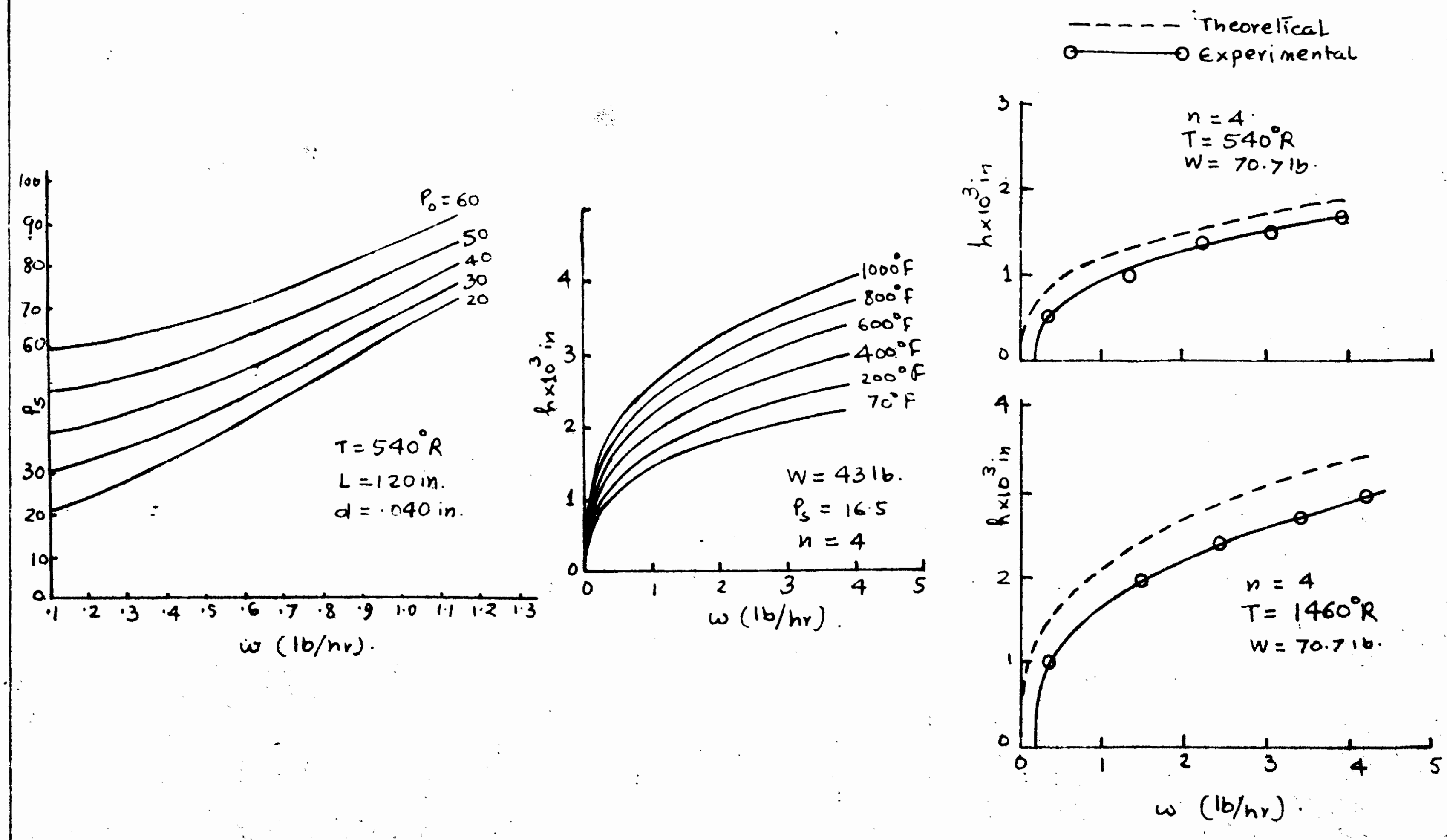

FIGURE (2·11) – EXPERIMENTAL RESULTS OF PIGOTT AND MACKS

3. STABILITY

The instability of gas bearings is one of the chief deterrents which have so far kept them out of use on a major scale. In hydrostatic thrust bearings the main reason for instability is the phenomenon known as "Air-hammer". The "Air-hammer" is caused by the longitudinal oscillations of the bearing disc. This phenomenon has been studied analytically in detail by various authors, and has been substantiated by experimental results. Roundebush (9) has given the simplest and probably the best analytical treatment of the problem along with curves showing the effects of various parameters on stability. (see Appendix 8) Licht et al (10) have determined the stability criteria by the application of Routh's stability criteria. They have found good agreement between theoretical predictions and experimental results. (see Appendix 9) The conclusions by both the authors can be summarized as follows:

1. For stability the air-storage capacity should be held to a minimum.
2. The recess depth D is the most important parameter affecting stability and hence it should be kept as small as possible. However, reduction of recess depth reduces the load carrying capacity and so a compromise should be sought.
3. The largest possible nozzle or orifice should be used.
4. The difference between the supply pressure P_s amd recess pressure P_o should be kept minimum.

5. The bearing should be operated at highest possible temperature.
6. The bearing should carry the maximum possible load within the safety limits of h.

From the above it is clear that the bearing parameters should be determined for a compromise of maximum load capacity and maximum stiffness. Practically the same considerations apply to journal bearings. Richardson (11) has shown that the inherent orifice compensated bearings as shown in figure 2.1b (where the recess depth is zero) are more stable than pool bearings. This seems to be logical.

In the case of spherical and conical bearings, spherical bearings are more stable. However, the stability of conical bearings can be increased by using two rings of inlet holes instead of one as shown in figure 2.4.

4. EFFECTS OF VARIOUS PARAMETERS ON THE PERFORMANCE

1. SPEED

It is generally agreed that the load carrying capacity of the bearing is augmented due to hydrodynamic action when the bearing is in rotation, but no quantitative data is available. Cole (12) also states that motion has a stabilizing effect so that unstable bearings will be stable at speed, but this seems unlikely to be generally true.

2. TEMPERATURE

As stated earlier, increase in temperature increases the load capacity and the stability of the bearing. In this connection it seems important to examine the assumptions of isothermal and adiabatic process in the bearing. Hughes and Osterle (13) have shown that air lubricated thrust bearings operate more nearly at isothermal conditions. So our analytical solutions are based on valid assumptions.

3. RATIO OF SPECIFIC HEATS

This can be determined experimentally by using different gases for lubrication. No information is available on this subject. However, it seems that the ratio of specific heats will have very little effect on the load capacity because bearings operate under isothermal conditions as shown earlier.

5. SOME PRACTICAL ASPECTS

To save the power consumed in the external pump system due to higher flow rates in comparison to liquid lubricated hydrostatic bearings, the clearances used are much smaller and so good filtration of gas supply is essential. It has been reported that with air filtered to exclude particles 4 micron and larger, maintenance is nil over periods of 2000 hours or better. About the effects of oil mist and moisture, the opinions are divided. Some authors claim that no trouble should be experienced if the bearings' materials are non-corrosive while others claim that the bearings become inoperative even with small quantities of oil mist or moisture. Due to small clearances the surface finish and geometric accuracies are of the same order as for hydrodynamic bearings.

Most journal bearing designs involve a symmetrical array of pressure holes or recesses even when the load is unidirectional. A simple way to assure equal volumes is to use cylindrical pockets made by drilling and plugging the bearing to a desired depth or to give the bearing an inner sleeve with predrilled pockets.

In the case of step bearings, to prevent galling, the steps and mating surfaces are flame plated with tungsten carbide--a fairly inexpensive but effective process. The step type bearings need not be kept clean. The best low cost material to date is 4130 steel shaft in 24 ST aluminium housing. Seal requirements for these bearings are almost negligible.

One particular form of bearing deserves mention in view of its simplicity. This makes use of porous (sintered) metal bush of the type normally used as oil impregnated, self-lubricated bearing. Used dry and supplied with air under pressure, it forms a useful self-regulating hydrostatic bearing and can be mounted in rubber O-rings to serve as anti-vibration mounts and as seals. In this form the bearing was first described by Montgomery and Sterry (14).

APPENDIX (4)

I. For an adiabatic flow through an orifice:

$$V = \sqrt{2gC_p(T_1-T_2)} \qquad \text{if approach velocity is small}$$

$$= \sqrt{\frac{2k}{k-1}R'T_1\left(1-\frac{T_2}{T_1}\right)} \qquad \left[\frac{T_2}{T_1} = \left(\frac{P_2}{P_1}\right)^{\frac{k-1}{k}}\right]$$

$$= \left[\frac{2k}{k-1}R'T_1\left\{1-\left(\frac{P_2}{P_1}\right)^{\frac{k-1}{k}}\right\}\right]^{1/2}$$

Weight flow $= C_d A_o V \rho_o g$ where C_d = discharge coefficient of orifice.

$$= C_d A_o g \rho_o\left[\frac{2k}{k-1}R'T_s\left\{1-\left(\frac{P_o}{P_s}\right)^{\frac{k-1}{k}}\right\}\right]^{1/2} \qquad \left[\rho_o = \frac{P_o}{R'T_s}\right]$$

$$= C_d A_o g\left[\frac{2k}{k-1}\frac{P_o^2}{R'T_s}\left(\frac{P_s}{P_o}\right)^{2-\frac{2}{k}}\left\{1-\left(\frac{P_o}{P_s}\right)^{\frac{k-1}{k}}\right\}\right]^{1/2}$$

$$= C_d A_o g\left[\frac{2k}{k-1}\frac{P_s^2}{R'T_s}\left\{\left(\frac{P_o}{P_s}\right)^{2/k}-\left(\frac{P_o}{P_s}\right)^{\frac{k+1}{k}}\right\}\right]^{1/2}$$

$$w_{in} = C_d A_o g P_s\left[\frac{2k}{(k-1)R'T_s}\left(f_o^{2/k}-f_o^{\frac{k+1}{k}}\right)\right]^{1/2} \qquad \text{------2.1}$$

II. For laminar, compressible viscous flow of a perfect gas under isothermal conditions through a narrow slot of rectangular shape.

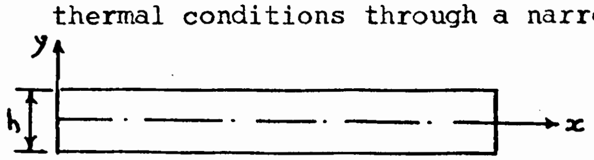

Consider a section of height $\pm$ y from the center line.

Balancing the forces:

$$P(2yb) - (P-dP)(2yb) - 2\tau b\,dx = 0$$

$$\text{or} \quad \tau = y\frac{dP}{dx}$$

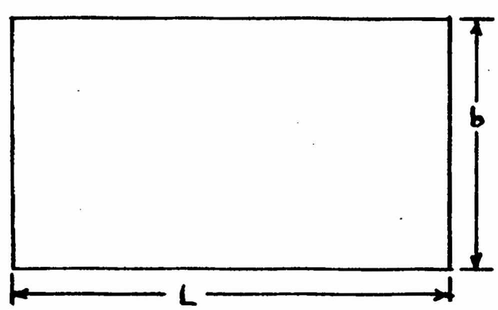

But for a Newtonian fluid

$$\tau = -\mu\frac{du}{dy}$$

$$\therefore\ du = -\frac{1}{\mu}\frac{dP}{dx}y\,dy$$

$$\int_0^u du = -\frac{1}{\mu}\frac{dP}{dx}\int_{h/2}^{y} y\,dy$$

$$u = \frac{1}{\mu}\frac{dP}{dx}\left(\frac{h^2}{8}-\frac{y^2}{2}\right)$$

Total volume flow, $Q = 2\int_0^{h/2}\frac{b}{\mu}\frac{dP}{dx}\left(\frac{h^2}{8}-\frac{y^2}{2}\right)dy = -\frac{bh^3}{12\mu}\frac{dP}{dx}$

Weight flow, $w = \rho g Q$ $\qquad \left[\rho = \frac{P}{R'T}\right]$

$$= -\frac{gbh^3}{12\mu R'T}P\frac{dP}{dx}$$

$$\therefore\ P\,dP = -\frac{12\mu R'Tw}{gbh^3}dx$$

$$\int_{P_1}^{P_2} P\,dP = -\int_0^L \frac{12\mu R' T_s w}{g b h^3}\,dx$$

$$\text{or } (P_2^2 - P_1^2) = -\frac{24\mu R' T_s w L}{g b h^3}$$

$$\text{or } \quad w = \frac{g b h^3}{24\mu R' T_s L}(P_1^2 - P_2^2)$$

$$\therefore\ w_{out} = \frac{g b h^3 P_s^2}{24\mu R' T_s L}(f_o^2 - f_e^2) \qquad \text{-------2.2}$$

III. For laminar, compressible viscous flow of a perfect gas under isothermal conditions through a narrow slot of circular shape. (radial flow)

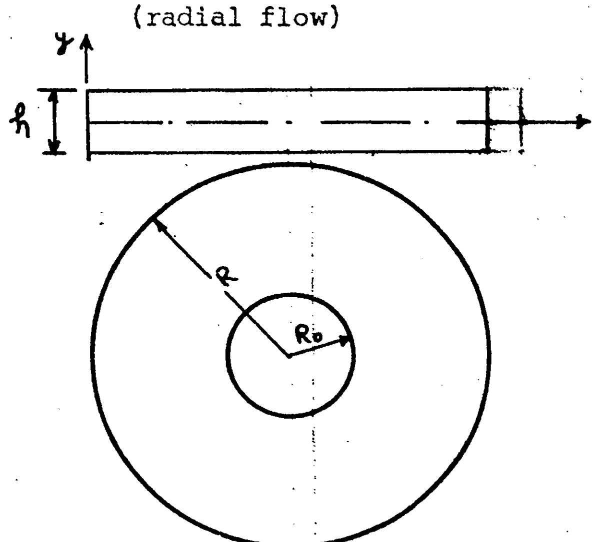

Consider a section of radius r of height $\pm$ y from the centre line. Balancing the forces:

$$P(2\pi r.2y) - (P-dP)(2\pi\,\overline{r+dr})2y - 2T(2\pi r dr) = 0$$

$$\text{or } T = y\frac{dP}{dr}$$

$$\text{But } \quad T = -\mu\frac{du}{dy}$$

$$\therefore\ du = -\frac{1}{\mu}\frac{dP}{dr}y\,dy$$

$$\int_0^u du = -\int_{h/2}^{y}\frac{1}{\mu}\frac{dP}{dr}y\,dy$$

$$u = \frac{1}{\mu}\frac{dP}{dr}\left(\frac{h^2}{8} - \frac{y^2}{2}\right)$$

Volume flow,

$$Q = \frac{1}{\mu}\frac{dP}{dr}2\pi r\int_0^{h/2} 2\left(\frac{h^2}{8} - \frac{y^2}{2}\right)dy$$

$$= -\frac{\pi}{\mu}\frac{dP}{dr}r\frac{h^3}{6}$$

Weight flow,

$$w = \rho g Q.$$

$$= \frac{-g\pi h^3}{6\mu R' T}P r\frac{dP}{dr}$$

$$P\,dP = -\frac{6\mu R' T w}{g\pi h^3}\frac{dr}{r}$$

$$\int_{P_1}^{P_2} P\,dP = -\frac{6\mu R' T w}{g\pi h^3}\int_{R_o}^{R}\frac{dr}{r}$$

$$(P_2^2 - P_1^2) = -\frac{12\mu R' T w}{g\pi h^3}\ln\frac{R}{R_o} \qquad \text{-------2.3}$$

$$w = \frac{g\pi h^3}{12\mu R' T \ln R/R_o}(P_1^2 - P_2^2)$$

For our case $P_1 = P_o$ and $P_2 = P_e$,

$$w_{out} = \frac{g\pi h^3 P_s^2}{12\mu R' T_s \ln R/R_o}(f_o^2 - f_e^2) \qquad \text{-------2.4}$$

IV. For laminar, compressible viscous flow of a perfect gas under isothermal conditions through a capillary:

Considering a section of radius y as shown and neglecting gravity and inertia forces:

Balancing the forces on the section:

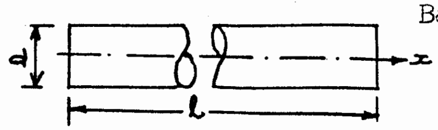

$$P(\pi y^2) - (P - dP)(\pi y^2) - \tau(2\pi y\,dx) = 0$$

$$\text{or} \quad \tau = y\frac{dP}{dx}$$

$$\text{But} \quad \tau = -\mu\frac{du}{dy}$$

$$\therefore \; du = -\frac{1}{\mu}\frac{dP}{dx}dy \quad \text{or} \quad \int_0^u du = -\int_{d/2}^{y}\frac{1}{\mu}\frac{dP}{dx}dy$$

$$\therefore \; u = \frac{1}{\mu}\frac{dP}{dx}\left(\frac{d^2}{8} - \frac{y^2}{2}\right)$$

Volume flow, $$Q = \frac{1}{\mu}\frac{dP}{dx}\int_0^{d/2}\left(\frac{d^2}{8} - \frac{y^2}{2}\right)2\pi y\,dy$$

$$= \frac{\pi d^4}{128\mu}\frac{dP}{dx}$$

Weight flow, $$w = \rho g Q = \frac{g\pi d^4}{128\mu}\frac{P}{R'T}\frac{dP}{dx}$$

$$\text{or} \quad P\,dP = \frac{128\mu R'Tw}{g\pi d^4}dx$$

$$\int_{P_1}^{P_2} P\,dP = \frac{128\mu R'Tw}{g\pi d^4}\int_0^l dx$$

$$(P_2^2 - P_1^2) = \frac{256\mu R'Tlw}{g\pi d^4}$$

$$w = \frac{g\pi d^4}{256\mu R'Tl}(P_2^2 - P_1^2)$$

For our case $P_2 = P_s$, $P_1 = P_o$

$$w_{in} = \frac{g\pi d^4 P_s^2}{256\mu R'T_s l}(1 - f_o^2) \qquad \text{------2.5}$$

APPENDIX (5)

Laub (1) considered circular pad thrust bearing. In steady state $\dot{W}$ in = $\dot{W}$ out. Therefore equating equations 2.1 and 2.4:

$$\frac{8\pi h^3 P_s^2}{12\mu R' T_s \ln R/R_o}(f_o^2 - f_e^2) = \dot{\omega} in$$

$$\text{or } h^3 = \left[\ln\frac{R}{R_o}\frac{12\mu}{\pi}\frac{R'T_s}{(P_s^2)(f_o^2-f_e^2)}\frac{\dot{w}in}{g}\right]$$

$$h = \left[\ln\frac{R}{R_o}\frac{12\mu}{\pi}\frac{1}{P_s(f_o^2-f_e^2)}Q_{in}\right]^{1/3} \qquad \text{------2.6}$$

This expression permits the calculation of h for varying pressure P_o, given bearing geometry and supply pressure P_s.

LOAD CARRYING CAPACITY: The capacity can be calculated from the force balance between the load W and the force F exerted on the load plate by the pressure P of the gas. The radial distribution of pressure between $r = R_o$ and $r = R$ can be derived from equation 2.3

$$\frac{P^2 - P_o^2}{P_e^2 - P_o^2} = \frac{\ln\frac{r}{R_o}}{\ln R/R_o}$$

$$\text{or } P = P_o\left\{1 - \frac{\ln\frac{r}{R_o}}{\ln R/R_o}(1 - f_a^2)\right\}^{1/2} \qquad \left[f_a = \frac{P_e}{P_o}\right] \qquad \text{------2.7}$$

Typical pressure profiles for two values of R/R_o are shown in figure 2.2.

Now $$W = F = \pi R_o^2 P_o + \int_{R_o}^{R} 2\pi r\,dr.P - \pi R^2 P_e$$

Inserting for P from equation 2.7 in above, we get

$$W = \pi P_o\left[R_o^2 + 2\int_{R_o}^{R}\left\{1 - \frac{\ln r/R_o}{\ln R/R_o}(1-f_a^2)\right\}^{1/2} r\,dr - R^2\frac{P_e}{P_o}\right] \text{--2.8}$$

In the integral, $\frac{1-f_a^2}{\ln R/R_o} = B =$ constant for a given load and so the integral can be written as:

$$I = \int_{R_o}^{R}\left\{1 - B\ln\frac{r}{R_o}\right\}^{1/2} r\,dr$$

The term in the bracket could be expanded into series but the convergence is very poor except at very small values of P_e/P_o which is not the usual case. But we can obtain a closed solution of I by substituting:

$$t = (1 - B\ln \tfrac{r}{R_o})^{1/2}$$

$$\text{or } r = R_o e^{\frac{1-t^2}{B}}$$

$$dr = -R_o \frac{2t}{B} e^{\frac{1-t^2}{B}} dt$$

$$I = -\int_1^{f_a} \frac{2R_o^2}{B} t^2 e^{\frac{2(1-t^2)}{B}} dt$$

$$= \frac{R_o^2 e^{2/B}}{2}\left[t e^{-\frac{2}{B}t^2}\Big|_1^{f_a} - \int_1^{f_a} e^{-\frac{2}{B}t^2} dt\right]$$

$$= \frac{R_o^2 e^{2/B}}{2}\left[f_a e^{-\frac{2}{B}f_a^2} - e^{-\frac{2}{B}} - \sqrt{\frac{B}{2}}\int_{\sqrt{\frac{2}{B}}}^{f_a\sqrt{\frac{2}{B}}} e^{-\frac{2}{B}t^2} d\left(\sqrt{\tfrac{2}{B}}t\right)\right]$$

$$= \frac{R_o^2}{2}\left[f_a e^{2\ln R/R_o} - 1 - e^{2/B}\sqrt{\frac{\pi B}{8}}\left\{\mathrm{Erf}\left(f_a\sqrt{\tfrac{2}{B}}\right) - \mathrm{Erf}\left(\sqrt{\tfrac{2}{B}}\right)\right\}\right]$$

Where Erf = Error Function.

Substituting this value of I in load equation 2.8 we get

$$F = \pi P_o\left[R_o^2 + 2I - R^2\frac{P_e}{P_o}\right]$$

$$= \pi P_o R_o^2 e^{2/B}\sqrt{\frac{\pi B}{8}}\left[\mathrm{Erf}\sqrt{\tfrac{2}{B}} - \mathrm{Erf}\left(f_a\sqrt{\tfrac{2}{B}}\right)\right]$$

In this putting

$$r' = R/R_o \quad \text{and} \quad A_R = \pi R^2 \quad \text{we get}$$

$$F = A_R P_o\left(\frac{1}{r'}\right)^2 e^{2/B}\sqrt{\frac{\pi B}{8}}\left[\mathrm{Erf}\sqrt{\tfrac{2}{B}} - \mathrm{Erf}\left(f_a\sqrt{\tfrac{2}{B}}\right)\right]$$

Load carried by a bearing of unit area:

$$H = P_o\left(\frac{1}{r'}\right)^2 e^{2/B}\sqrt{\frac{\pi B}{8}}\left[\mathrm{Erf}\sqrt{\tfrac{2}{B}} - \mathrm{Erf}\left(f_a\sqrt{\tfrac{2}{B}}\right)\right]$$

H has been plotted against r' for various values of P_o in figure 2.2. It is interesting to note how sharply the maximum load capacity increases at low ratios of r' corresponding to large recess areas. However, this gain in lift decreases h and the bearing becomes impracticable for safe operation.

APPENDIX (6)

McNeilly (2) has used orifice in which the recess depth is zero as shown in figure 2.12. This gives a smaller load capacity but a more stable bearing. This type is called inherent-orifice compensated bearing. McNeilly has shown that we get a bearing of maximum stiffness at a gap slightly less than that at which the orifice flow becomes 'choked' due to sonic velocity. So he has developed a design procedure for complete journal bearings operating under 'choked' flow conditions. By putting numerical values in equation 2.1 and assuming that complete recovery of velocity head occurs in the orifice he obtains the following equation for 'choked' flow corrected to exhaust conditions (P_e).

$$Q_{in} = 1250\, h\, d\, P_s \qquad \text{------2.9}$$

where $\frac{P_e}{P_s} = .53,\ A_o = \pi d h\ ,\ C_d = .76,\ k = 1.4\ ,\ P_e = 14.7$ and $\rho_e = 11.6 \times 10^{-8}$

He also defines a pressure efficiency as follows

$$\eta = \frac{W/\pi R^2}{P_s - P_e}$$

He has plotted the η against film thickness h as shown in figure 2.13.

Now suppose we have two such bearings opposing each other as illustrated schematically in figure 2.12. The resulting load capacity becomes the difference in the forces from the two individual thrust units and the gap on one side increases to a maximum of 2h while that on the other side decreases to zero. In order to avoid metal contact, we shall arbitrarily design for: (figure 2.12)

$$\epsilon = \frac{c}{h} = \frac{1}{2}$$

The load capacity for design in this case is:

$$W = F_{(h-e)} - F_{(h+e)}$$

$$= F_{h/2} - F_{3h/2}$$

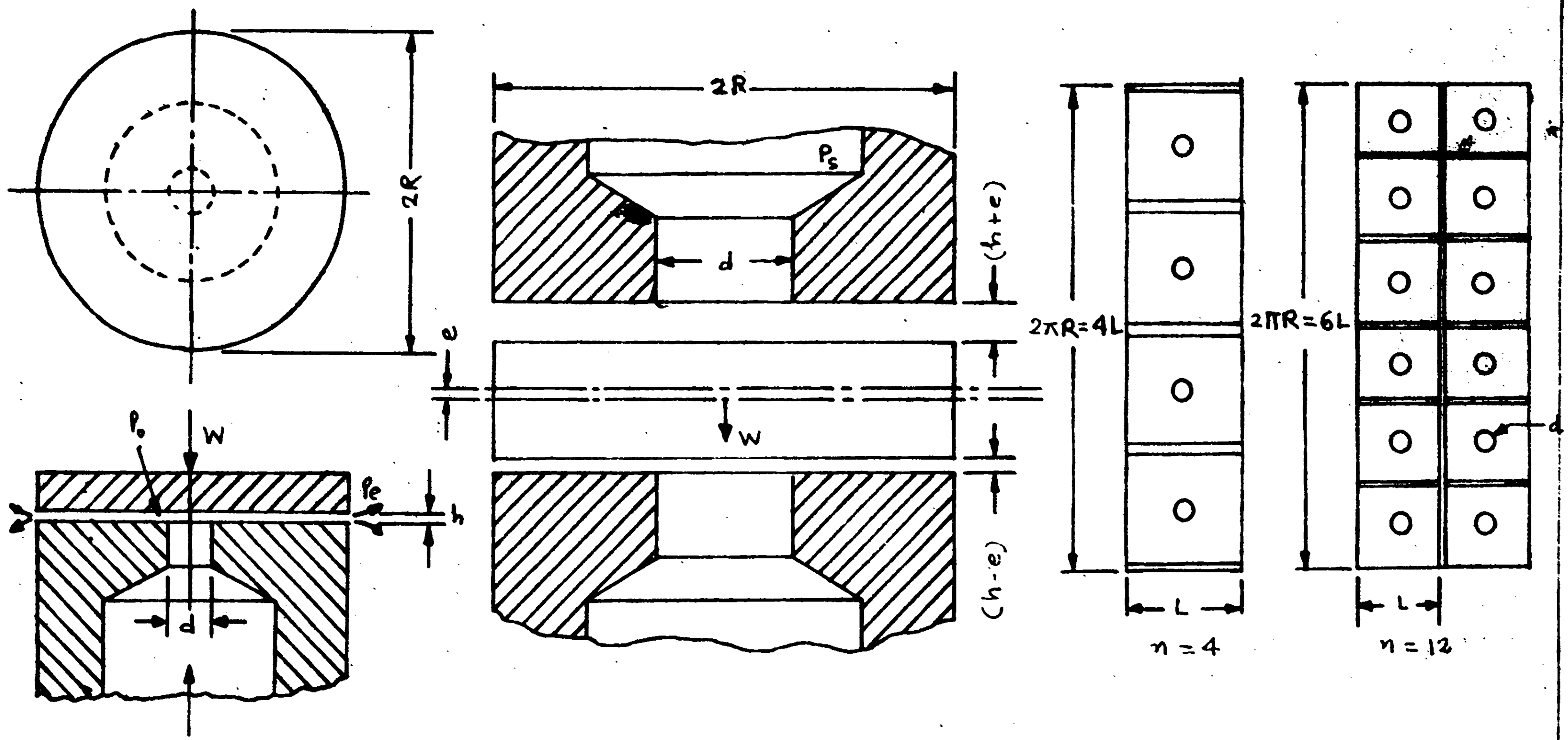

Single-Hole Circular Thrust Bearing, the Basic Unit for Design of Pneumostatic Bearings with Inherent Orifice Compensation.

Two Opposed Thrust Discs Acting on the Same Movable Member.

Examples of Developed Surfaces of Complete Journal Bearings. Projected Area $= \frac{4nR^2}{\pi}$

FIGURE (2.12) — OPPOSED THRUST DISCS OF McNEILLY

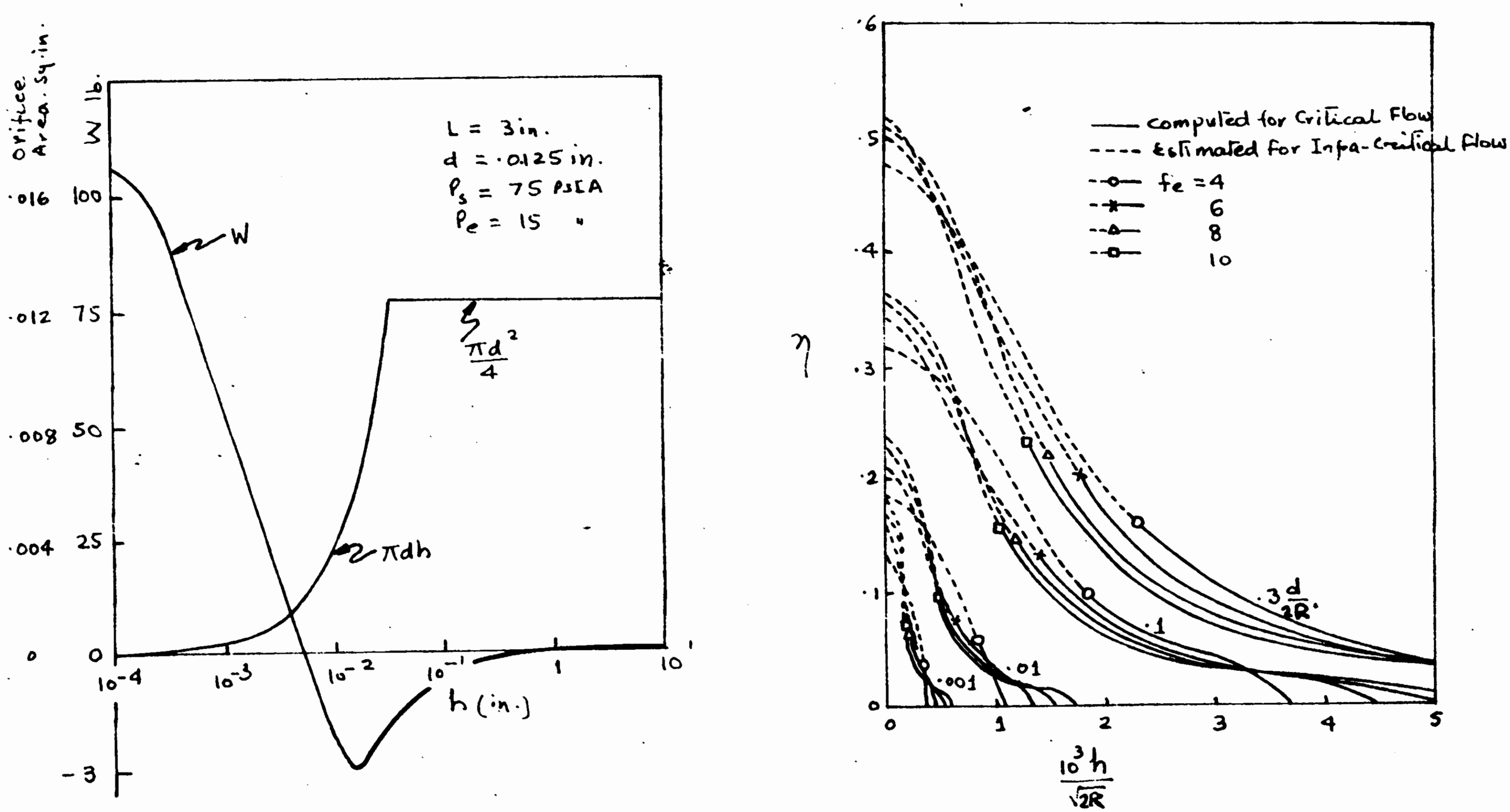

FIGURE (2.13) – DESIGN CURVES OF McNEILLY and the pressure η, defined as before is now

$$\frac{W/\pi R^2}{P_s - P_e} = \eta_{h/2} - \eta_{\frac{3h}{2}}$$

The total flow from equation 2.9 is merely

$$Q_{in} = 2500\, h d P_s$$

Q is independent of c because the increase in flow on one side is compensated by the decrease on the other.

COMPLETE JOURNAL BEARING: If we consider a complete cylindrical bearing we can use the same results with sufficient accuracy by proportioning the layout of the holes so as to approximate the radially outward symmetrical flow assumed above. Table III lists suggested number of holes and rows in terms of the overall length diameter ratio of the bearing. If there are n holes, the load capacity and gas flow are given by:

$$W = \frac{n}{2}(\pi R^2)(P_s - P_e)(\eta_{h/2} - \eta_{\frac{3h}{2}})$$

$$Q_{in} = 1250\, n \cdot h \cdot d \cdot P_s$$

So it is possible to design a bearing by choosing suitable values of P_s, h and d. McNeilly has given two examples in his paper.

TABLE III

RECOMMENDED HOLE LAYOUT FOR VARIOUS LENGTH/DIAMETER RATIOS

Length/Diameter Ratio	Row of Holes	Number of Holes Per Row	Total Holes
0.1	1	30	30
0.2	1	15	15
0,3	1	10	10
0.4	1	8	8
0.5	1	6	6
0.6	1	5	5
0.7	1	4	4
0.8	1	4	4
0.9	2	7	14
1.0	2	6	12
1.25	2	5	10
1.50	2	4	8
1.75	3	6	18
2.0	3	5	15
2.5	3	4	12

APPENDIX (7)

Richardson (3) has treated inherent orifice compensated bearings and he has introduced new variable F_o for plotting his design curves where: (figure 2.1b)

$$F_o = \sqrt{\frac{k-1}{2gkR'T_s}}\ \frac{bP_s}{24\mu\pi C_d}\ \frac{h^2}{Ld}$$

Physically the quantity F_o represents the ratio of the downstream laminar flow conductance $\frac{P_s^2 h^3 b}{\mu R' T_s}$ to the upstream orifice flow conductance $\frac{dhP_s}{R'T_s}$. He has shown that the stiffness and weight flow are functions of F_o, which he has plotted as shown in figure 2.14. In this figure

$$\eta = \frac{2\Delta F}{P_s LR}, \quad \epsilon = \frac{\Delta h}{h}, \quad \Delta = \text{small change}$$

It should also be noted that the ratio $\frac{\eta}{\epsilon}$ represents the stiffness of the bearing because

$$\frac{\eta}{\epsilon} = \frac{\Delta F}{\Delta h} \cdot \frac{2h}{P_s LR}$$

Therefore, if an optimum bearing is defined as one which has a maximum load carrying capacity per unit of supply pressure P_s, then the design value of F_o should be such as to place $\frac{\eta}{\epsilon}$ near the peak value of the stiffness curve of figure 2.14. Since the mass flow of air required to support a load increases with F_o, the minimum air flow is obtained when F_o is small, as shown in figure 2.14. As an

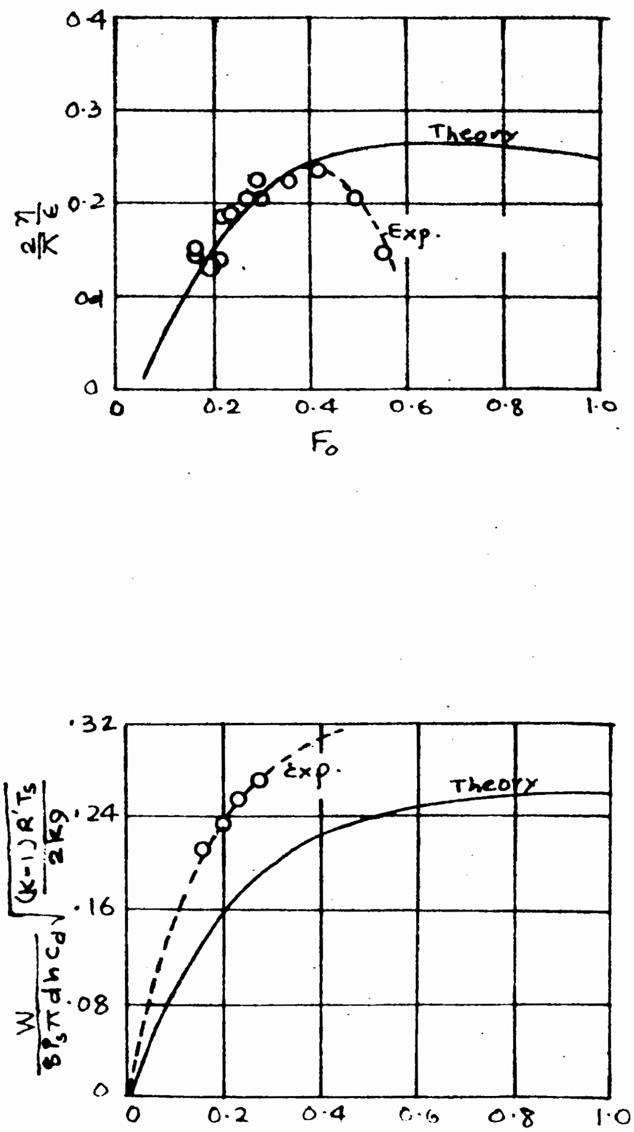

FIGURE (2·14) - RICHARDSON'S DESIGN CURVES.

example consider the design of a bearing for a load of 18 pounds and supply pressure of 150 psia taking a factor of safety 2, and number of feed holes = 8

$$\Delta F = 36 \text{ lbs.} \quad P_s = 150$$

To optimize the design as explained earlier, from figure 2.14

$$F_o = 0.4, \quad \frac{2}{\pi}\frac{\eta}{\epsilon} = 0.25, \quad \frac{W}{8 P_s \pi d h C_d}\sqrt{\frac{(k-1) R' T_s}{2 k g}} = 0.22$$

From these relations assuming the following values from practical considerations:

$$\epsilon = 0.5, \quad L = 1 \text{ in.} \quad C_d = 0.90 \text{ and } d = 0.020''$$

We get the geometric parameters of the bearing as follows

$$L = 1'', \quad R = 0.625 \text{ in.} \quad b = 0.49 \text{ in.}, \quad d = 0.020 \text{ in} \ \& \ h = .00075 \text{ in.}$$

APPENDIX (8)

From equation 2.7 the pressure profile in the circular pad thrust bearing is given by: (figure 2.1a)

$$P = P_o\left[1 - \frac{\ln r/R_o}{\ln R/R_o}(1-f_e^2)\right]^{1/2} \quad \text{where } R_o < r < R$$

A reasonable approximation is obtained by taking P to vary with r as a straight line which is true for larger values of R_o/R as seen from figure 2.2. With this simplification, the expression for P becomes:

$$P - P_e = \frac{P_o - P_e}{R_o - R}(r - R) \qquad \text{------2.10}$$

The force F exerted on the upper plate of the bearing is given by:

$$F = 2\pi\int_{R_o}^{R}(P-P_e)r\,dr + \pi R_o^2(P_o - P_e)$$

$$= 2\pi\int_{R_o}^{R}\frac{P_o-P_e}{R_o-R}(r-R)r\,dr + \pi R_o^2(P_o-P_e)$$

$$= \frac{\pi}{3}\left[R_o^2 + RR_o + R^2\right](P_o - P_e) \qquad \text{------2.11}$$

In non-steady state w in $\neq$ w out; but

$$\omega_{in} - \omega_{out} = \frac{d(\rho_o V_s)}{dt}$$

$$\left[V_s = \pi R_o^2(h+D)\right] \qquad \therefore \frac{\omega_{in} - \omega_{out}}{\pi R_o^2} = (h+D)\frac{d\rho_o}{dt} + \rho_o\frac{dh}{dt} \qquad \text{------2.12}$$

Noting that the subscript i denotes the initial conditions of parameters, for reversible adiabatic compression:

$$\rho_o = \rho_{o,i}\left(\frac{P_o}{P_{oi}}\right)^{1/k}$$

$$\frac{d\rho_o}{dt} = \frac{1}{k}\frac{\rho_{oi}}{P_{oi}^{1/k}}P_o^{\frac{1-k}{k}}\frac{dP_o}{dt} \qquad \text{------2.13}$$

Substituting equation 2.13 into 2.12, we get

$$\frac{\omega_{in} - \omega_{out}}{\pi R_o^2} = \rho_{oi}\left(\frac{f_o}{f_{oi}}\right)^{1/k}\left[\frac{h+D}{kf_o}\frac{df_o}{dt} + \frac{dh}{dt}\right]$$

The further assumption is made that the kinetic energy in the orifice flow is completely converted to internal energy in the bearing pad so that $T_{oi} = T_s$. Substituting for W in and W out from equation 2.1 and 2.4 and further reducing gives:

$$\frac{dh}{dt} = -\frac{1}{f_o}\left[\frac{h+D}{k}\frac{df_o}{dt} - \left(\frac{f_o}{f_{oi}}\right)^{\frac{k-1}{k}}\left\{\frac{gA_o\sqrt{R'T_s}}{\pi R_o^2\sqrt{\frac{k-1}{2k}}} f_o^{1/k}\left(1 - f_o^{\frac{k-1}{k}}\right)^{1/2} - \frac{\rho_s g(f_o^2 - f_e^2)h^3}{12R_o^2\mu \ln R/R_o}\right\}\right] \qquad \text{------2.14}$$

Similar reasoning for isothermal compression in the pad leads to:

$$\frac{dh}{dt} = -\frac{1}{f_o}\left[(h+D)\frac{df_o}{dt} - \frac{gA_o\sqrt{R'T_s}}{\pi R_o^2\sqrt{\frac{k-1}{2k}}} f_o^{1/k}\left(1 - f_o^{\frac{k-1}{k}}\right)^{1/2} + \frac{g\rho_s(f_o^2 - f_e^2)h^3}{12\mu R_o^2 \ln R/R_o}\right] \qquad \text{------2.15}$$

Either equation 2.14 or 2.15 is used as one of a pair of simultaneous differential equations in f and h. Another is obtained by equating the product of the mass and acceleration of the bearing to the forces acting on it.

$$M\frac{d^2h}{dt^2} = (F - W) - a\frac{dh}{dt}$$

Where a is the damping coefficient. In present analysis a = o. Substituting for F from equation 2.11 gives the second equation in h and f.

$$\frac{d^2h}{dt^2} = \frac{\pi}{3M}\left(R_o^2 + RR_o + R^2\right)(f_o - f_e)\rho_s - \frac{W}{M} \qquad \text{------2.16}$$

Equations 2.14 and 2.16 have been used in the analysis. In the present analysis the bearing is assumed to be in a state of initial equilibrium (denoted by subscript i) under a constant load F_i. At time t = 0, a change in the loading function occurs (usually a step change to a value F_f) which puts the bearing temporarily out of equilibrium. The bearing then begins to hunt for the new equilibrium clearance h_f corresponding to the new load F_f. If the bearing settles out or oscillates with constant amplitude, it is said to be stable. If it oscillates with increasing amplitude, it is unstable. It is convenient to plot the behavior of the bearing as dimensionless clearance parameter $(h - h_f)/(h_i - h_f)$.

As a standard example, an unstable bearing configuration is selected. The pertinent bearing parameters are then varied one at a time in order to examine the ability of each to stabilize the bearing. The standard example has the following characteristics:

R, in. 6

R_o, in. 4

A_e, sq in. 0.003

d, in. 0.008

k..1.4

W, lb...32.172

P_e, lb/sq in. 14.7

T, °R...530

F_i, lb...500

h_i, in...0.002

F_f, lb...550

The results are presented mostly as plots of the bearing clearance parameter $(h - h_f)/(h_i - h_f)$ against time as important bearing parameters are varied in figures 2.15 to 2.20.

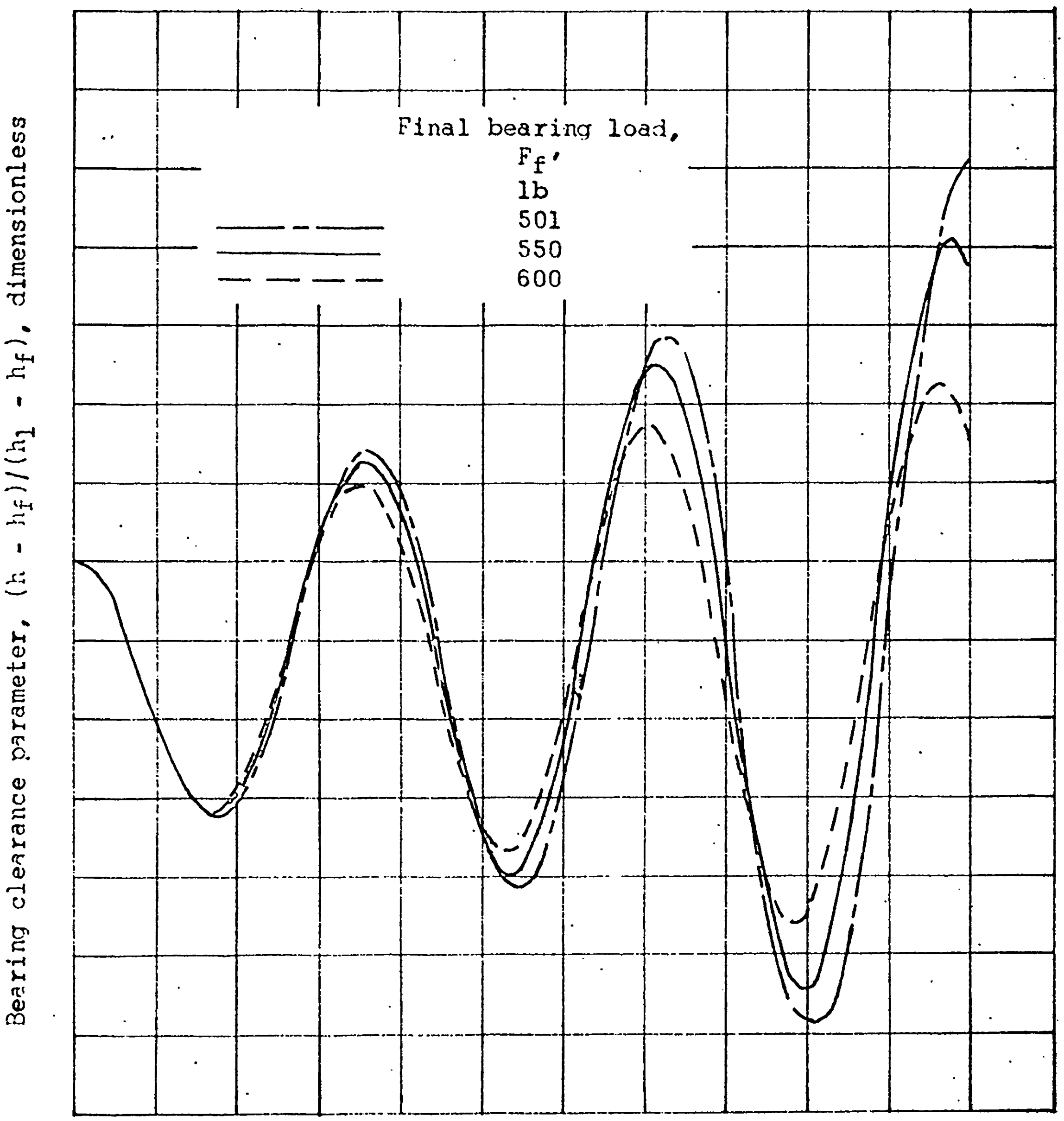

(b) Clearance parameter

Figure(2.15) ⟶ Effect of several values of final bearing load on time variation of bearing clearance and clearance parameter.

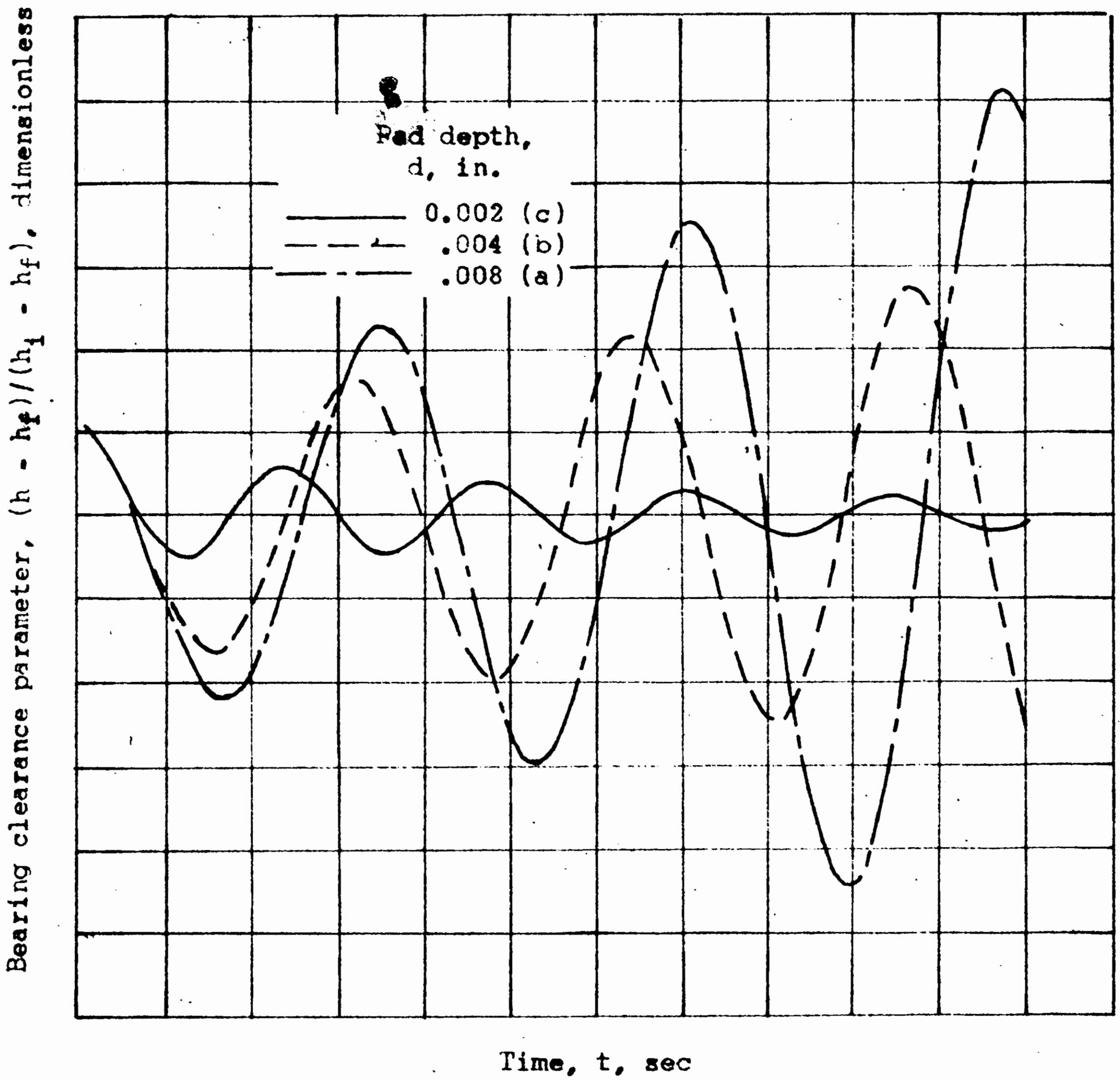

Figure(2.16)Effect of variation of pad depth on clearance parameter.

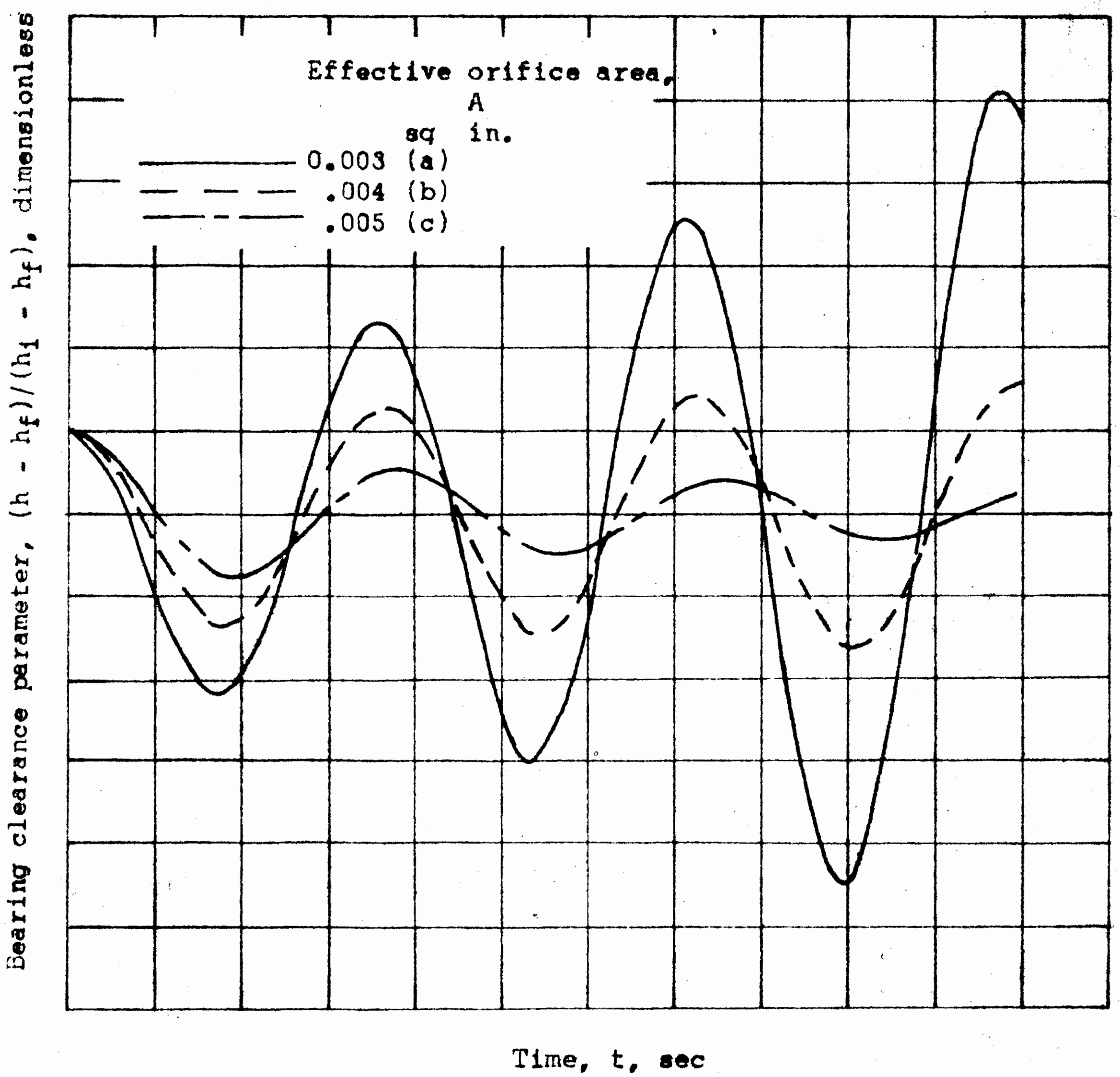

Figure(2.17)Effect of variarion of orifice area on clearance parameter.

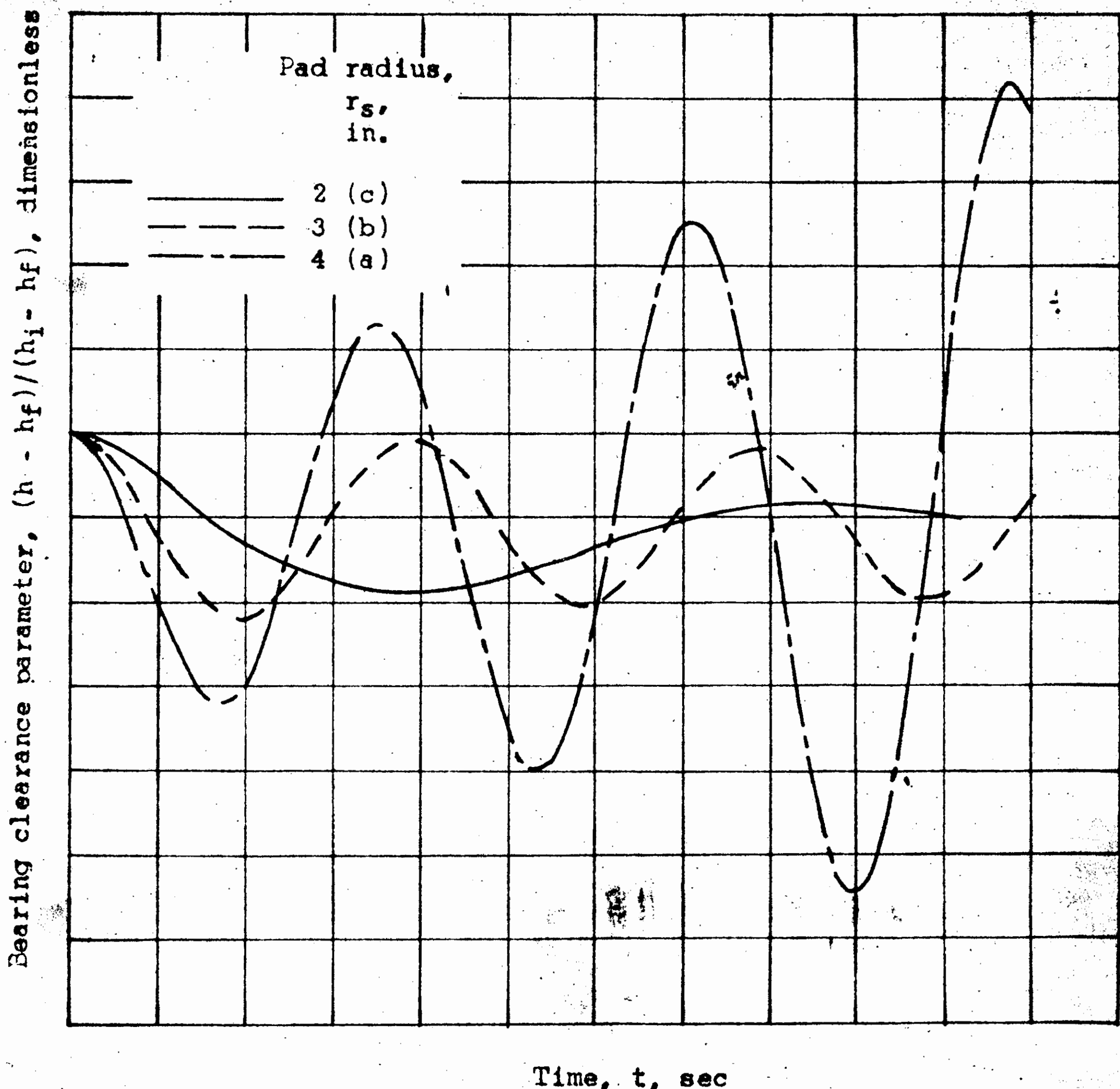

Figure (2.18) Effect of variation of pad radius on clearance parameter.

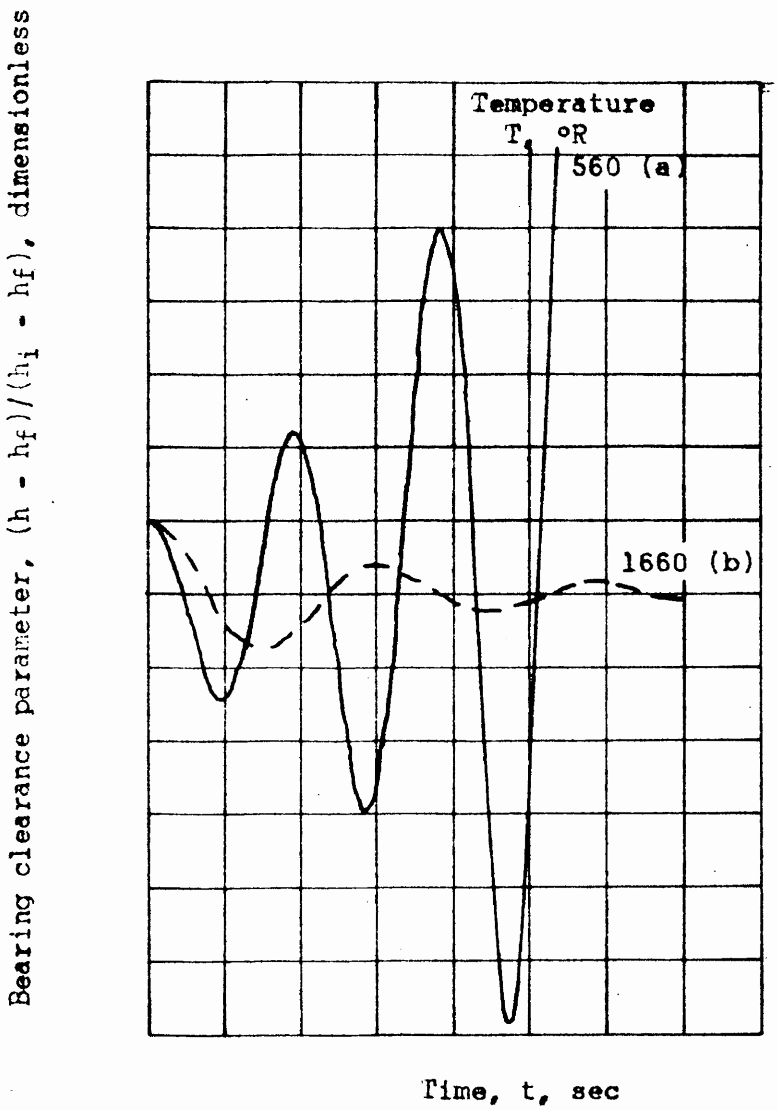

Figure(2·19) Effect of temperature on clearance parameter variation for high-load bearing. F_i = 15,000 pounds.

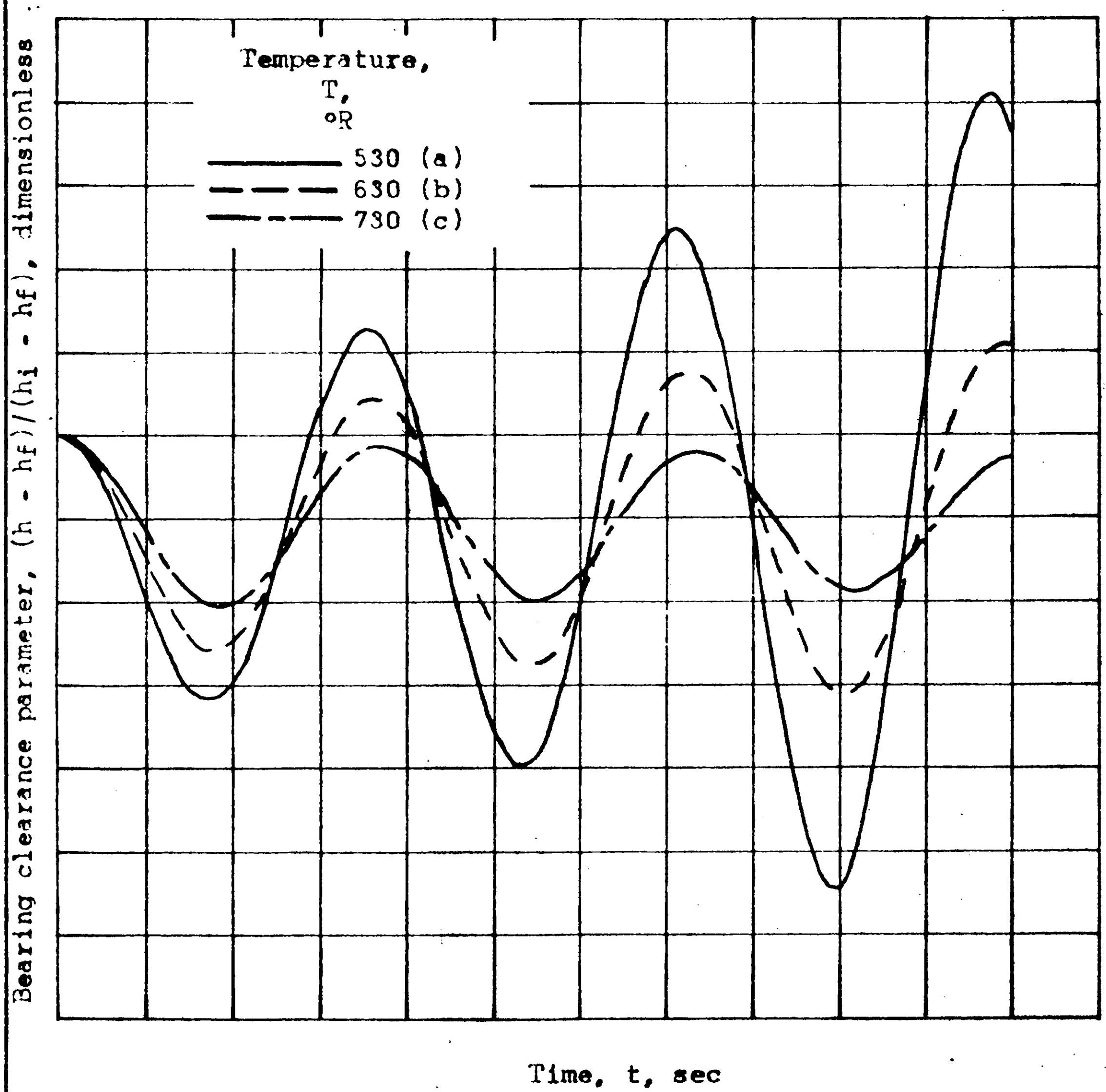

Figure(2.20) Effect of variation of air temperature on clearance parameter.

APPENDIX (9)

Assuming linear pressure distribution in the annulus

$$P = P_o - (P_o - P_e)\frac{r - R_o}{R - R_o} \quad \text{where } R_o < r < R \qquad \text{-----2.17}$$

Now for a small change of pressure p_o in the recess for a small change in film thickness δ, the change in force due to gas pressure on the upper bearing plate is given by:

$$\Delta F = \int_0^{R_o} (2\pi r dr)\, p_o + \int_{R_o}^{R} (2\pi r dr)\, \Delta P$$

Substituting for ΔP from equation 2.17,

$$\Delta F = \int_0^{R_o} (2\pi r dr)\, p_o + \int_{R_o}^{R} (2\pi r dr)\left[p_o - p_o \frac{r - R_o}{R - R_o}\right]$$

$$= 2\pi\left[\int_0^{R} p_o r dr - \int_{R_o}^{R} p_o \frac{r - R_o}{R - R_o} r dr\right]$$

$$= p_o \pi\left[R^2 - \frac{2R^3 + R_o^3 - 3R^2 R_o}{3(R - R_o)}\right]$$

$$= p_o \pi R_f^2$$

$$= p_o A_f$$

where subscript f means effective.

Where $R_f^2 = \left[R^2 - \dfrac{2R^3 + R_o^3 - 3R^2 R_o}{3(R - R_o)}\right]$ and $A_f = \pi R_f^2$ -----2.18

Now $$-\Delta F = M\frac{d^2\delta}{dt^2} = p_o A_f \qquad \text{-----2.19}$$

Licht et al (10) have shown that the mass flow into the bearing depends on the recess pressure only whereas the outflow is a function of the recess pressure p_o as well as the annulus height h. To small deviations from the equilibrium point (p_o and δ) there correspond variations in inflow and outflow which to the first degree of approximation, can be written respectively as:

$$\Delta w_{in} = \left(\frac{\partial w_{in}}{\partial P}\right)_q p_o = -\alpha p_o$$

$$\Delta\omega_{out} = \left(\frac{\partial \omega_{out}}{\partial P}\right)_q p_o + \left(\frac{\partial \omega_{out}}{\partial h}\right)_q \delta = \beta p_o + \Theta\delta \qquad \text{----2.20}$$

The time rate of change of the bearing air mass content then becomes:

$$\Delta\omega = \Delta\omega_{in} - \Delta\omega_{out} = -(\alpha+\beta)p_o - \Theta\delta \qquad \text{----2.21}$$

where α, β and Θ are all positive. (figure 2.21)

The air mass contained between the bearing surface is:

$$m = 2\pi\left[\int_0^{R_o}(h+D)\rho_o r\,dr + \int_{R_o}^{R} h\rho r\,dr\right]$$

Using the perfect gas law and equation 2.17 this gives:

$$m = \frac{1}{R'T_o}\left[hP_oA_f + DP_o\pi R_o^2 + hP_e(\pi R^2 - A_f)\right] \qquad \text{----2.22}$$

The time rate of change of m (P, h) is given by:

$$\frac{d(m)}{dt} = \left(\frac{\partial m}{\partial P}\right)_q \frac{dp_o}{dt} + \left(\frac{\partial m}{\partial h}\right)_q \frac{d\delta}{dt}$$

$$= q\dot{p}_o + s\dot{\delta}$$

and dot means $\frac{d}{dt}$.

From equation 2.22:

$$q = \left(\frac{\partial m}{\partial P}\right)_q = \frac{A_fh + D\pi R_o^2}{R'T_o}$$

$$s = \left(\frac{\partial m}{\partial h}\right)_q = \frac{A_f(P_o - P_e) + \pi R^2 P_e}{R'T_o}$$

$$\therefore \frac{q}{s} = \frac{A_fh + D\pi R_o^2}{A_f(P_o-P_e) + \pi R^2 P_e}$$

Equating the time rate of bearing mass:

$$q\dot{p}_o + s\dot{\delta} + (\alpha+\beta)p_o + \Theta\delta = 0 \qquad \text{----2.23}$$

from equation 2.19:

$$p_o = \frac{M}{A_f}\ddot{\delta}$$

$$\dot{p}_o = \frac{M}{A_f}\dddot{\delta}$$

Substituting the values of p_o and $\dot{p}_o$ in equation 2.23 we get

$$\dddot{\delta} + \frac{\alpha+\beta}{q}\ddot{\delta} + \frac{s}{q}\frac{A_f}{M}\dot{\delta} + \frac{\theta}{q}\frac{A_f}{M}\delta = 0 \qquad \text{----2.24}$$

where coefficients of δ and derivatives of δ are all positive. Hence applying Routh's stability criteria to equation 2.24, the following inequality must be satisfied in order to achieve stability:

$$\frac{\alpha+\beta}{q}\cdot\left(\frac{s}{q}\frac{A_f}{M}\right) > \frac{\theta}{q}\frac{A_f}{M}$$

$$\text{or } \frac{\alpha+\beta}{\theta} > \frac{q}{s} \qquad \text{----2.25}$$

Now we will discuss the effects of various parameters on stability. Referring to figure 2.21 we can conclude that for a fixed supply pressure P_s:

1) For stability the maximum possible load must be supported within the safety limits of h.

2) From equation of $\frac{q}{s}$, that D should be minimum.

3) The bearing is more stable for a larger diameter nozzle than for a smaller size nozzle or capillary.

The figure also shows comparison between experiment and theory which is quite satisfactory.

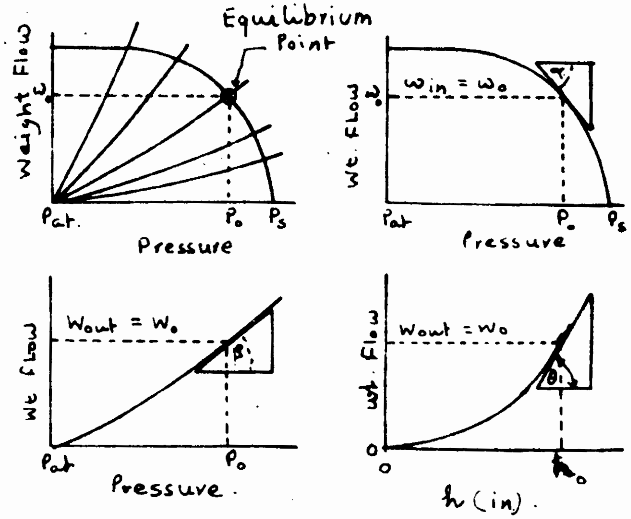

Rate of Change of Mass Flow about Equilibrium Point.

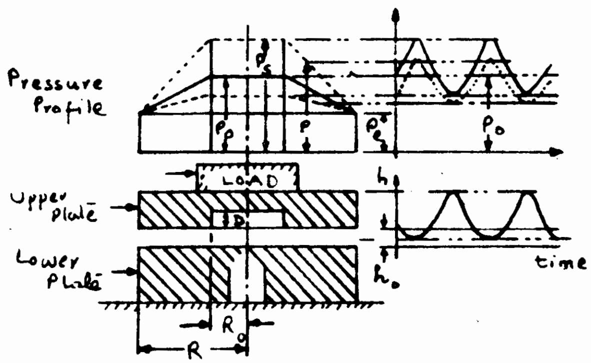

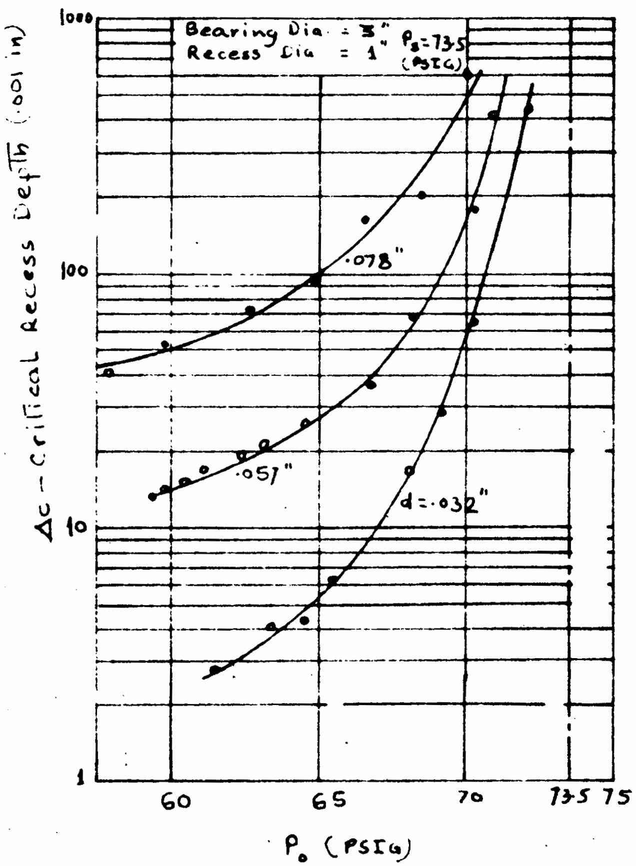

FIGURE (2.21) - EXPERIMENTAL RESULTS OF LICHT FOR THRUST BEARING.

BIBLIOGRAPHY - PART II

(Hydrostatic Lubrication)

1. LAUB, J.H. "Hydrostatic Gas Bearings". ASME Paper NO, 59-Lub-1.
2. MCNEILLY, V.H. "Design and Use of Pneumostatic Bearings". ASLE Paper No. 60 AM-5A-2.
3. RICHARDSON, H.H. and S.K. GRINNELL (1957) "Design Study of A Hydrostatic Gas Bearing with Inherent Orifice Compensation". Trans. ASME Vol. 79, No. 1, pp 11-21.
4. PIGOTT, J.D. and E.F. MACKS (1954) "Air Bearing Studies at Normal and Elevated Temperatures". Lubrication Engineering, Vol. 10, No. 1, pp 29-33.
5. COREY, T.L., TYLER, C.M. (Jr), ROWLAND, H.H. (Jr) and E.M. KIPP (1956) "Behaviour of Air in the Hydrostatic Lubrication of Loaded Spherical Bearings". Trans. ASME Vol. 78, pp 893-898.
6. GOTTAWALD, F. (1955) "Water Bearings and Air Bearings with Pressure Lubrication". Report PB 121405, U.S. Department of Commerce.
7. ADAMS, C.R. (1958) "Step Bearing, A New Concept in Air Lubrication". Produce Engineering, Vol. 29, pp 96-99.
8. WUNSCH, H.L. (1958) "Design Data on Flat Air Bearings When Operating under Steady Conditions of Load". Machinery, Vol. 93, No. 2394, pp 765-775.
9. ROUNDEBUSH, W.H. (1957) "An Analysis of the Effect of Several Parameters on the Stability of an Air lubricated

Hydrostatic Thrust Bearing". NACA Technical Note No. 4095.

10. LICHT, L., FULLER, D.D., and B. STERNLICHT. (1958) "Self Excited Vibrations of an Air Lubricated Thrust Bearing". Trans. ASME, Vol. 80, No. 2, pp 411-414.

11. RICHARDSON, H.H. (1958) "Static and Dynamic Characteristics of Compensated Gas Bearings". Trans. ASME, Vol. 80, No. 7, pp 1505-1508.

12. COLE, J.A. (1959) "Air Lubricated Bearings" Research Applied in Industry, Vol. 12, No. 8-9, pp 348-355.

13. HUGHES, W.F. and J.F. OSTERLE (1957) "Heat Transfer Effects in Hydrostatic Thrust Bearing Lubrication". Trans. ASME, Vol. 79, No. 6, pp. 1225-1228.

14. MONTGOMERY, A.G. and F. STERRY. (1956) A.E.R.E. Report ED/R1671.

15. MUELLER, P.M. (1951) "Air Lubricated Bearings" Product Engineering. August, 1951.

16. COMOLET, R. (1957) "Flow of Fluid Between two Parallel Planes; Contribution to the Study of Air Lubricated Bearings". (in French) Publ. Sci. Tech. Min. Air.France. No. 334.

17. DEUKER, E.A. and H. WOJTECH. (1951) "Radial Flow of a Viscous Fluid Between Two Neighboring Discs. Theory of an Air Bearing, I: Case of a Compressible Fluid". (in French) Rev. Gen. Hyd. 17, 65-66, pp 227-234.

18. SASAKI, T., MORI, H. and A. HIRAI. (1959) "Theoretical Study of Hydrostatic Thrust Bearings" Bull. Japan Society of Mech. Eng. 2,5, pp 75-79.

19. BROWN, E.C. (1951) "Development of a High Efficiency Air Lubricated Journal Bearing". Royal Aircraft Establishment, Tech. Note No. Aero 2107, Farnsborough, England.

20. SHIRES, G.L. (1957) "On a Type of Air Lubricated Journal Bearing". Aero. Res. Council, London. Curr. Papers 318.

21. ELROD, H.G. and L. LICHT. (1959) "A Study of the Stability of Externally Pressurized Gas Bearings". ASME Paper No. 60-APM-5.

22. LICHT, L. (1959) "Axial Relative Motion of a Circular Step Bearing". Trans. ASME, Series D. No. 2, pp 109-117.

23. LICHT, L. (1959) "Stability of Externally Pressurized Gas Journal Bearings". Franklin Institute Laboratories Interim Report No. I-A2049-8.

24. LICHT, L. (1959) "Extension of Conducting Sheet Analogy to Externally Pressurized Gas Bearings". Franklin Institute Laboratories Interim Report No. I-A2049-9.

CONCLUSIONS

From the discussion in Part I and Part II we can draw the following conclusions:

1. Current research in the field of self-acting gas bearings is concerned with three broad topics:

   a) The fluid mechanics of the gas lubrication process.

   b) Bearing materials.

   and c) Bearing stability.

Conventional film lubrication theory postulates the laminar flow of a viscous incompressible fluid in the thin bearing film and calls for fairly involved mathematics to obtain solutions even for highly idealized solutions. However, progress is now being made in the analysis of bearings lubricated with compressible fluids, with some surprising results. The most curious implications of gas lubrication theory are that even under light load conditions where pressure variations are quite small, the flow can still not be regarded as incompressible, and that under heavy loads the viscosity is not an important factor in load capacity.

Bearing materials present a problem because of starting and stopping conditions when the hydrodynamic film is inoperative and contact occurs. The corrosive properties of gases also present a problem. Hence a more detailed investigation of the starting and stopping conditions under various operating conditions must be made.

So far, only steady load conditions have been investigated and the whole field of dynamic loading due to rotor unbalance and other types of time varying loading awaits theoretical and experimental investigation.

Vapour lubrication, as distinct from gas lubrication, has received little attention and so it must be studied in the future because it is an attractive possibility for steam turbines and refrigerating plants.

2. Research and development work in the field of hydrostatic gas bearings is perhaps more active than in the case of hydrodynamic bearings, partly because of the wider range of configurations which can be employed and higher load capacity. Load capacity and friction in terms of pumping energy have been less studied. Other topics requiring further study are the choice of optimum gas supply arrangements and the influence of rotation on performance. The general questions of dynamic loading and stability of rotating hydrostatic bearings of different types offer scope for a great deal of research.

In the end, this survey of gas lubricated bearings shows that oil will not suffer large scale competition due to gas, but gas bearings do show promise for some specialized applications mentioned in the introductory chapter. The future in the field of gas lubrication is challenging both for the research worker and the designer.

VITA

The author was born on thirteenth of June, 1932, at a small town called Burhanpur in India. He finished his elementary and secondary education in a number of schools in Madhya Pradesh (India). He graduated in Mechanical Engineering in 1954 from Saugor University. After graduation he taught Mechanical Engineering at Government Polytechnic, Nagpur, for one year. After this he served as:

1) Research Assistant in the department of Atomic Energy, Government of India.
2) Junior Engineer in Larsen and Toubro, Limited, Bombay.
3) Junior Engineer (erection) in the Associated Cement Companies Limited, Bombay.

At present he is holding the post of lecturer in Mechanical Engineering at College of Engineering, Poona.

He was married on 9th May, 1958.